

Bethe Ansatz for Yangian Invariants: Towards Super Yang-Mills Scattering Amplitudes

Rouven Frassek^{a,b,c}, Nils Kanning^{b,c}, Yumi Ko^{b,d} and Matthias Staudacher^{b,c}

^a *Department of Mathematical Sciences, Durham University,
South Road, Durham DH1 3LE, United Kingdom*

^b *Institut für Mathematik und Institut für Physik, Humboldt-Universität zu Berlin,
IRIS-Adlershof, Zum Großen Windkanal 6, 12489 Berlin, Germany*

^c *Max-Planck-Institut für Gravitationsphysik, Albert-Einstein-Institut,
Am Mühlenberg 1, 14476 Potsdam, Germany*

^d *Asia Pacific Center for Theoretical Physics, Pohang, Gyeongbuk 790-784, Korea*

rouven.frassek@durham.ac.uk, kanning@mathematik.hu-berlin.de,
koyumi@mathematik.hu-berlin.de, matthias@aei.mpg.de

Abstract

We propose that Baxter's Z-invariant six-vertex model at the rational $\mathfrak{gl}(2)$ point on a planar but in general not rectangular lattice provides a way to study Yangian invariants. These are identified with eigenfunctions of certain monodromies of an auxiliary inhomogeneous spin chain. As a consequence they are special solutions to the eigenvalue problem of the associated transfer matrix. Excitingly, this allows to construct them using Bethe ansatz techniques. Conceptually, our construction generalizes to general (super) Lie algebras and general representations. Here we present the explicit form of sample invariants for totally symmetric, finite-dimensional representations of $\mathfrak{gl}(n)$ in terms of oscillator algebras. In particular, we discuss invariants of three- and four-site monodromies that can be understood respectively as intertwiners of the bootstrap and Yang-Baxter equation. We state a set of functional relations significant for these representations of the Yangian and discuss their solutions in terms of Bethe roots. They arrange themselves into exact strings in the complex plane. In addition, it is shown that the sample invariants can be expressed analogously to Grassmannian integrals. This aspect is closely related to a recent on-shell formulation of scattering amplitudes in planar $\mathcal{N} = 4$ super Yang-Mills theory.

Contents

1	Introduction and overview	3
2	Perimeter Bethe ansatz	5
2.1	Rational six-vertex model on Baxter lattices	5
2.2	Solution by Baxter	8
3	From vertex models to Yangian invariance	9
3.1	Vertex models on Baxter lattices	10
3.2	Partition function as eigenvalue problem	12
3.3	Yangian algebra and invariants	15
4	Yangian invariants in oscillator formalism	18
4.1	Oscillators, Lax operators and monodromies	19
4.2	Sample invariants	21
5	Toy model for super Yang-Mills scattering amplitudes	27
5.1	Graßmannian integral for (deformed) scattering amplitudes	28
5.2	Sample invariants as Graßmannian-like integrals	29
6	Bethe ansatz for Yangian invariants	33
6.1	Algebraic Bethe ansatz for $\mathfrak{gl}(2)$ spin chains	33
6.2	Bethe ansatz for invariants of Yangian $\mathcal{Y}(\mathfrak{gl}(2))$	36
6.3	Sample solutions of $\mathfrak{gl}(2)$ functional relations	37
6.4	Relation to perimeter Bethe ansatz	43
6.5	Outline of $\mathfrak{gl}(n)$ functional relations	46
7	Conclusion and outlook	47
A	Some oscillator algebra representations	48
A.1	Bargmann representation	49
A.2	Conjugate Bargmann representation	50

1 Introduction and overview

Some time ago, a remarkable observation has been made in the field of scattering amplitudes of planar $\mathcal{N} = 4$ super Yang-Mills theory, namely their Yangian structure [1]. It was obtained by combining superconformal symmetry and a hidden dual superconformal symmetry [2]. It holds for planar tree-level scattering amplitudes, and there are indications that it also plays a role at loop-level. Originally the Yangian algebra, commonly abbreviated to “Yangian”, was defined by Drinfeld as the algebraic consequence of the Yang-Baxter equation underlying one-dimensional quantum integrable models in the so-called rational case. It is an infinite generalization of finite-dimensional Lie algebras. Thus the Yangian structure appearing in the four-dimensional scattering amplitudes naturally suggests the existence of a hidden quantum integrability. Such a structure has already been unearthed in the last 11 years for the spectral problem of anomalous dimensions in $\mathcal{N} = 4$ theory, where it has led to spectacular progress. See [3] for a recent, fairly up-to-date multi-author review series, and specifically [4] for a juxtaposition of the Yangian symmetry in the scattering and spectral problems. However, while integrability has been essential for the (conjectured) solution of the spectral problem, in the scattering problem it has not yet directly led to any practical advantages in computations, with the notable exception of the recent, very promising conjectural approach of [5]. The reason is that the associated large integrability toolbox, the quantum inverse scattering method (QISM), is so far available only for the calculation of anomalous dimensions. Its application usually leads to powerful Bethe ansatz methods. In contradistinction, apparently no such methods exist to-date for directly exploiting Yangian invariance.

Our question starts here. What is the nature of Yangian symmetry, as it appears in the scattering amplitudes, from the view point of integrability and the QISM? In order to answer this question, we focus on *Yangian invariants* $|\Psi\rangle$, which are defined in the following way,

$$M_{ab}(u)|\Psi\rangle = \delta_{ab}|\Psi\rangle, \tag{1.1}$$

as a key to connect the scattering amplitudes and the Bethe ansatz. Here $M(u)$ is a monodromy matrix, given by a product of suitable R-matrices, u is a spectral parameter, and a, b are indices in an auxiliary space, taking values in the fundamental representation of the underlying symmetry algebra. The generators of the Yangian algebra are obtained as the coefficients $M_{ab}^{(r)}$ of an expansion of the monodromy matrix $M(u)$ in powers r of the inverse spectral parameter u^{-1} . From (1.1) with $M_{ab}^{(0)} = \delta_{ab}$ one then sees that $|\Psi\rangle$ is annihilated by all Yangian generators. By definition, $|\Psi\rangle$ is thus a Yangian invariant. Furthermore, finding all solutions of (1.1) for all suitable $M(u)$ should then lead to the complete set of such invariants.

The first main observation we would like to present in this paper is the following. In the simplest case of $\mathfrak{gl}(2)$ equation (1.1) can be derived from the rational limit of a two-dimensional integrable model, the so-called Z-invariant vertex model introduced by Baxter. It has a description as an inhomogeneous spin chain [6]. Introducing a certain oscillator formalism, and thereby considering more general representations, one can then obtain $\mathfrak{gl}(2)$ Yangian generators. Excitingly, they take forms analogous to the ones acting on the scattering amplitudes in $\mathcal{N} = 4$ super Yang-Mills theory [7]. Furthermore, the procedure readily generalizes to higher rank cases. Supersymmetry should also pose no obstacles.

A further interesting aspect of (1.1) is that it allows one to consider the Bethe ansatz

for the spin chain, which is the second main point of this paper. Equation (1.1) represents a system of eigenvalue problems for the matrix elements $M_{ab}(u)$ of the monodromy matrix $M(u)$, with rather trivial eigenvalues 0 or 1 for a common eigenvector $|\Psi\rangle$. In addition, by taking a trace on both sides, (1.1) becomes an eigenvalue problem for the transfer matrix $T(u)$ of the spin chain,

$$T(u) = \text{tr } M(u), \quad T(u)|\Psi\rangle = n|\Psi\rangle, \quad (1.2)$$

where we already generalized from $\mathfrak{gl}(2)$ to $\mathfrak{gl}(n)$, hence $M(u)$ is a $n \times n$ matrix in the auxiliary space. We conclude that any such Yangian invariant $|\Psi\rangle$ must then be a special eigenvector of the transfer matrix $T(u)$ with prescribed eigenvalue n . It is important to stress that the Yangian invariant $|\Psi\rangle$ in (1.2) and thus also in (1.1) does *not* depend on the spectral parameter u . This is a key feature of the QISM: The diagonalization of $T(u)$ involves an u -independent change of basis.

In this study we will content ourselves with compact representations of $\mathfrak{gl}(n)$. This should play the role of a toy model of the $\mathcal{N} = 4$ scattering amplitudes, where suitable non-compact representations of $\mathfrak{gl}(4|4)$ are needed instead. The latter are built from continuous generalizations of the oscillators mentioned above, which are essentially the spinor-helicity variables and their derivatives. The basic philosophy based on (1.1) should nevertheless remain applicable, at least in the case of the tree-level amplitudes, where Yangian invariance is unequivocal. Each L -particle tree-level amplitude should then be identical to an invariant $|\Psi\rangle$ solving (1.1) with a monodromy of “length” L , and thus amenable to analysis by the QISM. The monodromy is built from L suitable R-matrices, just as in the case of integrable spin chains. Thus amplitudes should turn into “special” spin chain states, similar, as we shall see, to $\mathfrak{gl}(n)$ symmetric antiferromagnetic ground states of the chain. The spin chain monodromy is again inhomogeneous, and the external scattering data is encoded in the representing “oscillators” = spinor-helicity variables. Alternatively, we can think of the tree-level amplitudes as appropriately generalized Baxter lattices, i.e. special vertex models.

Just like in the toy model, it is imperative that the Yangian invariants and therefore the tree-level amplitudes do not depend on the spectral parameter u . The latter merely serves as a suitable device for applying the QISM and for employing (a adequate generalization of) the Bethe ansatz to the problem. On the other hand, spectral parameters were recently introduced as certain natural “helicity” deformations of $\mathcal{N} = 4$ scattering amplitudes in [8, 9]. This is not a contradiction. In the present framework, these parameters simply correspond to a freedom in the choice of the inhomogeneities of the monodromy in (1.1). In the $\mathfrak{gl}(n)$ toy model, the representation labels in general do not fix the inhomogeneities completely. The same holds true in the $\mathcal{N} = 4$ case. In fact, R-matrices of rational models in arbitrary representations are also Yangian invariants. They may therefore be found from special solutions of (1.1). For instance, a standard four-legged $\mathfrak{gl}(n)$ R-matrix acting on the tensor product of two arbitrary compact representations may be deduced from the eigenvector $|\Psi\rangle$ of a length-four monodromy $M(u)$. Here a difference of *inhomogeneities*, denoted by z , in the monodromy $M(u)$ is to be interpreted as a *spectral parameter* of the R-matrix $R(z)$. But z is not the spectral parameter u used to solve the spectral problem (1.1) for Yangian invariants.

This paper is organized as follows. In section 2 we review Baxter’s Z-invariant six-vertex model in the $\mathfrak{gl}(2)$ limit, as well as its remarkable solution through the little-known perimeter Bethe ansatz [6]. Its key feature is, rather unusually, that the Bethe equations

may be explicitly solved with comparative ease. In section 3 we show that Baxter’s approach may be generalized to an important class of compact representations of $\mathfrak{gl}(n)$, and reinterpreted as a systematic way to define and derive Yangian invariants. This opens the way to derive a perimeter Bethe ansatz for the latter. In section 4 we illustrate the method for the case of compact oscillator representations of $\mathfrak{gl}(n)$ by presenting explicit Yangian invariants for three specific examples. Pictorially they correspond to a line, a three-vertex and a four-vertex. The invariants are expressed in oscillator notation. They look somewhat different from the Yangian-invariant tree-level scattering amplitudes, which is surely due to the different nature of the representations under investigation. However, in section 5 we demonstrate that our examples may be rewritten as Grassmannian contour integrals. Interestingly, this manifestly turns them into close analogues of the scattering amplitudes, see [10]. An added benefit of our approach is that the (multi)-contours are precisely defined by the construction. In section 6 we then discuss the perimeter Bethe ansatz for the Yangian invariants of our toy model. We illustrate it for $\mathfrak{gl}(2)$ for the sample invariants of section 4 and section 5. Remarkably, the Bethe roots assemble into exact strings in the complex spectral parameter plane, and are thus explicitly determined. We also sketch the generalization to $\mathfrak{gl}(n)$, where a nested perimeter Bethe ansatz is required. Finally section 7 provides conclusions and an outlook on the application of our novel approach to the computation of actual scattering amplitudes of $\mathcal{N} = 4$ Yang-Mills theory. Some facts useful in section 5 on the connections between oscillators and the well-known Bargmann representations as well as the less-known conjugate Bargmann representations are deferred to appendix A.

2 Perimeter Bethe ansatz

We begin our discussion with the six-vertex model, an important example of an exactly solvable lattice model in two-dimensional statistical mechanics, see e.g. [11]. This model is usually studied on a regular square lattice with periodic boundary conditions. Its exact solution for the partition function of finite size lattices is well known [12], albeit in an implicit form requiring the solution of Bethe ansatz equations. The six-vertex model has also been studied on more general planar lattices [13], the so-called Baxter lattices, which are typically non-rectangular. It is probably less known that the partition function on such lattices for fixed boundary conditions was also obtained using a *perimeter Bethe ansatz* by Baxter [6]. In this construction a Bethe wave function is identified with the partition function. Remarkably, in this case the solutions of the Bethe equations are given explicitly, in difference to most other applications of the Bethe ansatz.

Here we review the perimeter Bethe ansatz of the six-vertex model in the rational limit, which has $\mathfrak{su}(2)$ symmetry in the spin $\frac{1}{2}$ representation. However, our notation differs considerably from the original work [6]. In section 2.1 we introduce the Baxter lattice along with the model defined on it. Its solution in terms of the perimeter Bethe ansatz is discussed in section 2.2. For brevity we refrain from repeating Baxter’s proof of this result here. Instead, we will understand it later in section 6.4 as a special case of a more general connection between partition functions of vertex models and Bethe vectors.

2.1 Rational six-vertex model on Baxter lattices

The lattice is defined by N straight lines in the interior of a circle which start and end at points on the perimeter. The lines can be arranged in an arbitrary way. The intersection

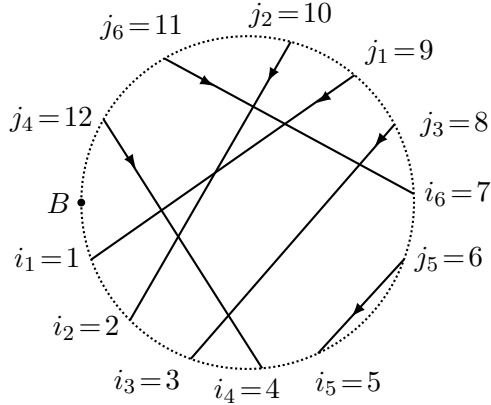


Figure 2.1: Sample Baxter lattice with $N = 6$ lines whose configuration is given by the endpoints $\mathbf{G} = ((1, 9), (2, 10), (3, 8), (4, 12), (5, 6), (7, 11))$. Each line k has endpoints (i_k, j_k) , an orientation indicated by an arrow and carries a rapidity θ_k , which is not shown in this figure.

points of the lines divide each line into a number of edges. However, only two lines are allowed to intersect at a point. An example is shown in figure 2.1, where the perimeter is represented by a dotted circle. The N lines and their $2N$ endpoints are labeled counter-clockwise starting at a reference point B on the perimeter. Each line has an orientation, which for the k -th line with endpoints (i_k, j_k) obeying $1 \leq i_k < j_k \leq 2N$ is given by an arrow pointing from j_k towards i_k . In addition, we assign a rapidity θ_k to the k -th line. We refer to this configuration of lines as a *Baxter lattice*. It is specified by the ordered sets

$$\mathbf{G} = ((i_1, j_1), \dots, (i_N, j_N)), \quad \boldsymbol{\theta} = (\theta_1, \dots, \theta_N). \quad (2.1)$$

To each vertex, i.e. intersection of two lines, we associate the Boltzmann weights of the six-vertex model in the rational limit, which may be conveniently expressed as elements of an R-matrix. They depend on the rapidities of the lines and state labels 1 or 2 which are assigned to the adjacent edges of the vertex:

$$\langle \alpha, \gamma | R(\theta - \theta') | \beta, \delta \rangle = \theta \alpha \begin{array}{c} \delta \\ \downarrow \\ \leftarrow \beta \\ \uparrow \\ \gamma \\ \theta' \end{array} . \quad (2.2)$$

These weights are defined as elements of an $\mathfrak{su}(2)$ spin $\frac{1}{2}$ R-matrix

$$R(\theta - \theta') = \frac{1}{\theta - \theta' + 1} \begin{pmatrix} \theta - \theta' + 1 & 0 & 0 & 0 \\ 0 & \theta - \theta' & 1 & 0 \\ 0 & 1 & \theta - \theta' & 0 \\ 0 & 0 & 0 & \theta - \theta' + 1 \end{pmatrix}. \quad (2.3)$$

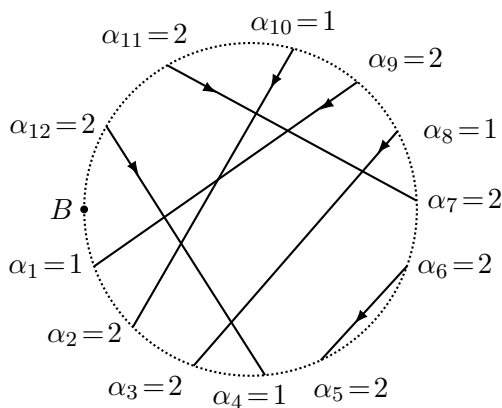


Figure 2.2: The sample Baxter lattice of figure 2.1 with a certain assignment of states, labeled by α , to the endpoints. Note that the number of endpoints i_k with a state labeled $\alpha_{i_k} = 1$ and that of endpoints j_k with $\alpha_{j_k} = 1$ agrees, i.e the ice rule (2.6) is satisfied. In this case α gives rise to $\mathbf{x} = (1, 4, 6, 9, 11, 12)$, see (2.11), which is used to express the partition function $\mathcal{Z}(\mathbf{G}, \boldsymbol{\theta}, \boldsymbol{\alpha})$ in terms of a Bethe wave function $\Phi(\mathbf{w}, \mathbf{z}, \mathbf{x})$ in (2.13).

The Greek indices $\alpha, \beta, \gamma, \delta$ assigned to the edges take the values 1 or 2. These correspond to the states $|1\rangle = \begin{pmatrix} 1 \\ 0 \end{pmatrix}$ or $|2\rangle = \begin{pmatrix} 0 \\ 1 \end{pmatrix}$, or the respective bras. The R-matrix acts on the tensor product of two states $|\beta, \delta\rangle := |\beta\rangle \otimes |\delta\rangle$ and the matrix element is built with $\langle \alpha, \gamma | := \langle \alpha | \otimes \langle \gamma |$. The six non-zero elements of the matrix denote the six configurations of a vertex for which the number of incoming states $|1\rangle, |2\rangle$ and outgoing states $\langle 1|, \langle 2|$ are equal, respectively. This “conservation law” is the so-called *ice rule*.

The boundary conditions of this vertex model are given by labels α_{i_k} and α_{j_k} that can take the values 1 or 2 and are assigned to the endpoints (i_k, j_k) of the lines, see figure 2.2. We denote them by

$$\boldsymbol{\alpha} = (\alpha_1, \dots, \alpha_{2N}). \quad (2.4)$$

These labels correspond to the states at the boundary edges of the lattice.

The partition function of a Baxter lattice is defined as

$$\mathcal{Z}(\mathbf{G}, \boldsymbol{\theta}, \boldsymbol{\alpha}) = \sum_{\substack{\text{internal vertices} \\ \text{state} \\ \text{config.}}} \prod \text{ Boltzmann weight}. \quad (2.5)$$

The sum runs over all possible state configurations of the internal edges. We have to add an additional prescription for lines not containing any vertex, see e.g. the line with endpoints (5, 6) in figure 2.2. If such a line k has equal state labels $\alpha_{i_k} = \alpha_{j_k}$ at the endpoints, it contributes a factor of unity to the partition function. In case of differing labels $\alpha_{i_k} \neq \alpha_{j_k}$, the partition function is set to zero.

As a consequence of the ice rule at each vertex, the partition function can only be non-zero if the number of endpoints i_k at outward pointing boundary edges with $\alpha_{i_k} = 1$ is equal to that of endpoints j_k at inward pointing edges with $\alpha_{j_k} = 1$,

$$|\{i_k \mid \alpha_{i_k} = 1\}| = |\{j_k \mid \alpha_{j_k} = 1\}|. \quad (2.6)$$

The same condition then also holds for endpoints with state labels 2.

The R-matrix (2.3) and thus the Boltzmann weights at the vertices satisfy a Yang-Baxter equation, see section 3 below. This means that the partition function does not change if a line of the lattice is moved through a vertex without changing the order of the endpoints in \mathbf{G} . This is usually referred to as Z-invariance.

2.2 Solution by Baxter

An exact expression for the partition function (2.5) was obtained in terms of a Bethe wave function in [6]. The wave function of the Heisenberg spin chain with $\mathfrak{su}(2)$ spin $\frac{1}{2}$ symmetry can be derived from a coordinate Bethe ansatz [14], as nicely explained e.g. in [15]. This was generalized to a spin chain with inhomogeneities in [16], which is the case needed here. For a spin chain of length L with P excitations (“magnons”) the wave function is parametrized by

$$\mathbf{w} = (w_1, \dots, w_L), \quad \mathbf{z} = (u_1, \dots, u_P), \quad \mathbf{x} = (x_1, \dots, x_P), \quad (2.7)$$

denoting respectively the inhomogeneities, Bethe roots and positions of the magnons with $1 \leq x_1 < \dots < x_P \leq L$. The wave function takes the form

$$\Phi(\mathbf{w}, \mathbf{z}, \mathbf{x}) = \sum_{\rho} \prod_{1 \leq k < l \leq P} \frac{u_{\rho(k)} - u_{\rho(l)} + 1}{u_{\rho(k)} - u_{\rho(l)}} \prod_{k=1}^P \phi_{x_k}(u_{\rho(k)}, \mathbf{w}), \quad (2.8)$$

where the sum is over all permutations ρ of P elements, and the single particle wave function is given by

$$\phi_x(u, \mathbf{w}) = \prod_{j=1}^{x-1} (u - w_j + 1) \prod_{j=x+1}^L (u - w_j). \quad (2.9)$$

Imposing periodicity of (2.8) in the magnon positions, one obtains the Bethe equations

$$\prod_{i=1}^L \frac{u_k - w_i + 1}{u_k - w_i} = - \prod_{i=1}^P \frac{u_k - u_i + 1}{u_k - u_i - 1} \quad (2.10)$$

with $1 \leq k \leq P$. They guarantee that the wave functions (2.8) for different magnon configurations \mathbf{x} build up a transfer matrix eigenvector of the closed inhomogeneous Heisenberg spin chain. See also section 6.1 below for a recap of the Bethe ansatz in the algebraic formulation. Often (2.8) for generic Bethe roots \mathbf{z} is referred to as “off-shell” Bethe wave-function, while it is “on-shell” in case the Bethe roots satisfy (2.10).

Now, we are ready to express the partition function (2.5) in terms of the Bethe wave function (2.8). It is only non-trivial if the ice rule (2.6) applies, hence we restrict to these cases. We stress again that our notation differs from [6]. The relation is established by the following procedure, where in particular the parameters \mathbf{w} , \mathbf{z} and \mathbf{x} of (2.8) are related to the variables \mathbf{G} , $\boldsymbol{\theta}$ and $\boldsymbol{\alpha}$ of (2.5):

1. For a Baxter lattice with N lines, we employ a wave function with length $L = 2N$ and $P = N$ excitations, a situation usually termed “half-filling”.
2. The magnon coordinates \mathbf{x} are related to $\boldsymbol{\alpha}$ and \mathbf{G} . They are given by the endpoint positions i_k at outward pointing edges with $\alpha_{i_k} = 1$ and j_k at edges directed inwards with $\alpha_{j_k} = 2$:

$$\{x_k\} = \{i_k | \alpha_{i_k} = 1\} \cup \{j_k | \alpha_{j_k} = 2\}. \quad (2.11)$$

These x_k are then ordered as $1 \leq x_1 < \dots < x_N \leq 2N$. See the example in figure 2.2.

3. Most importantly, the inhomogeneities \mathbf{w} and the Bethe roots \mathbf{z} are given in terms of the rapidities $\boldsymbol{\theta}$ and \mathbf{G} . For each line k with endpoints (i_k, j_k) we set

$$w_{i_k} = \theta_k + 1, \quad w_{j_k} = \theta_k + 2, \quad u_k = \theta_k + 1. \quad (2.12)$$

Remarkably, this is an explicit solution of the Bethe equations (2.10). It is easily seen after writing the Bethe equations in polynomial form in order to avoid divergencies, cf. section 6.1. Note also that the wave function (2.8) is invariant under a permutation of the Bethe roots.

Under these identifications, we finally obtain the desired expression for the partition function (2.5) in terms of the Bethe wave function (2.8):

$$\mathcal{Z}(\mathbf{G}, \boldsymbol{\theta}, \boldsymbol{\alpha}) = \mathcal{C}(\mathbf{G}, \boldsymbol{\theta})^{-1} (-1)^{\mathcal{K}(\mathbf{G}, \boldsymbol{\alpha})} \Phi(\mathbf{w}, \mathbf{z}, \mathbf{x}). \quad (2.13)$$

The exponent $\mathcal{K}(\mathbf{G}, \boldsymbol{\alpha})$ is the number of endpoints i_k with state label $\alpha_{i_k} = 2$,

$$\mathcal{K}(\mathbf{G}, \boldsymbol{\alpha}) = |\{i_k \mid \alpha_{i_k} = 2\}|. \quad (2.14)$$

The $\boldsymbol{\alpha}$ -independent normalization is given by

$$\mathcal{C}(\mathbf{G}, \boldsymbol{\theta}) = \Phi(\mathbf{w}, \mathbf{z}, \mathbf{x}_0), \quad (2.15)$$

where $\mathbf{x}_0 = (i_1, \dots, i_N)$ is obtained from (2.11) with $\boldsymbol{\alpha}_0 = (1, \dots, 1)$, which means the state labels are 1 at all $2N$ endpoints. Expression (2.13) is the *perimeter Bethe ansatz* solution of the six-vertex model on a Baxter lattice in the rational limit. A derivation of this solution, different from the original one in [6], will be presented in section 6.4 as a special case of a more general result.

3 From vertex models to Yangian invariance

In the previous section the computation of the partition function of vertex models on typically non-rectangular Baxter lattices using the perimeter Bethe ansatz was reviewed. Here we vastly generalize the class of vertex models, and we establish a new perspective on the computation of the partition functions \mathcal{Z} . This is achieved by connecting the problem to the powerful Quantum Inverse Scattering Method (QISM) and relating \mathcal{Z} to invariants $|\Psi\rangle$ of Yangian algebras. We are led to a characterization of invariants $|\Psi\rangle$, which provides the conceptual basis of all further studies. In particular, it will enable us later in section 6 to construct Yangian invariants using a Bethe ansatz.

In section 3.1 we generalize the Baxter lattice of section 2 in two respects. Firstly, we extend the algebra from $\mathfrak{su}(2) \subset \mathfrak{gl}(2)$ to $\mathfrak{gl}(n)$. Secondly, we replace the spin $\frac{1}{2}$ representation of $\mathfrak{su}(2)$ carried by every line with a more general representation Λ of $\mathfrak{gl}(n)$, which in addition may differ for each line. The resulting lattices will still be referred to as “Baxter lattices”, and we will define the partition function of vertex models associated to them. In section 3.2 we derive identities satisfied by these partition functions, which are then translated into a set of eigenvalue equations within the context of the QISM. To this end, the partition function \mathcal{Z} is identified with a component of a simultaneous eigenvector $|\Psi\rangle$ of all elements $M_{ab}(u)$ of a spin chain monodromy with specific representations and inhomogeneities. More precisely, the eigenvalue of this eigenvector $|\Psi\rangle$ is 1 for all diagonal monodromy elements $M_{aa}(u)$ and 0 for the off-diagonal ones. In section 3.3

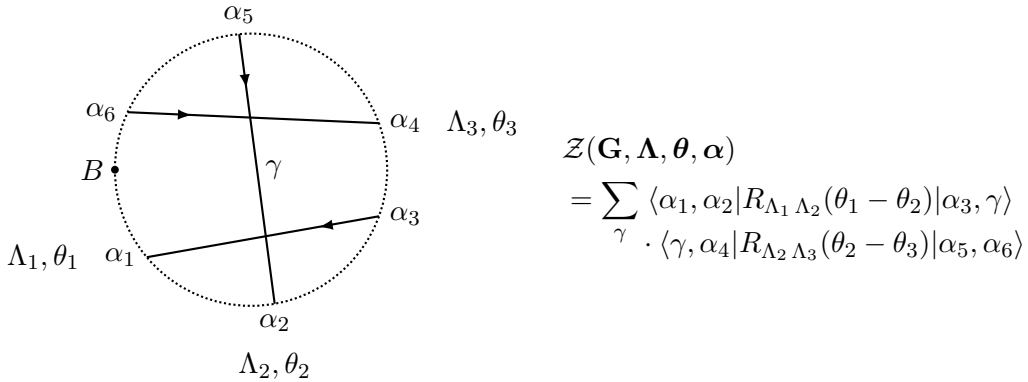


Figure 3.1: Example of a (generalized) Baxter lattice with $N = 3$ lines and $\mathbf{G} = ((1, 3), (2, 5), (4, 6))$, left side. Each line carries a $\mathfrak{gl}(n)$ representation Λ_k , a spectral parameter θ_k , two state labels α_{i_k} and α_{j_k} at the endpoints $i_k < j_k$ and an orientation indicated by an arrow. The dotted circle and the reference point B are not part of the Baxter lattice. The associated partition function $\mathcal{Z}(\mathbf{G}, \mathbf{\Lambda}, \boldsymbol{\theta}, \boldsymbol{\alpha})$ is shown on the right, cf. (3.6).

we free ourselves from specific representations and inhomogeneities, and consider the just derived set of eigenvalue equations for general spin chain monodromies. Noting that such monodromies provide realizations of the Yangian algebra $\mathcal{Y}(\mathfrak{gl}(n))$, we observe that the set of eigenvalue equations characterizes vectors $|\Psi\rangle$ that are Yangian invariant. Later, in section 4.2.2, we will come across examples of Yangian invariants that fall outside the framework of Baxter lattices in the sense of section 3.2. These require the generalizations of section 3.3.

3.1 Vertex models on Baxter lattices

Let us repeat the definition of the Baxter lattice spelled out in section 2, and extend it by the generalizations just mentioned. See also the simple example lattice in the left part of figure 3.1. We start with a dotted circle on which we mark a reference point B . Notice that the circle and the reference point are only used for the construction and will not become part of the Baxter lattice itself. N straight lines, each connecting two points on the dotted circle, are specified in such a way that in the interior of the circle only two of the lines intersect at a single point. Starting at the reference point, the N lines and the $2N$ endpoints of these lines are labeled counterclockwise. Each line has an orientation, which for the k -th line with endpoints $i_k < j_k$ is given by an arrow pointing from j_k towards i_k . The choice of the reference point clearly affects the orientation of the lines. In addition, we assign a $\mathfrak{gl}(n)$ representation Λ_k and a complex spectral parameter θ_k to the k -th line. To the endpoints of this line we assign states of the representation Λ_k labeled by α_{i_k} and α_{j_k} . A (generalized) *Baxter lattice* including boundary conditions is defined with this data by the ordered sets

$$\begin{aligned} \mathbf{G} &= ((i_1, j_1), \dots, (i_N, j_N)), \\ \mathbf{\Lambda} &= (\Lambda_1, \dots, \Lambda_N), \quad \boldsymbol{\theta} = (\theta_1, \dots, \theta_N), \quad \boldsymbol{\alpha} = (\alpha_1, \dots, \alpha_{2N}). \end{aligned} \tag{3.1}$$

In order to introduce a vertex model on such a Baxter lattice we also have to generalize the Boltzmann weights of section 2. We introduce them as

$$\langle \alpha, \gamma | R_{\Lambda \Lambda'}(\theta - \theta') | \beta, \delta \rangle = \Lambda, \theta \begin{array}{c} \delta \\ \downarrow \\ \alpha \text{ --- } \rightarrow \beta \\ \uparrow \\ \gamma \\ \Lambda', \theta' \end{array} , \quad (3.2)$$

which are matrix elements of the R-matrix

$$R_{\Lambda \Lambda'}(\theta - \theta') = \Lambda, \theta \begin{array}{c} \downarrow \\ \text{---} \leftarrow \\ \uparrow \\ \Lambda', \theta' \end{array} . \quad (3.3)$$

This R-matrix is an operator acting on the tensor product $V_{\Lambda} \otimes V_{\Lambda'}$ of the spaces of the two $\mathfrak{gl}(n)$ representations Λ and Λ' with spectral parameters θ and θ' . The Boltzmann weights are defined using orthonormal basis states of V_{Λ} and $V_{\Lambda'}$ labeled by Greek indices α , β and γ , δ , respectively. Graphically each space is associated with one line. The orientation of (i.e. arrow on) a line specifies the order of multiple R-matrices acting on one space. R-matrices “earlier” on the line are right of “later” ones in the corresponding formula. In this sense the arrows in (3.3) point from the “inputs” of the R-matrix towards the “outputs” or, in component language (3.2), from the kets towards the bras. We will switch between the operator language and the Boltzmann weights whenever it is convenient. The R-matrix (3.3) is required to be a solution of the Yang-Baxter equation

$$\begin{aligned} R_{\Lambda \Lambda'}(\theta - \theta') R_{\Lambda \Lambda''}(\theta - \theta'') R_{\Lambda' \Lambda''}(\theta' - \theta'') \\ = R_{\Lambda' \Lambda''}(\theta' - \theta'') R_{\Lambda \Lambda''}(\theta - \theta'') R_{\Lambda \Lambda'}(\theta - \theta') , \end{aligned} \quad (3.4)$$

which acts in the tensor product $V_{\Lambda} \otimes V_{\Lambda'} \otimes V_{\Lambda''}$ and reads graphically

$$\begin{array}{c} \swarrow \quad \searrow \\ \Lambda, \theta \text{ --- } \rightarrow \\ \nwarrow \quad \nearrow \\ \Lambda', \theta' \quad \Lambda'', \theta'' \end{array} = \begin{array}{c} \Lambda, \theta \text{ --- } \rightarrow \\ \swarrow \quad \searrow \\ \nwarrow \quad \nearrow \\ \Lambda', \theta' \quad \Lambda'', \theta'' \end{array} . \quad (3.5)$$

Now we can define the partition function of a vertex model on a (generalized) Baxter lattice, see again the example in figure 3.1, employing the component language of Boltzmann weights. To each internal edge of the lattice we assign a state of the given representation Λ , while the states at the boundary edges are naturally fixed by α . Recall that Λ is associated to the entire line, and therefore all internal and boundary edges which make up the line carry states in this representation. Each vertex of the lattice is then translated into a Boltzmann weight as shown in (3.2). The partition function $\mathcal{Z}(\mathbf{G}, \Lambda, \theta, \alpha)$ is the sum, ranging over all possible configurations of states at the internal edges, of the product of all Boltzmann weights of the lattice. As already in (2.13), we write symbolically

$$\mathcal{Z}(\mathbf{G}, \Lambda, \theta, \alpha) = \sum_{\substack{\text{internal} \\ \text{state} \\ \text{config.}}} \prod \text{ Boltzmann weight} . \quad (3.6)$$

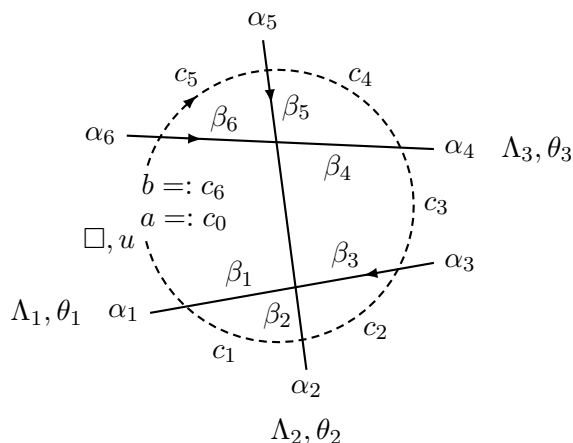


Figure 3.2: The Baxter lattice introduced in the example of figure 3.1 after the dotted circle has been replaced by a dashed auxiliary space line in the fundamental representation \square with spectral parameter u and states labeled a, b at the endpoints. The indices c_i are assigned to the edges of this auxiliary space. The states at the edges connecting this space with the Baxter lattice are labeled β_i .

If there is a line consisting of a single edge with differing states at the boundary, the partition function vanishes.

In the operator description this partition function is a matrix element of a product of R-matrices. These R-matrices and their order in the product are given by the form of the Baxter lattice. A line with a single edge is translated into an identity operator on the corresponding representation space. The matrix element is specified by α , and the sum and product in (3.6) translate into matrix multiplication.

3.2 Partition function as eigenvalue problem

As a first step to understand the partition function of a Baxter lattice as an eigenvalue problem within the QISM, we derive an identity satisfied by $\mathcal{Z}(\mathbf{G}, \mathbf{\Lambda}, \boldsymbol{\theta}, \boldsymbol{\alpha})$. Recall that the construction of Baxter lattices involves a dotted circle. Here we replace this circle by an arc, which is opened at the reference point B and is to represent an actual *space* called auxiliary space. In addition, the lines of the Baxter lattice are slightly extended such that they intersect the arc. This is depicted by the dashed line in figure 3.2. The auxiliary space $V_{\square} = \mathbb{C}^n$ carries the fundamental representation \square of $\mathfrak{gl}(n)$ as well as a spectral parameter u . The orientation is chosen counterclockwise. The bra and ket states at the endpoints of the dashed line are labeled by the indices a and b , respectively, which may take the values $1, \dots, n$. As auxiliary space intersects all other lines twice, it introduces a layer of additional vertices at the boundary of the Baxter lattice. The Boltzmann weights at these vertices correspond to elements of R-matrices of the type $R_{\square\Lambda}(u - \theta)$ or $R_{\Lambda\square}(\theta - u)$, which are referred to as Lax operators. These Lax operators also satisfy a Yang-Baxter

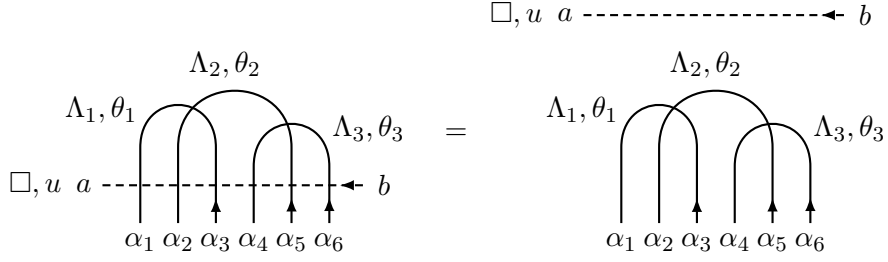


Figure 3.3: An identity for $\mathcal{Z}(\mathbf{G}, \mathbf{\Lambda}, \boldsymbol{\theta}, \boldsymbol{\alpha})$ of the sample Baxter lattice in figure 3.1 is derived by disentangling the dashed auxiliary line from the solid lines using (3.7) and (3.8). The lattice has been deformed to emphasize that the row of vertices involving the auxiliary line will be written as a monodromy shortly, cf. figure 3.4.

equation of the form

$$\square, u \begin{array}{c} \nearrow \\ \searrow \\ \dashrightarrow \\ \nearrow \\ \searrow \end{array} \begin{array}{c} \Lambda, \theta \\ \Lambda', \theta' \end{array} = \begin{array}{c} \square, u \dashrightarrow \\ \nearrow \\ \searrow \\ \nearrow \\ \searrow \end{array} \begin{array}{c} \Lambda, \theta \\ \Lambda', \theta' \end{array}, \quad (3.7)$$

which is a special case of (3.5). In addition, we demand the unitarity condition

$$R_{\square\Lambda}(u - \theta)R_{\Lambda\square}(\theta - u) = 1, \quad \text{i.e.} \quad \square, u \begin{array}{c} \dashrightarrow \\ \updownarrow \\ \dashrightarrow \end{array} \Lambda, \theta = \begin{array}{c} \updownarrow \\ \dashrightarrow \end{array} \Lambda, \theta \quad (3.8)$$

using the graphical notation.

Making use of the Yang-Baxter equation (3.7) and the unitarity condition (3.8) we can completely disentangle the auxiliary space (dashed line) from the N spaces defining the Baxter lattice (solid lines). Graphically one easily sees that this leads to a non-trivial identity for the partition function $\mathcal{Z}(\mathbf{G}, \mathbf{\Lambda}, \boldsymbol{\theta}, \boldsymbol{\alpha})$ of a Baxter lattice, see the example in figure 3.3. To obtain this identity for a general Baxter lattice, we start by denoting the Boltzmann weights involving the auxiliary space by

$$\begin{aligned} & \mathcal{M}_{ab}(u, \mathbf{G}, \mathbf{\Lambda}, \boldsymbol{\theta}, \boldsymbol{\alpha}, \boldsymbol{\beta}) \\ &= \sum_{c_1, \dots, c_{2N-1}=1}^n \left(\prod_{k=1}^N \langle c_{i_k-1}, \alpha_{i_k} | R_{\square\Lambda_k}(u - \theta_k) | c_{i_k}, \beta_{i_k} \rangle \right. \\ & \quad \left. \cdot \langle \beta_{j_k}, c_{j_k-1} | R_{\Lambda_k\square}(\theta_k - u) | \alpha_{j_k}, c_{j_k} \rangle \right)_{\substack{c_0:=a \\ c_{2N}:=b}}, \end{aligned} \quad (3.9)$$

where each of the N lines of the lattice contributes two weights. In figure 3.2 we see an example for the assignment of the indices c_i and β_i to the edges. Also, recall from (3.1) that the k -th line of a Baxter lattice has the endpoints $i_k < j_k$. The states labeled

c_i with $i = 0, \dots, 2N$ are assigned to the edges of the auxiliary space. The state labels $\beta = (\beta_1, \dots, \beta_{2N})$ are placed at the edges that connect the layer of vertices involving the auxiliary space to the Baxter lattice on which the partition function is defined. Equating the Baxter lattice entangled with the auxiliary space to the disentangled situation, we find

$$\sum_{\beta} \mathcal{M}_{ab}(u, \mathbf{G}, \mathbf{\Lambda}, \boldsymbol{\theta}, \boldsymbol{\alpha}, \beta) \mathcal{Z}(\mathbf{G}, \mathbf{\Lambda}, \boldsymbol{\theta}, \beta) = \delta_{ab} \mathcal{Z}(\mathbf{G}, \mathbf{\Lambda}, \boldsymbol{\theta}, \boldsymbol{\alpha}). \quad (3.10)$$

We see that the unraveled auxiliary line simply translates into δ_{ab} on the r.h.s. of (3.10). The entire equation is depicted for an example in figure 3.3.

As will be shown next, the summed-over Boltzmann weights in $\mathcal{M}_{ab}(u, \mathbf{G}, \mathbf{\Lambda}, \boldsymbol{\theta}, \boldsymbol{\alpha}, \beta)$ can be rewritten as matrix elements of an inhomogeneous spin chain monodromy $M(u)$ with L sites. This allows us to link with the QISM. The monodromy is introduced as

$$M(u) = R_{\square \Xi_1}(u - v_1) \cdots R_{\square \Xi_L}(u - v_L) = \square, u \begin{array}{c} \downarrow \\ \vdots \\ \vdots \\ \downarrow \\ \Xi_1, v_1 \end{array} \cdots \begin{array}{c} \downarrow \\ \vdots \\ \vdots \\ \downarrow \\ \Xi_L, v_L \end{array}. \quad (3.11)$$

The j -th site carries a $\mathfrak{gl}(n)$ representation Ξ_j acting on the local quantum space V_j and it has an inhomogeneity $v_j \in \mathbb{C}$. The total quantum space of the spin chain is the tensor product $V_1 \otimes \cdots \otimes V_L$. The auxiliary space carries the fundamental representation \square and the matrix elements of the monodromy with respect to this space are denoted by

$$M_{ab}(u) := \langle a | M(u) | b \rangle. \quad (3.12)$$

They are still operators in the total quantum space. In what follows, we require the Lax operators associated to the Boltzmann weights in (3.9) to satisfy the crossing relation

$$R_{\square \bar{\Lambda}}(u - \theta + \kappa_{\Lambda}) = R_{\Lambda \square}(\theta - u)^{\dagger}, \quad (3.13)$$

where κ_{Λ} is a representation-dependent crossing parameter, and the conjugation only acts on the space V_{Λ} . For a representation Λ realized by $\mathfrak{gl}(n)$ generators J_{ab} on V_{Λ} , the conjugate representation $\bar{\Lambda}$ appearing in (3.13) is defined by the generators

$$\bar{J}_{ab} = -J_{ab}^{\dagger}. \quad (3.14)$$

Assuming the matrix elements $\langle \alpha | J_{ab} | \beta \rangle$ of the generators to be real, we obtain from (3.13)

$$\begin{aligned} \langle c, \beta | R_{\square \bar{\Lambda}}(u - \theta + \kappa_{\Lambda}) | d, \alpha \rangle & \quad \text{i.e.} \quad \square, u \begin{array}{c} \alpha \\ \downarrow \\ \vdots \\ \vdots \\ \downarrow \\ \beta \end{array} \begin{array}{c} \leftarrow d \\ \vdots \\ \vdots \\ \leftarrow c \end{array} \\ = \langle \alpha, c | R_{\Lambda \square}(\theta - u) | \beta, d \rangle, & \quad \bar{\Lambda}, \theta - \kappa_{\Lambda} \end{array} = \begin{array}{c} \square, u \begin{array}{c} \alpha \\ \downarrow \\ \vdots \\ \vdots \\ \downarrow \\ \beta \end{array} \begin{array}{c} \leftarrow d \\ \vdots \\ \vdots \\ \leftarrow c \end{array} \\ \Lambda, \theta \end{array}, \quad (3.15) \end{aligned}$$

where we have given both the equation and its graphic representation. Applying (3.15) to the weights in the second line of (3.9) yields

$$\begin{aligned} & \mathcal{M}_{ab}(u, \mathbf{G}, \mathbf{\Lambda}, \boldsymbol{\theta}, \boldsymbol{\alpha}, \beta) \\ &= \sum_{c_1, \dots, c_{2N-1}=1}^n \left(\prod_{k=1}^N \langle c_{i_k-1}, \alpha_{i_k} | R_{\square \Lambda_k}(u - \theta_k) | c_{i_k}, \beta_{i_k} \rangle \right. \\ & \quad \left. \cdot \langle c_{j_k-1}, \alpha_{j_k} | R_{\square \bar{\Lambda}_k}(u - \theta_k + \kappa_{\Lambda_k}) | c_{j_k}, \beta_{j_k} \rangle \right)_{\substack{c_0:=a \\ c_{2N}:=b}}. \end{aligned} \quad (3.16)$$

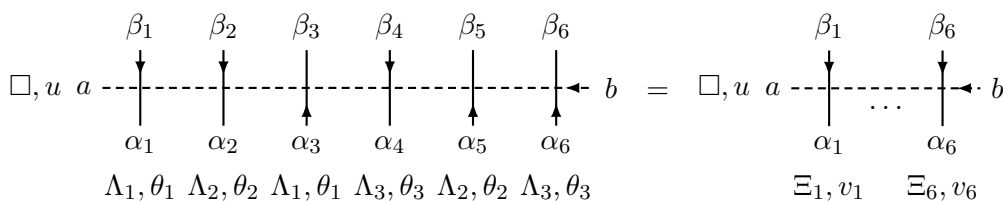


Figure 3.4: Rewriting of the summed Boltzmann weights in $\mathcal{M}_{ab}(u, \mathbf{G}, \mathbf{\Lambda}, \boldsymbol{\theta}, \boldsymbol{\alpha}, \boldsymbol{\beta})$ on the l.h.s. as a matrix element $\langle \boldsymbol{\alpha} | M_{ba}(u) | \boldsymbol{\beta} \rangle$ of a monodromy on the r.h.s. for the example discussed in figure 3.3. After applying (3.15) to the l.h.s. all vertical lines have the same orientation. Ξ_i and v_i of the resulting monodromy are given by (3.18) with \mathbf{G} specified in the caption of figure 3.1.

In this form the index structure is such that all weights combine into matrix elements of the monodromy (3.11) with $L = 2N$ sites,

$$\mathcal{M}_{ab}(u, \mathbf{G}, \mathbf{\Lambda}, \boldsymbol{\theta}, \boldsymbol{\alpha}, \boldsymbol{\beta}) = \langle \boldsymbol{\alpha} | M_{ab}(u) | \boldsymbol{\beta} \rangle. \quad (3.17)$$

As is usual for a monodromy, the labels of the total quantum space are hidden. Thus there is no analogue of the labels $\mathbf{G}, \mathbf{\Lambda}, \boldsymbol{\theta}$ on the r.h.s. of (3.17). Here we use the notation $|\boldsymbol{\beta}\rangle := |\beta_1\rangle \otimes \cdots \otimes |\beta_{2N}\rangle \in V_1 \otimes \cdots \otimes V_{2N}$. For each line k of the Baxter lattice with endpoints $i_k < j_k$ specified in \mathbf{G} , see (3.1), we obtain two spin chain sites with representations and inhomogeneities

$$\Xi_{i_k} = \Lambda_k, \quad v_{i_k} = \theta_k \quad \text{and} \quad \Xi_{j_k} = \bar{\Lambda}_k, \quad v_{j_k} = \theta_k - \kappa_{\Lambda_k}. \quad (3.18)$$

See also the example in figure 3.4. In addition, the partition function of the vertex model defines a vector $|\Psi\rangle$ in the total quantum space of the spin chain via

$$\langle \boldsymbol{\alpha} | \Psi \rangle := \mathcal{Z}(\mathbf{G}, \mathbf{\Lambda}, \boldsymbol{\theta}, \boldsymbol{\alpha}). \quad (3.19)$$

With (3.12), (3.19) and the orthonormality of the states $|\boldsymbol{\beta}\rangle$ the identity (3.10) for the partition function translates into

$$\langle \boldsymbol{\alpha} | M_{ab}(u) | \Psi \rangle = \delta_{ab} \langle \boldsymbol{\alpha} | \Psi \rangle. \quad (3.20)$$

Dropping the bra $\langle \boldsymbol{\alpha} |$, (3.20) is the sought-for set of eigenvalue equations. These equations characterize the vector $|\Psi\rangle$, which, according to (3.19), is built out of the partition functions of a Baxter lattice for all possible boundary configurations $\boldsymbol{\alpha}$. Equation (3.20) tells us that $|\Psi\rangle$ is a *special* simultaneous eigenvector of all matrix elements of the *specific* monodromy defined by (3.11) with (3.18). The eigenvector $|\Psi\rangle$ is special because its eigenvalues are fixed to be 1 for diagonal monodromy elements and 0 for off-diagonal ones. Remarkably, (3.20) is an eigenvalue problem within the realm of the QISM.

3.3 Yangian algebra and invariants

In this section we will analyze (3.20) in the context of Yangians. We will continue to employ the monodromy (3.11). However, we shall allow for general representations Ξ_i

and inhomogeneities v_i , which in general do not have to obey the restrictions (3.18). Furthermore, an odd number of sites L is now also permitted. This was not meaningful in the context of section 3.2, where each line of the Baxter lattice gave rise to exactly two sites.

Let us use the well-known explicit expression for the Lax operators at the sites of the monodromy,

$$R_{\square\Xi}(u-v) = f_{\Xi}(u-v) \left(1 + (u-v)^{-1} \sum_{a,b=1}^n e_{ab} J_{ba} \right) = \begin{array}{c} \square, u \text{ --- } | \text{ --- } \leftarrow \\ \Xi, v \end{array}, \quad (3.21)$$

where the generators J_{ab} of the representation Ξ satisfy the $\mathfrak{gl}(n)$ algebra

$$[J_{ab}, J_{cd}] = \delta_{cb} J_{ad} - \delta_{ad} J_{cb}. \quad (3.22)$$

The $n \times n$ matrices e_{ab} are generators of the fundamental representation \square of $\mathfrak{gl}(n)$. Their components are $\langle c | e_{ab} | d \rangle = \delta_{ac} \delta_{bd}$, where $|a\rangle$ with $a = 1, \dots, n$ are the standard basis vectors of $V_{\square} = \mathbb{C}^n$. Hence, $e_{ab} e_{cd} = \delta_{bc} e_{ad}$. Moreover, $f_{\Xi}(u-v)$ is a scalar normalization factor and 1 stands for the appropriate identity operator. Here it is that in $\mathbb{C}^n \otimes V_{\Xi}$. The monodromy (3.11) built out of these Lax operators satisfies the RTT-relation¹

$$R_{\square\square'}(u-u') M(u) M'(u') = M'(u') M(u) R_{\square\square'}(u-u'). \quad (3.23)$$

This is proven with the so-called ‘‘train argument’’, see e.g. [17], making use of the Yang-Baxter equations for the individual Lax operators. The RTT-relation is an equation in the tensor product of two fundamental auxiliary spaces $V_{\square} = \mathbb{C}^n$ and $V_{\square'} = \mathbb{C}^n$, and the total quantum space of the spin chain $V_1 \otimes \dots \otimes V_L$. The monodromies $M(u)$ and $M'(u')$ act respectively on the auxiliary spaces V_{\square} and $V_{\square'}$, and on the same total quantum space. The remaining R-matrix in (3.23) is

$$R_{\square\square'}(u-u') = 1 + (u-u')^{-1} \sum_{a,b=1}^n e_{ab} e'_{ba}, \quad (3.24)$$

where the sum in the last term is the permutation operator on $\mathbb{C}^n \otimes \mathbb{C}^n$. Written in terms of the monodromy elements (3.12), the RTT-relation (3.23) becomes

$$(u'-u)[M_{ab}(u), M_{cd}(u')] = M_{cb}(u) M_{ad}(u') - M_{cb}(u') M_{ad}(u). \quad (3.25)$$

Importantly, the RTT-relation (3.23) is the defining relation of the *Yangian algebra* $\mathcal{Y}(\mathfrak{gl}(n))$ in the QISM language, see e.g. [18]. A formal Laurent expansion of the monodromy elements (3.12) in inverse powers of the spectral parameter u ,

$$M_{ab}(u) = M_{ab}^{(0)} + M_{ab}^{(1)} u^{-1} + M_{ab}^{(2)} u^{-2} + \dots, \quad (3.26)$$

yields the generators $M_{ab}^{(r)}$ of the Yangian, where one demands

$$M_{ab}^{(0)} = \delta_{ab}. \quad (3.27)$$

¹The name stems from the frequent use of the symbol ‘‘ $T(u)$ ’’ for the monodromy $M(u)$ in the literature.

section 3.2. Hence $|\Psi\rangle$ is symbolized in (3.31) by a dotted “black box” without specifying the interior. In section 4.2.2 we will indeed find solutions of the Yangian invariance condition (3.30) that go beyond the Baxter lattices of section 3.2. The graphical representation of these solutions not only contains lines and four-valent vertices, i.e R-matrices, but also trivalent-vertices, which are associated with solutions of bootstrap equations, see [21] and e.g. [22], [23].

We end this section with a remark on a reformulation of Yangian invariance. The condition in the form (3.30) can naturally be understood as an intertwining relation of the tensor product of the first K with the remaining $L - K$ spaces of the total quantum space. For this purpose we split the monodromy (3.11) as

$$M(u) = R_{\square \Xi_1}(u - v_1) \cdots R_{\square \Xi_K}(u - v_K) \cdot R_{\square \Xi_{K+1}}(u - v_{K+1}) \cdots R_{\square \Xi_L}(u - v_L). \quad (3.33)$$

Conjugating (3.30) in the first K spaces and using (3.8) and (3.13) for these spaces yields the intertwining relation

$$R_{\square \Xi_{K+1}}(u - v_{K+1}) \cdots R_{\square \Xi_L}(u - v_L) \mathcal{O}_\Psi = \mathcal{O}_\Psi R_{\square \Xi_K}(u - v_K + \kappa_{\Xi_K}) \cdots R_{\square \Xi_1}(u - v_1 + \kappa_{\Xi_1}), \quad (3.34)$$

where $\mathcal{O}_\Psi := |\Psi\rangle^{\dagger 1 \cdots \dagger K}$. This is depicted graphically as

In case \mathcal{O}_Ψ corresponds to the partition function \mathcal{Z} of a vertex model, this equation is nothing but a consequence of Z-invariance, c.f. [13] and also section 2.1: The (dashed) fundamental auxiliary line is moved through the entire Baxter lattice. An equation of the type (3.34) also appeared recently in [9] in the context of a spectral parameter deformation of planar $\mathcal{N} = 4$ super Yang-Mills scattering amplitudes. There it was referred to as “generalized Yang-Baxter equation”. In the scattering problem, Yangian invariance of undeformed tree-level amplitudes is usually formulated in the sense of (3.32), see [1] and e.g. [4]. Bearing in mind our ambitions to construct Yangian invariants using a Bethe ansatz in section 6, we focus in this paper on (3.30) instead of (3.32) or (3.34).

4 Yangian invariants in oscillator formalism

In section 3.3 we characterized Yangian invariants by the (system of) eigenvalue equations (3.30) for matrix elements of a monodromy and equivalently by the associated intertwining relation (3.34). Here we will begin our study of (3.30) by working out explicit solutions $|\Psi\rangle$ in a number of concrete examples. We restrict our analysis to monodromies $M(u)$, where the total quantum space is built by tensoring finite-dimensional totally symmetric

representations \mathfrak{s} and their conjugates $\bar{\mathfrak{s}}$, i.e. $\Xi_i = \mathfrak{s}_i$ or $\Xi_i = \bar{\mathfrak{s}}_i$ for all $i = 1, \dots, L$ in (3.11). We need these conjugate representations to make sure that the total quantum space contains a $\mathfrak{gl}(n)$ singlet, which is a necessary criterion for Yangian invariants, see (3.32) for the case $r = 1$.

The representations \mathfrak{s} and $\bar{\mathfrak{s}}$ are realized in terms of oscillator algebras, see section 4.1. Since the non-zero eigenvalues appearing in (3.30) are identical to 1, the normalization of the Lax operators used in the construction is clearly important and will be discussed in some detail. After that we are in place to construct the sought solutions in section 4.2. Our first and simplest examples are the two-site monodromies of section 4.2.1, where the representations of the two sites are necessarily conjugate to each other. The inhomogeneities are then fixed by demanding Yangian invariance, i.e. (3.30). This solution $|\Psi\rangle$ is graphically represented by a Baxter lattice consisting of a single line. In section 4.2.2 we construct three-site invariants. The corresponding intertwiner \mathcal{O}_Ψ satisfying (3.34) is to be interpreted as a solution of a bootstrap equation in analogy with [21]. Although these invariants leave the framework of section 3.2, they are naturally included in our definition of Yangian invariants. Finally, in section 4.2.3 we study the Yangian invariant related to the first non-trivial Baxter lattice consisting of two intersecting lines. The associated intertwiner \mathcal{O}_Ψ contains a free parameter z and actually turns out to be the $\mathfrak{gl}(n)$ symmetric R-matrix $R_{\mathfrak{s}, \mathfrak{s}'}(z)$ for arbitrary totally symmetric representations $\mathfrak{s}, \mathfrak{s}'$. We obtain a compact expression for this R-matrix in a certain oscillator basis. The spectral parameter z of the R-matrix should not be confused with that of the auxiliary space in section 3 denoted by u .

4.1 Oscillators, Lax operators and monodromies

We start by specifying the two types of oscillator representations \mathfrak{s} and $\bar{\mathfrak{s}}$ of the $\mathfrak{gl}(n)$ algebra (3.22), which will be used for the local quantum spaces of the monodromy (3.11). These representations are labeled by their highest weight. Consider the totally symmetric representation of $\mathfrak{gl}(n)$ with highest weight $\mathfrak{s} = (s, 0, \dots, 0)$, where s is a non-negative integer. We build these representations from a single family of oscillators \mathfrak{a}_a with $a = 1, \dots, n$. Furthermore, consider the $\mathfrak{gl}(n)$ representation with highest weight $\bar{\mathfrak{s}} = (0, \dots, 0, -s)$, and construct it using a second family of n oscillators \mathfrak{b}_a . The n^2 generators J_{ab} of the representation \mathfrak{s} and the second set of n^2 generators \bar{J}_{ab} of $\bar{\mathfrak{s}}$ are given by

$$\begin{aligned} J_{ab} &= +\bar{\mathfrak{a}}_a \mathfrak{a}_b & \text{with} & & [\mathfrak{a}_a, \bar{\mathfrak{a}}_b] &= \delta_{ab}, & \mathfrak{a}_a |0\rangle &= 0, & \bar{\mathfrak{a}}_a &= \mathfrak{a}_a^\dagger, \\ \bar{J}_{ab} &= -\bar{\mathfrak{b}}_b \mathfrak{b}_a & \text{with} & & [\mathfrak{b}_a, \bar{\mathfrak{b}}_b] &= \delta_{ab}, & \mathfrak{b}_a |0\rangle &= 0, & \bar{\mathfrak{b}}_a &= \mathfrak{b}_a^\dagger. \end{aligned} \quad (4.1)$$

Commutators of oscillators that are not specified by these relations vanish. See e.g. [24] for a review of such Jordan-Schwinger-type realizations of the $\mathfrak{gl}(n)$ algebra. The generators (4.1) act on the representation spaces $V_{\mathfrak{s}}$ and $V_{\bar{\mathfrak{s}}}$. These spaces consist of homogeneous polynomials of degree s in, respectively, the creation operators $\bar{\mathfrak{a}}_a$ and $\bar{\mathfrak{b}}_a$ acting on the Fock vacuum $|0\rangle$. Therefore the number operators $\sum_{a=1}^n \bar{\mathfrak{a}}_a \mathfrak{a}_a$ and $\sum_{a=1}^n \bar{\mathfrak{b}}_a \mathfrak{b}_a$ both take the value s . The highest weight states in $V_{\mathfrak{s}}$ and $V_{\bar{\mathfrak{s}}}$ are, respectively,

$$\begin{aligned} |\sigma\rangle &= (\bar{\mathfrak{a}}_1)^s |0\rangle & \text{with} & & J_{aa} |\sigma\rangle &= s \delta_{1a} |\sigma\rangle, & J_{ab} |\sigma\rangle &= 0 & \text{for } a < b, \\ |\bar{\sigma}\rangle &= (\bar{\mathfrak{b}}_n)^s |0\rangle & \text{with} & & \bar{J}_{aa} |\bar{\sigma}\rangle &= -s \delta_{na} |\bar{\sigma}\rangle, & \bar{J}_{ab} |\bar{\sigma}\rangle &= 0 & \text{for } a < b. \end{aligned} \quad (4.2)$$

The representation $\bar{\mathfrak{s}}$ is conjugate to \mathfrak{s} in the sense of (3.14),

$$\bar{J}_{ab} |_{\mathfrak{b}_a \mapsto \mathfrak{a}_a} = -J_{ab}^\dagger. \quad (4.3)$$

The Lax operators (3.21) for the two representations defined in (4.1) read

$$R_{\square_{\mathbf{s}}}(u-v) = f_{\mathbf{s}}(u-v) \left(1 + (u-v)^{-1} \sum_{a,b=1}^n e_{ab} \bar{\mathbf{a}}_b \mathbf{a}_a \right) = \square, u \begin{array}{c} \downarrow \\ \text{---} \text{---} \text{---} \\ \uparrow \\ \mathbf{s}, v \end{array}, \quad (4.4)$$

$$R_{\square_{\bar{\mathbf{s}}}}(u-v) = f_{\bar{\mathbf{s}}}(u-v) \left(1 - (u-v)^{-1} \sum_{a,b=1}^n e_{ab} \bar{\mathbf{b}}_a \mathbf{b}_b \right) = \square, u \begin{array}{c} \downarrow \\ \text{---} \text{---} \text{---} \\ \uparrow \\ \bar{\mathbf{s}}, v \end{array}. \quad (4.5)$$

As discussed in section 3.2, we require these Lax operators to possess the properties of unitarity (3.8) and crossing (3.13), which will impose constraints on the normalizations $f_{\mathbf{s}}(u)$ and $f_{\bar{\mathbf{s}}}(u)$. The first property (3.8) yields

$$R_{\square_{\mathbf{s}}}(u-v) R_{\square_{\mathbf{s}}}(v-u) = 1, \quad R_{\square_{\bar{\mathbf{s}}}}(u-v) R_{\square_{\bar{\mathbf{s}}}}(v-u) = 1. \quad (4.6)$$

These equations contain the two additional Lax operators

$$R_{\square_{\mathbf{s}}}(v-u) = \begin{array}{c} \mathbf{s}, v \\ \text{---} \text{---} \text{---} \\ \downarrow \\ \square, u \end{array}, \quad R_{\square_{\bar{\mathbf{s}}}}(v-u) = \begin{array}{c} \bar{\mathbf{s}}, v \\ \text{---} \text{---} \text{---} \\ \downarrow \\ \square, u \end{array} \quad (4.7)$$

with exchanged order of auxiliary and quantum space. These are obtained as solutions of the Yang-Baxter equation in $V_{\square} \otimes V_{\mathbf{s}} \otimes V_{\square}$ and $V_{\square} \otimes V_{\bar{\mathbf{s}}} \otimes V_{\square}$, respectively, where they are the only unknowns, cf. (3.4). The Lax operators (4.7) are symmetric in the sense that, up to a shift of the spectral parameter, they can be expressed in terms of (4.4) and (4.5),

$$R_{\square_{\mathbf{s}}}(v-u) = R_{\square_{\mathbf{s}}}(v-u-s+1), \quad R_{\square_{\bar{\mathbf{s}}}}(v-u) = R_{\square_{\bar{\mathbf{s}}}}(v-u+n+s-1). \quad (4.8)$$

Then the unitarity conditions in (4.6) turn into constraints on the normalization of the Lax operators,

$$f_{\mathbf{s}}(u) f_{\mathbf{s}}(-u-s+1) = \frac{u(u+s-1)}{u(u+s-1)-s}, \quad f_{\bar{\mathbf{s}}}(u) f_{\bar{\mathbf{s}}}(-u+s-1+n) = 1. \quad (4.9)$$

The other condition, the crossing relation (3.13), reads for the representations \mathbf{s} and $\bar{\mathbf{s}}$, respectively,

$$R_{\square_{\bar{\mathbf{s}}}}(u+\kappa_{\bar{\mathbf{s}}})|_{\mathbf{b}_a \mapsto \mathbf{a}_a} = R_{\square_{\mathbf{s}}}(-u)^\dagger, \quad R_{\square_{\mathbf{s}}}(u+\kappa_{\mathbf{s}}) = R_{\square_{\bar{\mathbf{s}}}}(-u)^\dagger|_{\mathbf{b}_a \mapsto \mathbf{a}_a}, \quad (4.10)$$

where $\kappa_{\mathbf{s}}$ and $\kappa_{\bar{\mathbf{s}}}$ are the crossing parameters. These conditions imply

$$\kappa_{\mathbf{s}} = s-1, \quad \kappa_{\bar{\mathbf{s}}} = -s+1-n, \quad f_{\bar{\mathbf{s}}}(u) = f_{\mathbf{s}}(-u). \quad (4.11)$$

Notice that the two equations in (4.10) lead to only one constraint on the normalizations. Relations (4.9) and (4.11) are solved by the well-known normalization

$$f_{\mathbf{s}}(u) = \frac{\Gamma(\frac{1-u}{n}) \Gamma(\frac{n+u}{n})}{\Gamma(\frac{1-s-u}{n}) \Gamma(\frac{n+s+u}{n})}. \quad (4.12)$$

For $s = 1$ this solution was obtained in [25]. The solution for higher integer values of s can be constructed using the additional recursion relation

$$f_{\mathbf{s}}(u)f_{\mathbf{s}'}(u+s) = f_{\mathbf{s}+\mathbf{s}'}(u), \quad (4.13)$$

where $\mathbf{s} + \mathbf{s}' = (s + s', 0, \dots, 0)$ denotes the addition of weights. Note that the solution (4.12) is not unique.

Now, we concentrate on monodromies $M(u)$ of the form (3.11), which are built entirely out of the two types of Lax operators (4.4) and (4.5) with the proper normalization (4.12). Consequently, at the i -th site of the monodromy the representation of the local quantum space is $\Xi_i = \mathbf{s}_i$ or $\Xi_i = \bar{\mathbf{s}}_i$ and the oscillator families building these representations are labeled \mathbf{a}_a^i or \mathbf{b}_a^i , respectively. Further restricting to monodromies that allow for solutions $|\Psi\rangle$ of the Yangian invariance condition (3.30), one finds severe constraints on the representation labels s_i and inhomogeneities v_i .

One large class of such monodromies is obtained by considering Baxter lattices in the sense of section 3.2, where each line carries either a symmetric representation or a conjugate one. If the k -th line of the Baxter lattice with endpoints $i_k < j_k$ and spectral parameter θ_k carries a symmetric representation labeled by $\Lambda_k = \mathbf{s}_{i_k}$, then according to (3.18) and using (4.11) the monodromy $M(u)$ contains two sites

$$\begin{aligned} \Xi_{i_k} = \mathbf{s}_{i_k}, \quad v_{i_k} = \theta_k \quad \text{and} \quad \Xi_{j_k} = \bar{\mathbf{s}}_{j_k}, \quad v_{j_k} = \theta_k - s_{i_k} + 1 \\ \text{with} \quad s_{i_k} = s_{j_k}. \end{aligned} \quad (4.14)$$

As a consequence, in $M(u)$ the Lax operator $R_{\square_{\mathbf{s}_{i_k}}}(u - v_{i_k})$ with the symmetric representation is placed left of $R_{\square_{\bar{\mathbf{s}}_{j_k}}}(u - v_{j_k})$ with the conjugate representation. If instead the k -th line carries the conjugate representation $\Lambda_k = \bar{\mathbf{s}}_{i_k}$, we obtain from (3.18) with (4.11)

$$\begin{aligned} \Xi_{i_k} = \bar{\mathbf{s}}_{i_k}, \quad v_{i_k} = \theta_k \quad \text{and} \quad \Xi_{j_k} = \mathbf{s}_{j_k}, \quad v_{j_k} = \theta_k + s_{i_k} - 1 + n \\ \text{with} \quad s_{i_k} = s_{j_k}. \end{aligned} \quad (4.15)$$

In this case the Lax operator with the conjugate representation is to the left of the one with the symmetric representation. In the following, we will also study solutions $|\Psi\rangle$ of (3.30) where the representation labels and inhomogeneities do not obey (4.14) or (4.15). These do not correspond to a Baxter lattice in the sense of section 3.2.

Let us comment on the normalization of the monodromies considered in the remainder of section 4. The constraints on their representation labels and inhomogeneities guarantee that the gamma functions in the normalizations of the different Lax operators cancel and only a rational function in u remains.

4.2 Sample invariants

After these preparations, we are in a position to actually solve (3.30) in a number of simple examples. From now on, we label the monodromies $M_{L,K}(u)$ and the Yangian invariants $|\Psi_{L,K}\rangle$ by the total number of sites L and the number K of sites carrying a conjugate representation of type $\bar{\mathbf{s}}$. This is motivated by section 5, where the invariant $|\Psi_{L,K}\rangle$ is compared with the L -particle N^{K-2} MHV tree-level scattering amplitude of planar $\mathcal{N} = 4$ super Yang-Mills theory. In addition, we focus on monodromies $M_{L,K}(u)$ whose sites with conjugate representations of type $\bar{\mathbf{s}}$ are all to the left of the sites with \mathbf{s} . This order corresponds to the gauge fixing used in the Grassmannian integral formulation in section 5.

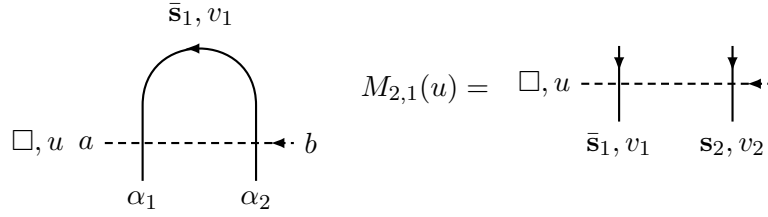


Figure 4.1: A Baxter lattice with one line specified by $\mathbf{G} = ((1, 2))$, $\mathbf{\Lambda} = (\bar{s}_1)$, $\boldsymbol{\theta} = (v_1)$, $\boldsymbol{\alpha} = (\alpha_1, \alpha_2)$, cf. (3.1), and intersected by a dashed auxiliary space, left part. This arrangement of Boltzmann weights corresponds to the l.h.s. of the invariance condition (3.30) for $|\Psi_{2,1}\rangle$, i.e. to $M_{2,1}(u)|\Psi_{2,1}\rangle$. The elements of the monodromy $M_{2,1}(u)$ in the right part of the figure are obtained from the Boltzmann weights on the left side using the crossing relation (3.15). The representation labels and inhomogeneities of this monodromy obey (4.17).

4.2.1 Line and identity operator

The simplest Yangian invariant $|\Psi_{2,1}\rangle$ solving (3.30) corresponds to a Baxter lattice consisting of a single line. In order to obtain the associated monodromy $M_{2,1}(u)$ where the site with the conjugate representation is situated to the left of the symmetric one, we choose the line in the Baxter lattice to carry a conjugate representation, cf. (4.15) and see figure 4.1.

This leads to the length-two monodromy

$$M_{2,1}(u) = R_{\square \bar{s}_1}(u - v_1) R_{\square s_2}(u - v_2) \quad (4.16)$$

with the following constraints on the representation labels and inhomogeneities:

$$v_1 = v_2 - n - s_2 + 1, \quad s_1 = s_2. \quad (4.17)$$

Recalling the Baxter lattice associated to this particular monodromy, we happily notice that (4.17) agrees with (4.15). The overall normalization of the monodromy (4.16) originating from those of the Lax operators (4.4) and (4.5) trivializes,

$$f_{\bar{s}_1}(u - v_1) f_{s_2}(u - v_2) = 1, \quad (4.18)$$

where we used (4.17) and subsequently the unitarity condition for $f_{\bar{s}}(u)$ in (4.9) and the relation between the two normalizations $f_s(u)$ and $f_{\bar{s}}(u)$ in (4.11). We can now easily solve (3.30) to obtain the explicit form of the invariant,

$$|\Psi_{2,1}\rangle = (\bar{\mathbf{b}}^1 \cdot \bar{\mathbf{a}}^2)^{s_2} |0\rangle \quad \text{with} \quad \bar{\mathbf{b}}^i \cdot \bar{\mathbf{a}}^j := \sum_{a=1}^n \bar{\mathbf{b}}_a^i \bar{\mathbf{a}}_a^j, \quad (4.19)$$

where we recall that the upper indices on the oscillators refer to the sites of the monodromy. This solution is unique up to a scalar factor, which clearly drops out of (3.30). To obtain the intertwiner associated to the invariant $|\Psi_{2,1}\rangle$ we employ (3.34) with $K = 1$ and use the value of the crossing parameter $\kappa_{\bar{s}_1}$ given in (4.11). This leads to

$$R_{\square s_2}(u - v_2) \mathcal{O}_{\Psi_{2,1}} = \mathcal{O}_{\Psi_{2,1}} R_{\square s_1}(u - v_2) \quad (4.20)$$

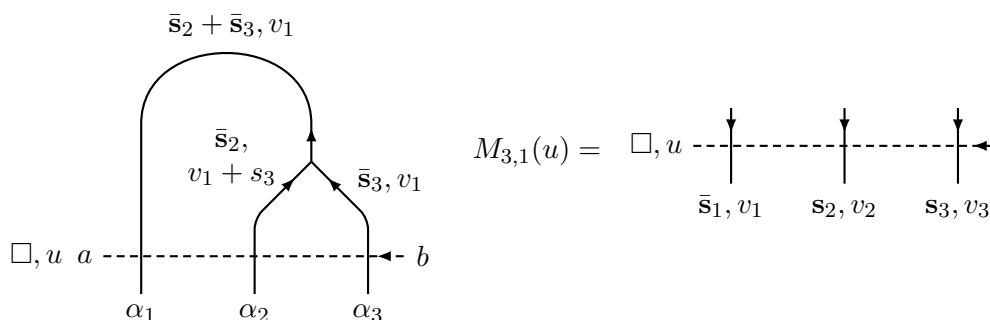


Figure 4.2: The left part corresponds to the l.h.s. of (3.30) for $|\Psi_{3,1}\rangle$, i.e. $M_{3,1}(u)|\Psi_{3,1}\rangle$. It contains a (solid) trivalent vertex, which is an extension of the usual Baxter lattice, and a dashed auxiliary line. Using the crossing relation (3.15) and the crossing parameters in (4.11), the Boltzmann weights involving the auxiliary line can be reformulated as elements of the monodromy $M_{3,1}(u)$, as is shown on the right side. The necessary constraints on the representation labels and inhomogeneities of the monodromy may be found in (4.23).

with

$$\mathcal{O}_{\Psi_{2,1}} := |\Psi_{2,1}\rangle^{\dagger 1} = \sum_{a_1, \dots, a_{s_2}=1}^n \bar{\mathbf{a}}_{a_1}^2 \cdots \bar{\mathbf{a}}_{a_{s_2}}^2 |0\rangle \langle 0| \mathbf{b}_{a_1}^1 \cdots \mathbf{b}_{a_{s_2}}^1. \quad (4.21)$$

After identifying the representation spaces V_{s_1} and V_{s_2} , which is possible because of $s_1 = s_2$ in (4.17), we see that $\mathcal{O}_{\Psi_{2,1}}$ reduces to $s_2!$ times the identity operator.

4.2.2 Three-vertices and bootstrap equations

The next simplest Yangian invariants are characterized by monodromies with three sites and are of the type $|\Psi_{3,1}\rangle$ or $|\Psi_{3,2}\rangle$. We restrict once more to the case where the sites with conjugate representations are to the left of those with symmetric ones. These three-site invariants clearly leave the framework of section 3.2. We represent them graphically by an extension of the Baxter lattice, which in this case consists of a trivalent vertex. See figures 4.2 and 4.3 for the invariants $|\Psi_{3,1}\rangle$ and $|\Psi_{3,2}\rangle$, respectively.

We start with a monodromy containing one conjugate site,

$$M_{3,1}(u) = R_{\square \bar{s}_1}(u - v_1) R_{\square s_2}(u - v_2) R_{\square s_3}(u - v_3), \quad (4.22)$$

see also the right part of figure 4.2. Now the Yangian invariance condition (3.30) can be easily solved if the parameters obey

$$v_2 = v_1 + n + s_2 + s_3 - 1, \quad v_3 = v_1 + n + s_3 - 1, \quad s_1 = s_2 + s_3. \quad (4.23)$$

In this case the normalizations of the Lax operators of type (4.4) and (4.5) appearing in (4.22) trivializes using the relation (4.13) for $f_s(u)$, the unitarity condition for $f_{\bar{s}}(u)$ and finally expressing $f_{\bar{s}}(u)$ in terms of $f_s(u)$ with the help of (4.11):

$$f_{\bar{s}_1}(u - v_1) f_{s_2}(u - v_2) f_{s_3}(u - v_3) = 1. \quad (4.24)$$

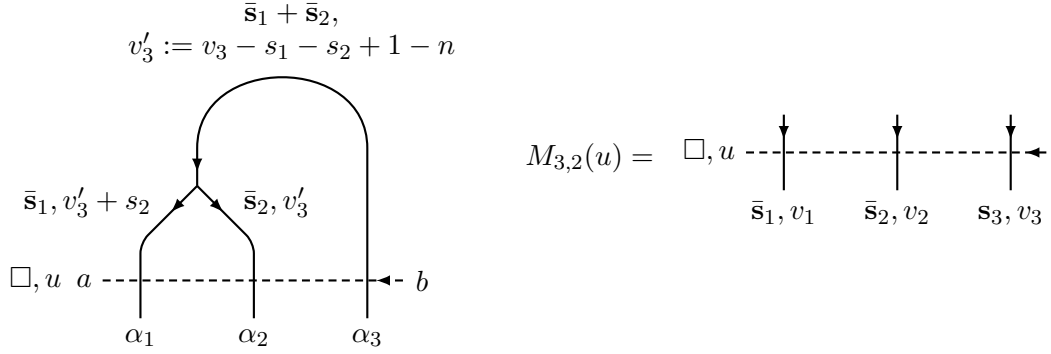


Figure 4.3: The l.h.s. $M_{3,2}(u)|\Psi_{3,2}\rangle$ of (3.30) for $|\Psi_{3,2}\rangle$ corresponds to the lattice in the left part. It consists of an extended Baxter lattice in form of a trivalent vertex and a dashed auxiliary space. The Boltzmann weights containing the auxiliary space can be formulated as elements of a monodromy $M_{3,2}(u)$ using the crossing relation (3.15) with (4.11). This monodromy is shown in the right part and the parameters of the monodromy obey the constraints (4.29).

Then one immediately checks that the solution of (3.30) is given by

$$|\Psi_{3,1}\rangle = (\bar{\mathbf{b}}^1 \cdot \bar{\mathbf{a}}^2)^{s_2} (\bar{\mathbf{b}}^1 \cdot \bar{\mathbf{a}}^3)^{s_3} |0\rangle, \quad (4.25)$$

where we fixed a possible scalar prefactor. We once again proceed to the corresponding intertwining relation. From its general form in (3.34) we obtain for $K = 1$ and $\kappa_{\bar{\mathbf{s}}_1}$ given by (4.11) the relation

$$R_{\square_{s_2}}(u - v_2) R_{\square_{s_3}}(u - v_2 + s_2) \mathcal{O}_{\Psi_{3,1}} = \mathcal{O}_{\Psi_{3,1}} R_{\square_{s_1}}(u - v_2) \quad (4.26)$$

with

$$\mathcal{O}_{\Psi_{3,1}} := |\Psi_{3,1}\rangle^{\dagger 1} = \sum_{\substack{a_1, \dots, a_{s_2} \\ b_1, \dots, b_{s_3}}} \bar{\mathbf{a}}_{a_1}^2 \cdots \bar{\mathbf{a}}_{a_{s_2}}^2 \bar{\mathbf{a}}_{b_1}^3 \cdots \bar{\mathbf{a}}_{b_{s_3}}^3 |0\rangle \langle 0| \mathbf{b}_{a_1}^1 \cdots \mathbf{b}_{a_{s_2}}^1 \mathbf{b}_{b_1}^1 \cdots \mathbf{b}_{b_{s_3}}^1. \quad (4.27)$$

The intertwining relation (4.26) is known as bootstrap equation.

We move on to a monodromy with two conjugate sites on the left,

$$M_{3,2}(u) = R_{\square_{\bar{s}_1}}(u - v_1) R_{\square_{\bar{s}_2}}(u - v_2) R_{\square_{s_3}}(u - v_3), \quad (4.28)$$

see also the right part of figure 4.3. Looking for solutions $|\Psi_{3,2}\rangle$ of (3.30) with this monodromy again leads to constraints on the representation labels and inhomogeneities,

$$v_1 = v_3 - n - s_1 + 1, \quad v_2 = v_3 - n - s_3 + 1, \quad s_3 = s_1 + s_2. \quad (4.29)$$

Analogously to the discussion of the other three-site invariant, the normalization of the monodromy (4.28) trivializes using (4.29):

$$f_{\bar{s}_1}(u - v_1) f_{\bar{s}_2}(u - v_2) f_{s_3}(u - v_3) = 1. \quad (4.30)$$

The explicit expression for the solution of (3.30) turns out to be

$$|\Psi_{3,2}\rangle = (\bar{\mathbf{b}}^1 \cdot \bar{\mathbf{a}}^3)^{s_1} (\bar{\mathbf{b}}^2 \cdot \bar{\mathbf{a}}^3)^{s_2} |0\rangle. \quad (4.31)$$

Again we fixed a scalar prefactor. We employ the intertwining relation (3.34) in this case with $K = 2$ and $\kappa_{\bar{\mathbf{s}}_1}, \kappa_{\bar{\mathbf{s}}_2}$ specified in (4.11) to derive the bootstrap equation

$$R_{\square_{\mathbf{s}_3}}(u - v_3) \mathcal{O}_{\Psi_{3,2}} = \mathcal{O}_{\Psi_{3,2}} R_{\square_{\mathbf{s}_2}}(u - v_3 + s_1) R_{\square_{\mathbf{s}_1}}(u - v_3) \quad (4.32)$$

with the solution

$$\mathcal{O}_{\Psi_{3,2}} := |\Psi_{3,2}\rangle^{\dagger_1 \dagger_2} = \sum_{\substack{a_1, \dots, a_{s_1} \\ b_1, \dots, b_{s_2}}} \bar{\mathbf{a}}_{a_1}^3 \cdots \bar{\mathbf{a}}_{a_{s_1}}^3 \bar{\mathbf{a}}_{b_1}^3 \cdots \bar{\mathbf{a}}_{b_{s_2}}^3 |0\rangle \langle 0| \mathbf{b}_{a_1}^1 \cdots \mathbf{b}_{a_{s_1}}^1 \mathbf{b}_{b_1}^2 \cdots \mathbf{b}_{b_{s_2}}^2. \quad (4.33)$$

4.2.3 Four-vertex and Yang-Baxter equation

Let us proceed to Yangian invariants associated to four-site monodromies. As an important check of our formalism we will rederive the well-known $\mathfrak{gl}(n)$ invariant R-matrix [26]. We therefore leave aside the rather trivial cases where the Baxter lattice consists of two non-intersecting lines, and focus on the invariants of type $|\Psi_{4,2}\rangle$, where the Baxter lattice is a four-vertex. Once again, we may a priori vary the positions of the conjugate sites within the monodromy. We picked a particular assignment, where all sites with conjugate representations are left of those with symmetric representations, see figure 4.4.

We use the four-site monodromy

$$M_{4,2}(u) = R_{\square_{\bar{\mathbf{s}}_1}}(u - v_1) R_{\square_{\bar{\mathbf{s}}_2}}(u - v_2) R_{\square_{\mathbf{s}_3}}(u - v_3) R_{\square_{\mathbf{s}_4}}(u - v_4) \quad (4.34)$$

with

$$v_1 = v_3 - n - s_1 + 1, \quad v_2 = v_4 - n - s_2 + 1, \quad s_1 = s_3, \quad s_2 = s_4. \quad (4.35)$$

This identification of the inhomogeneities and representation labels corresponds to a Baxter lattice with two lines of type (4.15). In order to simplify the normalizations of the Lax operators in (4.34), we note that the relations in (4.35) are two sets of conditions of the form appearing for the two site-invariant in (4.17). Hence the normalization factors are simplified analogously to the discussion in section 6.3.1, which leads to

$$f_{\bar{\mathbf{s}}_1}(u - v_1) f_{\bar{\mathbf{s}}_2}(u - v_2) f_{\mathbf{s}_3}(u - v_3) f_{\mathbf{s}_4}(u - v_4) = 1. \quad (4.36)$$

For the solution of the eigenvalue equation (3.30) with this monodromy we make the $\mathfrak{gl}(n)$ invariant ansatz

$$|\Psi_{4,2}(v_3 - v_4)\rangle := |\Psi_{4,2}\rangle = \sum_{k=0}^{\min(s_3, s_4)} d_k(v_3 - v_4) |\Upsilon_k\rangle \quad (4.37)$$

with

$$|\Upsilon_k\rangle = (\bar{\mathbf{b}}^1 \cdot \bar{\mathbf{a}}^3)^{s_3 - k} (\bar{\mathbf{b}}^2 \cdot \bar{\mathbf{a}}^4)^{s_4 - k} (\bar{\mathbf{b}}^2 \cdot \bar{\mathbf{a}}^3)^k (\bar{\mathbf{b}}^1 \cdot \bar{\mathbf{a}}^4)^k |0\rangle. \quad (4.38)$$

In our formalism, the spectral parameter dependence of this four-site invariant emerges in a natural fashion as the difference of two inhomogeneities which from now on is denoted by

$$z := v_3 - v_4. \quad (4.39)$$

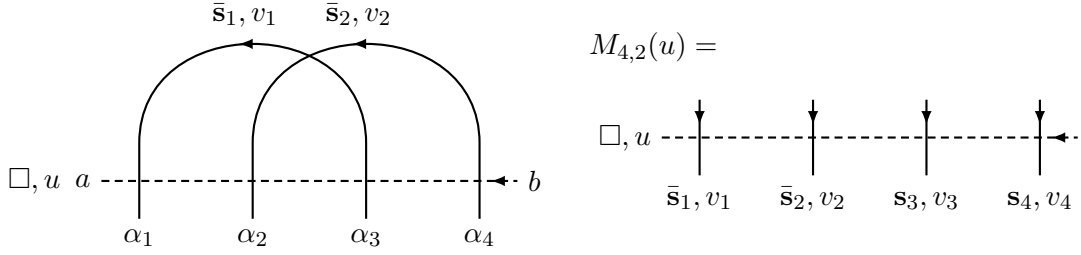


Figure 4.4: The left part shows a Baxter lattice with two lines specified by $\mathbf{G} = ((1, 3), (2, 4))$, $\mathbf{\Lambda} = (\bar{s}_1, \bar{s}_2)$, $\boldsymbol{\theta} = (v_1, v_2)$, $\boldsymbol{\alpha} = (\alpha_1, \alpha_2, \alpha_3, \alpha_4)$ and a dashed auxiliary space. It corresponds to $M_{4,2}(u)|\Psi_{4,2}\rangle$ as the l.h.s. of (3.30). The right part contains the monodromy $M_{4,2}(u)$, which is associated to this Baxter lattice. The necessary identifications of the representation labels and the inhomogeneities are written in (4.35).

We have made this manifest by using the notation $|\Psi_{4,2}(z)\rangle$. Substituting (4.37) into (3.30) yields a recursion relation for the coefficients d_k ,

$$\frac{d_k(z)}{d_{k+1}(z)} = \frac{(k+1)(z-s_3+k+1)}{(s_3-k)(s_4-k)}. \quad (4.40)$$

It is solved, up to a function periodic in the index k with period 1, by

$$d_k(z) = \frac{1}{(s_3-k)!(s_4-k)!k!^2} \frac{k!}{\Gamma(z-s_3+k+1)}. \quad (4.41)$$

Following the same logic as before we obtain the equation, which determines the intertwiner corresponding to $|\Psi_{4,2}(z)\rangle$, from (3.34) with $K=2$ and $\kappa_{\bar{s}_1}, \kappa_{\bar{s}_2}$ found in (4.11). This yields the Yang-Baxter equation in the form

$$R_{\square s_3}(u-v_3)R_{\square s_4}(u-v_4)\mathcal{O}_{\Psi_{4,2}(z)} = \mathcal{O}_{\Psi_{4,2}(z)}R_{\square s_2}(u-v_4)R_{\square s_1}(u-v_3), \quad (4.42)$$

where

$$\mathcal{O}_{\Psi_{4,2}(z)} := |\Psi_{4,2}(z)\rangle^{\dagger 1 \dagger 2} = \sum_{k=0}^{\min(s_3, s_4)} d_k(z) \mathcal{O}_{\Upsilon_k}, \quad (4.43)$$

with

$$\begin{aligned} \mathcal{O}_{\Upsilon_k} := |\Upsilon_k\rangle^{\dagger 1 \dagger 2} = & \sum_{\substack{a_1, \dots, a_{s_3} \\ b_1, \dots, b_{s_4}}} \bar{a}_{a_1}^3 \cdots \bar{a}_{a_{s_3}}^3 \bar{a}_{b_1}^4 \cdots \bar{a}_{b_{s_4}}^4 |0\rangle \\ & \cdot \langle 0 | \mathbf{b}_{a_1}^1 \cdots \mathbf{b}_{a_{s_3-k}}^1 \mathbf{b}_{b_{s_4-k+1}}^1 \cdots \mathbf{b}_{b_{s_4}}^1 \\ & \cdot \mathbf{b}_{b_1}^2 \cdots \mathbf{b}_{b_{s_4-k}}^2 \mathbf{b}_{a_{s_3-k+1}}^2 \cdots \mathbf{b}_{a_{s_3}}^2. \end{aligned} \quad (4.44)$$

In order to rewrite this form of the Yang-Baxter equation in a more standard way, we identify space V_{s_1} with V_{s_3} and V_{s_2} with V_{s_4} , and simultaneously $\mathcal{O}_{\Psi_{4,2}(z)}$ with $R_{s_3 s_4}(z)$. This then yields

$$R_{\square s_3}(u-v_3)R_{\square s_4}(u-v_4)R_{s_3 s_4}(z) = R_{s_3 s_4}(z)R_{\square s_4}(u-v_4)R_{\square s_3}(u-v_3). \quad (4.45)$$

Indeed, (4.45) establishes that $R_{s_3 s_4}(z)$ must be the $\mathfrak{gl}(n)$ invariant R-matrix [26] for symmetric representations.

In our approach $R_{\mathbf{s}_3 \mathbf{s}_4}(z)$ is expressed in an oscillator basis. To be as explicit as possible, it is convenient to introduce the hopping operators²

$$\text{Hop}_k = \frac{1}{k!^2} \sum_{\substack{a_1, \dots, a_k \\ b_1, \dots, b_k}} \bar{\mathbf{a}}_{a_1}^3 \cdots \bar{\mathbf{a}}_{a_k}^3 \bar{\mathbf{a}}_{b_1}^4 \cdots \bar{\mathbf{a}}_{b_k}^4 \mathbf{a}_{b_1}^3 \cdots \mathbf{a}_{b_k}^3 \mathbf{a}_{a_1}^4 \cdots \mathbf{a}_{a_k}^4. \quad (4.46)$$

On $V_{\mathbf{s}_3} \otimes V_{\mathbf{s}_4}$ the operator Hop_k agrees with \mathcal{O}_{Υ_k} , after the said identification of spaces, up to a trivial combinatorial factor. This hopping basis allows us to express the R-matrix in the form

$$R_{\mathbf{s}_3 \mathbf{s}_4}(z) = \sum_{k=0}^{\min(s_3, s_4)} \frac{k!}{\Gamma(z - s_3 + k + 1)} \text{Hop}_k. \quad (4.47)$$

The operator Hop_k produces a sum of states containing all possibilities to exchange k of the oscillators in space $V_{\mathbf{s}_3}$ with k of the oscillators in space $V_{\mathbf{s}_4}$, i.e. it ‘‘hops’’ k oscillators between the two spaces. See also [9] for its supersymmetric and non-compact version. Note that we can extend the summation range in (4.47) to infinity as Hop_k with $k > \min(s_3, s_4)$ will annihilate any state. Note also that in (4.47) the dependence on the representation labels of the coefficients can be absorbed by a shift of the spectral parameter. Taken in conjunction, these two observations allow to interpret the expression (4.47) in a way that does not depend on a specific symmetric representation \mathbf{s} .

Apart from the invariant (4.37) discussed so far, which corresponds to the R-matrix, there exists another class of invariants based on the monodromy (4.34). Relaxing the conditions in (4.35) one finds further solutions with $s_1 + s_2 = s_3 + s_4$. However, in the general case with $s_1 \neq s_3$ these invariants do not depend on a free complex spectral parameter.

5 Toy model for super Yang-Mills scattering amplitudes

The main result of section 4 is summarized by explicit formulas for the sample invariants (4.19), (4.25), (4.31) and (4.37) of the Yangian $\mathcal{Y}(\mathfrak{gl}(n))$. The aim of this section is to establish a relation between these expressions and tree-level scattering amplitudes of planar $\mathcal{N} = 4$ super Yang-Mills theory, which will often simply be referred to as ‘‘scattering amplitudes’’. See e.g. [27] for a recent review of the latter.

The essential connection between the expressions of section 4, which are formulated using oscillator algebras, and these amplitudes is Yangian invariance. For the amplitudes this was shown in [1] employing spinor-helicity variables.³ A formal relation between these variables and certain oscillators was indicated in [4]. Nevertheless, the Yangian is different in both cases. In the present paper we are focusing on finite-dimensional representations of $\mathcal{Y}(\mathfrak{gl}(n))$ and not on the infinite-dimensional representation of the Yangian of $\mathfrak{psu}(2, 2|4) \subset \mathfrak{gl}(4|4)$, which is the one relevant for amplitudes. Furthermore, at first sight the said formulas of section 4 look somewhat different from known expressions for super Yang-Mills scattering amplitudes.

In order to compare and relate these two different types of Yangian invariants, it turns out to be most appropriate to formulate the scattering amplitudes as Grassmannian integrals in terms of super twistors [30]. In these variables the generators of the superconformal

²This formalism has been developed in joint discussions with Tomek Łukowski. See [9], where these hopping operators are also employed.

³Special diligence is required if the particle momenta are not in generic position, but there are collinear particles [28], see also [29].

algebra, i.e. the lowest level Yangian generators, are realized as first order differential operators [31]. The Yangian invariance of these integrals was proven in [32], see also [7, 33]. Furthermore, the super twistor variables together with the associated differential operators obey the commutation relations of the oscillator algebra. In the way the invariants of section 4 are formulated within the framework of the QISM, they naturally contain spectral parameters in the form of inhomogeneities. Hence, we are led to compare these invariants to a recent spectral parameter deformation [8, 9] of these amplitudes.

Those aspects of the Graßmannian integral for undeformed and deformed scattering amplitudes which are important for our discussion are briefly summarized in section 5.1. In section 5.2 we reformulate the invariants obtained in section 4 with the aim of comparing them to the deformed amplitudes. As a first step, the invariants are expressed as multi-dimensional contour integrals over exponential functions of creation operators. Next, the oscillator algebras are realized in terms of multiplication and differentiation operators, see appendix A for details. This turns the exponential functions into certain delta functions, which are characteristic of Graßmannian integrals.

Rewritten in this way, the Yangian invariants of section 4 are essentially $\mathfrak{gl}(n)$ analogues of the deformed tree-level scattering amplitudes of planar $\mathcal{N} = 4$ super Yang-Mills theory. Hence, we may think of them as a “toy model” for scattering amplitudes. Note that we will be able to explicitly specify the multi-dimensional integration contour for the sample invariants at hand.

5.1 Graßmannian integral for (deformed) scattering amplitudes

All tree-level scattering amplitudes of planar $\mathcal{N} = 4$ super Yang-Mills theory can be packaged into a single compact Graßmannian integral formula using super twistor variables, see [30] for a recent formulation, and [10] for the original proposal. In this formalism the undeformed L -point N^{K-2} MHV amplitude is given by

$$\mathcal{A}_{L,K} = \int \frac{\prod_{k=1}^K \prod_{i=K+1}^L dc_{ki}}{(1 \dots K)(2 \dots K+1) \dots (L \dots L+K-1)} \prod_{k=1}^K \delta^{4|4} \left(\mathcal{W}^k + \sum_{i=K+1}^L c_{ki} \mathcal{W}^i \right). \quad (5.1)$$

These amplitudes are organized by the deviation $K - 2$ from the maximally helicity violating (MHV) configuration. The minor $(i \dots i + K)$, i.e. the $K \times K$ subdeterminant, is built from the columns $i, \dots, i + K$ of the $K \times L$ matrix

$$\begin{pmatrix} 1 & 0 & c_{1K+1} & \dots & c_{1L} \\ & \ddots & \vdots & & \vdots \\ 0 & 1 & c_{KK+1} & \dots & c_{KL} \end{pmatrix}. \quad (5.2)$$

A $\mathfrak{gl}(K)$ gauge symmetry of the Graßmannian integral (5.1) has already been fixed by the choice of the first K columns in (5.2). The delta functions $\delta^{4|4}$ in (5.1) are given by the product of four bosonic and four fermionic delta functions depending on the super twistor variables \mathcal{W}_a^i with a point index i and a fundamental $\mathfrak{gl}(4|4)$ index a ,

$$\delta^{4|4} \left(\mathcal{W}^k + \sum_{i=K+1}^L c_{ki} \mathcal{W}^i \right) := \prod_{a=1}^{4+4} \delta \left(\mathcal{W}_a^k + \sum_{i=K+1}^L c_{ki} \mathcal{W}_a^i \right). \quad (5.3)$$

The Graßmannian integral (5.1) is often treated in a formal sense, neither explicitly specifying the domain of integration nor the meaning of the delta functions of *complex* variables. See, however, e.g. [34] for a mathematically more rigorous approach.

Recently, a spectral parameter deformation of the Grassmannian integral for scattering amplitudes has been introduced [8, 9] in order to establish connections with the common language of quantum integrable systems. Here we consider the deformations of the 3-point MHV amplitude $\overline{\mathcal{A}}_{3,1}$, the 3-point MHV amplitude $\mathcal{A}_{3,2}$, and the 4-point MHV amplitude $\mathcal{A}_{4,2}$. These will shortly be compared with the Yangian invariants constructed in section 4. The two 3-point amplitudes are of special importance as they provide the building blocks for general L -point amplitudes. The 4-point MHV amplitude is the first non-trivial example that can be constructed using these building block. The deformations of these amplitudes read [9]

$$\tilde{\mathcal{A}}_{3,1} = \int \frac{dc_{12} dc_{13}}{c_{12}^{s_2+1} c_{13}^{s_3+1}} \delta^{n|m}(\mathcal{W}^1 + c_{12}\mathcal{W}^2 + c_{13}\mathcal{W}^3), \quad (5.4)$$

$$\tilde{\mathcal{A}}_{3,2} = \int \frac{dc_{13} dc_{23}}{c_{13}^{s_1+1} c_{23}^{s_2+1}} \delta^{n|m}(\mathcal{W}^1 + c_{13}\mathcal{W}^3) \delta^{n|m}(\mathcal{W}^2 + c_{23}\mathcal{W}^3), \quad (5.5)$$

$$\begin{aligned} \tilde{\mathcal{A}}_{4,2}(z) = \int \frac{dc_{13} dc_{14} dc_{23} dc_{24}}{c_{13}c_{24}(c_{13}c_{24} - c_{23}c_{14})} \left(-\frac{c_{13}c_{24}}{c_{13}c_{24} - c_{23}c_{14}} \right)^z \frac{c_{24}^{s_3-s_4}}{(-c_{13}c_{24} + c_{23}c_{14})^{s_3}} \\ \cdot \delta^{n|m}(\mathcal{W}^1 + c_{13}\mathcal{W}^3 + c_{14}\mathcal{W}^4) \delta^{n|m}(\mathcal{W}^2 + c_{23}\mathcal{W}^3 + c_{24}\mathcal{W}^4), \end{aligned} \quad (5.6)$$

where the deformation parameters $s_i \in \mathbb{C}$ can be understood as representation labels. For these low values of L and K a spectral parameter z appears only in the last expression (5.6). In addition, in these deformations the super twistors are generalized to variables \mathcal{W}_a^i with a fundamental $\mathfrak{gl}(n|m)$ index a and the delta functions are to be understood as the corresponding extension of (5.3). In case of $n|m = 4|4$, $s_i = 0$ and $z = 0$ the deformations $\tilde{\mathcal{A}}_{L,K}$ reduce to the undeformed scattering amplitudes $\mathcal{A}_{L,K}$ obtained from the Grassmannian integral (5.1). For our comparison in the next section we will need the case $n|0$ with positive integer values of s_i , because we will be dealing with finite-dimensional, purely bosonic representations, and generic complex z .

5.2 Sample invariants as Grassmannian-like integrals

Let us collect the invariants (4.19), (4.25), (4.31), (4.37) of the Yangian $\mathcal{Y}(\mathfrak{gl}(n))$ constructed in section 4 in terms of oscillators:

$$|\Psi_{2,1}\rangle = (\bar{\mathbf{b}}^1 \cdot \bar{\mathbf{a}}^2)^{s_2} |0\rangle, \quad (5.7)$$

$$|\Psi_{3,1}\rangle = (\bar{\mathbf{b}}^1 \cdot \bar{\mathbf{a}}^2)^{s_2} (\bar{\mathbf{b}}^1 \cdot \bar{\mathbf{a}}^3)^{s_3} |0\rangle, \quad (5.8)$$

$$|\Psi_{3,2}\rangle = (\bar{\mathbf{b}}^1 \cdot \bar{\mathbf{a}}^3)^{s_1} (\bar{\mathbf{b}}^2 \cdot \bar{\mathbf{a}}^3)^{s_2} |0\rangle, \quad (5.9)$$

$$\begin{aligned} |\Psi_{4,2}(z)\rangle = \sum_{k=0}^{\min(s_3, s_4)} \frac{1}{(s_3 - k)!(s_4 - k)!k!^2} \frac{k!}{\Gamma(z - s_3 + k + 1)} \\ \cdot (\bar{\mathbf{b}}^1 \cdot \bar{\mathbf{a}}^3)^{s_3 - k} (\bar{\mathbf{b}}^2 \cdot \bar{\mathbf{a}}^4)^{s_4 - k} (\bar{\mathbf{b}}^2 \cdot \bar{\mathbf{a}}^3)^k (\bar{\mathbf{b}}^1 \cdot \bar{\mathbf{a}}^4)^k |0\rangle. \end{aligned} \quad (5.10)$$

At first sight there seems to be little resemblance between these formulas and the deformed amplitudes (5.4), (5.5) and (5.6). Nevertheless, in this section we will reformulate these sample $\mathcal{Y}(\mathfrak{gl}(n))$ invariants $|\Psi_{L,K}\rangle$ and compare to the $\mathfrak{gl}(n)$ version of the deformed amplitudes $\tilde{\mathcal{A}}_{L,K}$.

We start by introducing complex contour integrals in some auxiliary variables c_{ki} . In case of the simplest two-site invariant (5.7) this is particularly easy and we write

$$|\Psi_{2,1}\rangle = (\bar{\mathbf{b}}^1 \cdot \bar{\mathbf{a}}^2)^{s_2} |0\rangle = \frac{s_2!(-1)^{s_2}}{2\pi i} \oint \frac{dc_{12}}{c_{12}^{s_2+1}} e^{-c_{12} \bar{\mathbf{b}}^1 \cdot \bar{\mathbf{a}}^2} |0\rangle, \quad (5.11)$$

where the closed contour encircles the pole at the origin of the complex c_{12} -plane counterclockwise. In the same way each product $\bar{\mathbf{b}}^k \cdot \bar{\mathbf{a}}^i$ of oscillators appearing in the further invariants (5.8), (5.9) and (5.10) is translated into one complex contour integral in the variable c_{ki} ,

$$|\Psi_{3,1}\rangle = \frac{s_2!s_3!(-1)^{s_2+s_3}}{(2\pi i)^2} \oint \frac{dc_{12} dc_{13}}{c_{12}^{s_2+1} c_{13}^{s_3+1}} e^{-c_{12}\bar{\mathbf{b}}^1 \cdot \bar{\mathbf{a}}^2 - c_{13}\bar{\mathbf{b}}^1 \cdot \bar{\mathbf{a}}^3} |0\rangle, \quad (5.12)$$

$$|\Psi_{3,2}\rangle = \frac{s_1!s_2!(-1)^{s_1+s_2}}{(2\pi i)^2} \oint \frac{dc_{13} dc_{23}}{c_{13}^{s_3+1} c_{23}^{s_2+1}} e^{-c_{13}\bar{\mathbf{b}}^1 \cdot \bar{\mathbf{a}}^3 - c_{23}\bar{\mathbf{b}}^2 \cdot \bar{\mathbf{a}}^3} |0\rangle, \quad (5.13)$$

$$|\Psi_{4,2}(z)\rangle = \frac{(-1)^{s_3+s_4}}{(2\pi i)^4} \oint \frac{dc_{13} dc_{14} dc_{23} dc_{24}}{c_{13}^{s_3+1} c_{24}^{s_4+1} c_{14}c_{23}} \sum_{k=0}^{\min(s_3, s_4)} \frac{k!}{\Gamma(z - s_3 + k + 1)} \left(\frac{c_{13}c_{24}}{c_{14}c_{23}} \right)^k \cdot e^{-c_{13}\bar{\mathbf{b}}^1 \cdot \bar{\mathbf{a}}^3 - c_{14}\bar{\mathbf{b}}^1 \cdot \bar{\mathbf{a}}^4 - c_{23}\bar{\mathbf{b}}^2 \cdot \bar{\mathbf{a}}^3 - c_{24}\bar{\mathbf{b}}^2 \cdot \bar{\mathbf{a}}^4} |0\rangle, \quad (5.14)$$

where the contour in each of the variables c_{ki} is again a closed counterclockwise circle around the origin. The four-site invariant (5.14) can also be expressed in a slightly more compact form. We notice that the range of the summation in (5.14) can be extended to infinity without changing the value of the integral because the additional terms have a vanishing residue. Furthermore, choosing a contour that satisfies $|c_{13}c_{24}| < |c_{14}c_{23}|$, the infinite sum is a series expansion of a hypergeometric function leading to⁴

$$|\Psi_{4,2}(z)\rangle = \frac{(-1)^{s_3+s_4}}{(2\pi i)^4} \oint \frac{dc_{13} dc_{14} dc_{23} dc_{24}}{c_{13}^{s_3+1} c_{24}^{s_4+1} c_{14}c_{23}} \frac{{}_2F_1\left(1, 1; z - s_3 + 1; \frac{c_{13}c_{24}}{c_{14}c_{23}}\right)}{\Gamma(z - s_3 + 1)} \cdot e^{-c_{13}\bar{\mathbf{b}}^1 \cdot \bar{\mathbf{a}}^3 - c_{14}\bar{\mathbf{b}}^1 \cdot \bar{\mathbf{a}}^4 - c_{23}\bar{\mathbf{b}}^2 \cdot \bar{\mathbf{a}}^3 - c_{24}\bar{\mathbf{b}}^2 \cdot \bar{\mathbf{a}}^4} |0\rangle. \quad (5.15)$$

After these reformulations the integral structure of the invariants $|\Psi_{L,K}\rangle$ already matches the one of the deformed amplitudes $\tilde{\mathcal{A}}_{L,K}$, in the sense that in both cases there are $L \cdot K$ integration variables. The exponential functions of creation operators in the integrands of the sample invariants $|\Psi_{L,K}\rangle$ are reminiscent of the link representation of scattering amplitudes [10, 36].

Next, we turn to the form of the integrand with the aim to express the exponential functions of creation operators as appropriate delta functions like those in (5.4), (5.5) and (5.6). For this purpose we employ different representations of the oscillator algebras at sites carrying symmetric representations of type \mathbf{s} and at sites with conjugate representations of type $\bar{\mathbf{s}}$, respectively:

$$\begin{aligned} \bar{\mathbf{a}} &\hat{=} \mathcal{W}, & \mathbf{a} &\hat{=} \partial_{\mathcal{W}}, & |0\rangle &\hat{=} 1 & \text{for sites with } \mathbf{s}, \\ \bar{\mathbf{b}} &\hat{=} -\partial_{\mathcal{W}}, & \mathbf{b} &\hat{=} \mathcal{W}, & |0\rangle &\hat{=} \delta(\mathcal{W}) & \text{for sites with } \bar{\mathbf{s}}. \end{aligned} \quad (5.16)$$

The oscillators are realized as multiplication and differentiation operators in a complex variable \mathcal{W} . Consequently, as we already stressed above, $\delta(\mathcal{W})$ is a delta function of a complex variable. These representations of the oscillator algebra are discussed in detail in appendix A.

Before we apply (5.16) to the integral expressions of the invariants $|\Psi_{L,K}\rangle$ given in (5.11), (5.12), (5.13) and (5.15), it is instructive to first look at the form of the Yangian

⁴Naively this expression does not seem to be valid at the special points $s_3 - z = 1, 2, 3, \dots$ because in this case the series expansion of the hypergeometric function is not defined. However, the divergence of the expansion is regularized by the gamma function, see e.g. [35], and (5.15) is also valid at these points.

generators annihilating these invariants, recall (3.32). The corresponding monodromies all have a trivial overall normalization factor, cf. (4.18), (4.24), (4.30) and (4.36). Hence, their expansion (3.26) leads to the common Yangian generators

$$M_{ab}^{(1)} = \sum_{i=1}^L J_{ba}^i, \quad M_{ab}^{(2)} = \sum_{\substack{i,j=1 \\ i < j}}^L \sum_{c=1}^n J_{ca}^i J_{bc}^j + \sum_{i=1}^L v_i J_{ba}^i, \quad (5.17)$$

where the $\mathfrak{gl}(n)$ generators at the sites are

$$J_{ab}^i = \begin{cases} \bar{\mathbf{a}}_a^i \mathbf{a}_b^i \cong \mathcal{W}_a^i \partial_{\mathcal{W}_b^i} & \text{for sites with } \mathbf{s}_i, \\ -\bar{\mathbf{b}}_b^i \mathbf{b}_a^i \cong \mathcal{W}_a^i \partial_{\mathcal{W}_b^i} + \delta_{ab} & \text{for sites with } \bar{\mathbf{s}}_i. \end{cases} \quad (5.18)$$

The inhomogeneities v_i depend on the chosen invariant and are specified in section 4. In this formulation, the variables \mathcal{W}_a^i can be thought of as analogous to the super twistors used in scattering amplitudes, where in case of the latter a is a fundamental $\mathfrak{gl}(4|4)$ index. While the oscillator form of the $\mathfrak{gl}(n)$ generators in (5.18) has a different structure at the two distinct types of sites, the generators are, up to the shift δ_{ab} , identical when written in terms of \mathcal{W}_a^i . The two distinct types of representations, \mathbf{s}_i and $\bar{\mathbf{s}}_i$, nevertheless manifests themselves in the structure of the states: The invariants are polynomials in \mathcal{W}_a^i if the i -th site carries a representation \mathbf{s}_i , and they contain delta functions with argument \mathcal{W}_a^i and derivatives thereof for a site with $\bar{\mathbf{s}}_i$. In discussions of the Yangian invariance of scattering amplitudes the $\mathfrak{gl}(4|4)$ generators also take an identical form for all points of the amplitude, see e.g. [7].

Let us return to our main goal of applying (5.16) to the sample invariants $|\Psi_{L,K}\rangle$ in the form (5.11), (5.12), (5.13) and (5.15). Note that with (5.16) an exponential of creation operators becomes

$$e^{-c_{ki} \bar{\mathbf{a}}_a^i \bar{\mathbf{b}}_b^k} |0\rangle \cong e^{c_{ki} \mathcal{W}_a^i \partial_{\mathcal{W}_b^k}} \delta(\mathcal{W}_b^k) = \delta(\mathcal{W}_b^k + c_{ki} \mathcal{W}_a^i). \quad (5.19)$$

Here $|0\rangle$ denotes the tensor product of the Fock vacua of the two oscillator algebras. The vacuum of the oscillators \mathbf{a}_a^i is realized as 1 and that of \mathbf{b}_b^k as a delta function. For the invariants $|\Psi_{L,K}\rangle$, the symbol $|0\rangle$ stands more generally for the tensor product of the Fock vacua of all involved oscillator algebras. This means, using (5.16), that

$$|0\rangle \cong \prod_{k \in \{\text{sites with } \bar{\mathbf{s}}\}} \delta^n(\mathcal{W}^k) \quad \text{with} \quad \delta^n(\mathcal{W}^k) := \prod_{a=1}^n \delta(\mathcal{W}_a^k), \quad (5.20)$$

where the range of the first product extends over all sites carrying a conjugate representation of type $\bar{\mathbf{s}}$. Using (5.16), (5.19) and (5.20) the two-site invariant (5.11) is expressed as

$$|\Psi_{2,1}\rangle \cong \left(- \sum_{a=1}^n \mathcal{W}_a^2 \partial_{\mathcal{W}_a^1} \right)^{s_2} \delta^n(\mathcal{W}^1) = \frac{s_2! (-1)^{s_2}}{2\pi i} \oint \frac{dc_{12}}{c_{12}^{s_2+1}} \delta^n(\mathcal{W}^1 + c_{12} \mathcal{W}^2). \quad (5.21)$$

To show the equality of the middle and the right expression in this formula explicitly, we have to evaluate a contour integral where the integrand contains a delta function. This is done by first acting on a holomorphic test function depending only on the variables \mathcal{W}_a^1 of the conjugate site and subsequently evaluating a standard contour integral. Such test functions are discussed in more detail in appendix A. Note that such test functions do not

introduce new poles in the c_{12} -plane. Proceeding analogously in the cases of the invariants (5.12), (5.13), (5.15) we obtain⁵

$$|\Psi_{3,1}\rangle \cong \frac{s_2!s_3!(-1)^{s_2+s_3}}{(2\pi i)^2} \oint \frac{dc_{12} dc_{13}}{c_{12}^{s_2+1} c_{13}^{s_3+1}} \delta^n(\mathcal{W}^1 + c_{12}\mathcal{W}^2 + c_{13}\mathcal{W}^3), \quad (5.22)$$

$$|\Psi_{3,2}\rangle \cong \frac{s_1!s_2!(-1)^{s_1+s_2}}{(2\pi i)^2} \oint \frac{dc_{13} dc_{23}}{c_{13}^{s_1+1} c_{23}^{s_2+1}} \delta^n(\mathcal{W}^1 + c_{13}\mathcal{W}^3)\delta^n(\mathcal{W}^2 + c_{23}\mathcal{W}^3), \quad (5.23)$$

$$|\Psi_{4,2}(z)\rangle \cong \frac{(-1)^{s_3+s_4}}{(2\pi i)^4} \oint \frac{dc_{13} dc_{14} dc_{23} dc_{24}}{c_{13}^{s_3+1} c_{24}^{s_4+1} c_{14}c_{23}} \frac{{}_2F_1\left(1, 1; z - s_3 + 1; \frac{c_{13}c_{24}}{c_{14}c_{23}}\right)}{\Gamma(z - s_3 + 1)} \cdot \delta^n(\mathcal{W}^1 + c_{13}\mathcal{W}^3 + c_{14}\mathcal{W}^4)\delta^n(\mathcal{W}^2 + c_{23}\mathcal{W}^3 + c_{24}\mathcal{W}^4). \quad (5.24)$$

Recall that for these invariants the integrations in all variables c_{ki} are closed counterclockwise contours encircling the origin and for (5.24) we have to assume in addition $|c_{13}c_{24}| < |c_{14}c_{23}|$.

Finally, we want to compare this version of the invariants to the deformed amplitudes summarized in section 5.1. The integrations and the delta functions appearing in these deformed amplitudes are normally only understood in a formal sense, cf. [9]. To be able to make the comparison, we chose closed counterclockwise circles around the coordinate origins for the integration contours in (5.4), (5.5) and (5.6). Furthermore, we interpret the delta functions in these expressions in the sense of appendix A as for our invariants.

First of all, no deformed amplitude $\tilde{\mathcal{A}}_{2,1}$ is presented in [9]. However, at least for $s_2 = 0$ the two-site invariant (5.21) is contained up to a normalization factor in the general formula (5.1) for $\mathcal{A}_{L,K}$ after replacing the delta function $\delta^{4|4}$ by δ^n . Both three-site invariants (5.22) and (5.23) agree (again up to a constant normalization) with the $\mathfrak{gl}(n|0)$ version of the deformed amplitudes provided in (5.4) and (5.5),

$$|\Psi_{3,1}\rangle \propto \tilde{\mathcal{A}}_{3,1}\Big|_{n|0}, \quad |\Psi_{3,2}\rangle \propto \tilde{\mathcal{A}}_{3,2}\Big|_{n|0}. \quad (5.25)$$

As already mentioned, the 3-point amplitudes can be understood as the basic building blocks for more general amplitudes. Hence, (5.25) is an important check of our formalism. Interestingly, however, the integrand of the deformed amplitude $\tilde{\mathcal{A}}_{4,2}(z)$ given in (5.6) does not fully agree with that of $|\Psi_{4,2}(z)\rangle$ found in (5.24). To relate these two expressions we note that at the special points $s_3 - z = 1, 2, 3, \dots$ of the spectral parameter the series expansion of the hypergeometric function in (5.24) simplifies to

$$|\Psi_{4,2}(z)\rangle \cong \frac{(-1)^{s_3+s_4}}{(2\pi i)^4} \oint \frac{dc_{13} dc_{14} dc_{23} dc_{24}}{c_{13}c_{24}(c_{13}c_{24} - c_{23}c_{14})} \frac{1}{c_{13}^{s_3}c_{24}^{s_4}} \left(-\frac{c_{13}c_{24}}{c_{13}c_{24} - c_{23}c_{14}}\right)^{z-s_3} \cdot \delta^n(\mathcal{W}^1 + c_{13}\mathcal{W}^3 + c_{14}\mathcal{W}^4)\delta^n(\mathcal{W}^2 + c_{23}\mathcal{W}^3 + c_{24}\mathcal{W}^4). \quad (5.26)$$

This agrees up to a shift of the spectral parameter (and again a normalization factor) with the deformed amplitude:

$$|\Psi_{4,2}(z)\rangle \propto \tilde{\mathcal{A}}_{4,2}(z - 2s_3)\Big|_{n|0} \quad \text{for } s_3 - z = 1, 2, 3, \dots \quad (5.27)$$

In [9] $\tilde{\mathcal{A}}_{4,2}(z)$ is also used for generic values of z . However, at least for our choice of the integration contours around zero this is problematic due to the branch cut of the complex

⁵Similar formulas for invariants of the Yangian of $\mathfrak{gl}(n)$ were also obtained recently in [37]. This was extended in [38] to $\mathfrak{gl}(n|m)$, which includes the $\mathfrak{gl}(4|4)$ case relevant to scattering amplitudes.

power function in (5.6). We want to stress that in the present formulation (5.26) is only valid at the special points of the spectral parameter and the full four-site invariant, i.e. the invariant corresponding to the R-matrix, is given by (5.24) involving a hypergeometric function. The interesting question whether a $\mathfrak{gl}(4|4)$ version of (5.24) might be a more appropriate deformation of the four-point MHV amplitude $\mathcal{A}_{4,2}$ than (5.6) should definitely be clarified.

6 Bethe ansatz for Yangian invariants

In section 4 we discussed some sample Yangian invariants. Their relation to (deformed) super Yang-Mills scattering amplitudes was then established in section 5. We will proceed to a systematic construction of Yangian invariants based on their characterization as solutions of the set of eigenvalue equations (3.30), which involves the monodromy matrix elements $M_{ab}(u)$. This characterization shows that the invariant $|\Psi\rangle$ is a special eigenstate of the transfer matrix

$$T(u) = \text{tr } M(u), \quad (6.1)$$

where the trace is taken over the auxiliary space $V_{\square} = \mathbb{C}^n$. Indeed, (3.30) implies

$$T(u)|\Psi\rangle = n|\Psi\rangle \quad (6.2)$$

with the fixed eigenvalue n . The transfer matrix (6.1) can be diagonalized by means of a Bethe ansatz, see e.g. the introduction [39] and [40] for the $\mathfrak{gl}(n)$ case. Therefore a Yangian invariant $|\Psi\rangle$ is a special Bethe vector. This is the key observation leading to the construction of $|\Psi\rangle$ by a *Bethe ansatz for Yangian invariants* in this section.

For simplicity, we first focus on $\mathfrak{gl}(2)$ monodromies with finite-dimensional highest weight representations in the quantum space. After a brief reminder of the general algebraic Bethe ansatz technique for $\mathfrak{gl}(2)$ spin chains in section 6.1, we specialize in section 6.2 to the case of Yangian invariant Bethe vectors. This leads to a set of functional relations characterizing Yangian invariants, which are equivalent to a degenerate case of the Baxter equation [41]. These equations determine the Bethe roots and, in addition, constrain the allowed representation labels and inhomogeneities of the monodromy. Remarkably, a large class of explicit solutions of these functional relations can be obtained. They show an interesting structure which is discussed in section 6.3. The Bethe roots form *exact* strings in the complex plane. The positions of these strings depend on the inhomogeneities of the monodromy. The length of the strings, i.e. the number of Bethe roots per string, is determined by the representation labels. We illustrate this structure using the sample invariants already known from section 4. We also present solutions to the functional relations corresponding to Baxter lattices with N lines. In particular, this includes lattices where all lines carry the spin $\frac{1}{2}$ representation of $\mathfrak{su}(2)$. In section 6.4 this special case is shown to reproduce Baxter's original perimeter Bethe ansatz, cf. section 2. Finally, in section 6.5 we sketch the generalization of the set of functional relations characterizing Yangian invariants from the $\mathfrak{gl}(2)$ to the $\mathfrak{gl}(n)$ case, postponing the details to a future publication [42].

6.1 Algebraic Bethe ansatz for $\mathfrak{gl}(2)$ spin chains

An extensive review of the algebraic Bethe ansatz for $\mathfrak{gl}(2)$ invariant spin chains can be found e.g. in [39]. Here we only recapitulate the essential ideas and highlight those features

that are of importance for the construction of Yangian invariants.

The algebraic Bethe ansatz allows to diagonalize transfer matrices defined as traces of suitable monodromies. We begin with a monodromy matrix $M(u)$ satisfying the RTT-relation (3.23). In the $\mathfrak{gl}(2)$ case the auxiliary space is $V_{\square} = \mathbb{C}^2$. Thus, it is convenient to think about the monodromy as a 2×2 matrix with operatorial entries acting on the total quantum space,

$$M(u) = \begin{pmatrix} A(u) & B(u) \\ C(u) & D(u) \end{pmatrix}. \quad (6.3)$$

We define a transfer matrix $T(u)$ as the trace of the monodromy (6.3) over the auxiliary space:

$$T(u) = A(u) + D(u). \quad (6.4)$$

Its diagonalization can then be achieved in an efficient way using the algebraic relations imposed on (6.3) by the RTT-equation (3.23).

We assume the existence of a vacuum state $|\Omega\rangle$ characterized by the action of the monodromy elements as

$$A(u)|\Omega\rangle = \alpha(u)|\Omega\rangle, \quad D(u)|\Omega\rangle = \delta(u)|\Omega\rangle, \quad C(u)|\Omega\rangle = 0. \quad (6.5)$$

The operators $A(u)$ and $D(u)$ act diagonally on the reference state $|\Omega\rangle$ and hence $\alpha(u)$ and $\delta(u)$ are scalar functions. The conditions in (6.5) are satisfied for monodromies (3.11) built up from Lax operators (3.21), where the i -th local quantum space carries a $\mathfrak{gl}(2)$ representation $\Xi_i = (\xi_i^{(1)}, \xi_i^{(2)})$ with a highest weight state $|\sigma_i\rangle$ defined by

$$J_{11}^i|\sigma_i\rangle = \xi_i^{(1)}|\sigma_i\rangle, \quad J_{22}^i|\sigma_i\rangle = \xi_i^{(2)}|\sigma_i\rangle, \quad J_{12}^i|\sigma_i\rangle = 0. \quad (6.6)$$

For such a monodromy the reference state is

$$|\Omega\rangle = |\sigma_1\rangle \otimes \cdots \otimes |\sigma_L\rangle, \quad (6.7)$$

and we immediately obtain

$$\alpha(u) = \prod_{i=1}^L f_{\Xi_i}(u - v_i) \frac{u - v_i + \xi_i^{(1)}}{u - v_i}, \quad \delta(u) = \prod_{i=1}^L f_{\Xi_i}(u - v_i) \frac{u - v_i + \xi_i^{(2)}}{u - v_i}. \quad (6.8)$$

However, here and also in section 6.2 we do not use these explicit expressions for $\alpha(u)$ and $\delta(u)$. It suffices to demand (6.5). To proceed, we make an ansatz for the eigenstates of the transfer matrix:

$$|\Psi\rangle = B(u_1) \cdots B(u_P)|\Omega\rangle, \quad (6.9)$$

where the P complex parameters u_k are referred to as Bethe roots. In general the vector (6.9) is not an eigenvector of the transfer matrix $T(u)$. It is, however, if the Bethe roots satisfy a set of Bethe equations. To derive them, we need some of the commutation relations between the monodromy elements encoded in (3.25). With the notation introduced in (6.3) the relevant commutators are

$$\begin{aligned} A(u)B(u') &= \frac{u - u' - 1}{u - u'} B(u')A(u) + \frac{1}{u - u'} B(u)A(u'), \\ D(u)B(u') &= \frac{u - u' + 1}{u - u'} B(u')D(u) - \frac{1}{u - u'} B(u)D(u'), \\ B(u)B(u') &= B(u')B(u). \end{aligned} \quad (6.10)$$

In the next step we act with the operators $A(u)$ and $D(u)$ appearing in the transfer matrix (6.4) on the vector (6.9). Using (6.10) one commutes these operators to the right and obtains after some algebra, see [39],

$$\begin{aligned} A(u)|\Psi\rangle &= \alpha(u)\frac{Q(u-1)}{Q(u)}|\Psi\rangle - \sum_{k=1}^P \frac{\alpha(u_k)Q(u_k-1)}{u-u_k} B(u) \prod_{\substack{i=1 \\ i \neq k}}^P \frac{B(u_i)}{u_k-u_i} |\Omega\rangle, \\ D(u)|\Psi\rangle &= \delta(u)\frac{Q(u+1)}{Q(u)}|\Psi\rangle - \sum_{k=1}^P \frac{\delta(u_k)Q(u_k+1)}{u-u_k} B(u) \prod_{\substack{i=1 \\ i \neq k}}^P \frac{B(u_i)}{u_k-u_i} |\Omega\rangle. \end{aligned} \quad (6.11)$$

Here we introduced Baxter's Q-function, which is defined as a polynomial of degree P in the spectral parameter and its zeros are located at the Bethe roots u_i ,

$$Q(u) = \prod_{i=1}^P (u - u_i). \quad (6.12)$$

For $|\Psi\rangle$ of (6.9) to be an eigenstate of the transfer matrix we have to impose the *Bethe equations*

$$\alpha(u_k)Q(u_k-1) + \delta(u_k)Q(u_k+1) = 0 \quad (6.13)$$

for $k = 1, \dots, P$. These equations assure that the “unwanted terms”, namely the sums on the right hand sides of each of the two equations in (6.11), cancel each other upon addition of the equations.

A more common form of (6.13) is achieved by solving for the fraction of the two Q-functions, and inserting (6.8) and (6.12):

$$\prod_{i=1}^L \frac{u_k - v_i + \xi_i^{(1)}}{u_k - v_i + \xi_i^{(2)}} = - \prod_{j=1}^P \frac{u_k - u_j + 1}{u_k - u_j - 1}. \quad (6.14)$$

However, it turns out that for those solutions which are of particular interest in the following sections we would divide by zero in (6.14). Therefore, we keep the Bethe equations in the original form (6.13).

The eigenvalue $\tau(u)$ of $T(u)$ corresponding to the eigenstate $|\Psi\rangle$ is then given by the *Baxter equation*

$$\tau(u) = \alpha(u)\frac{Q(u-1)}{Q(u)} + \delta(u)\frac{Q(u+1)}{Q(u)}. \quad (6.15)$$

It is important to notice that, assuming the regularity of $\tau(u)$, $\alpha(u)$ and $\delta(u)$ at the Bethe roots u_k , the Bethe equations (6.13) are a consequence of the Baxter equation (6.15). This is easily seen by taking the residue of (6.15) at $u = u_k$ and using the form of the Q-function in (6.12).

With this algebraic Bethe ansatz the problem of diagonalizing the transfer matrix (6.4), i.e determining its eigenvalues (6.15) and the corresponding eigenvectors (6.9), is reduced to solving the Bethe equations (6.13). Although this method is very powerful, it is in general difficult to obtain solutions of the Bethe equations analytically and often one relies on approximations and numerical methods. In the case of Yangian invariants the situation will turn out to be much more favorable.

6.2 Bethe ansatz for invariants of Yangian $\mathcal{Y}(\mathfrak{gl}(2))$

Let us explicitly spell out the definition (3.30) of Yangian invariants for the $\mathfrak{gl}(2)$ case using the notation (6.3) for the monodromy elements,

$$A(u)|\Psi\rangle = 1, \quad D(u)|\Psi\rangle = 1, \quad (6.16)$$

$$B(u)|\Psi\rangle = 0, \quad C(u)|\Psi\rangle = 0. \quad (6.17)$$

Here we separated the equations into (6.16) involving the diagonal monodromy elements and (6.17) with the off-diagonal elements. To construct Yangian invariants $|\Psi\rangle$ we first solve (6.16) by specializing the Bethe ansatz of section 6.1. In a second step, we show that for finite-dimensional representations the Bethe vectors $|\Psi\rangle$ obtained in this way automatically obey also (6.17). The result of this procedure yields a characterization of Yangian invariants in terms of functional relations that will be summarized at the end of this section.

Let us first concentrate on the diagonal part (6.16). Usually, cf. section 6.1, one wants to construct eigenvectors of the transfer matrix, i.e. eigenvectors of the sum $A(u) + D(u)$. However, here we additionally require that $|\Psi\rangle$ is a common eigenvector of $A(u)$ and $D(u)$. As in section 6.1 we make the ansatz (6.9) for the eigenvector and use the commutation relations (6.10) to derive (6.11). However, we now need to demand that the “unwanted terms” are identical to zero separately for each of the two equations in (6.11). This is guaranteed by

$$\alpha(u_k)Q(u_k - 1) = 0, \quad \delta(u_k)Q(u_k + 1) = 0, \quad (6.18)$$

which is the degenerate case of the Bethe equations (6.13) where each term vanishes individually. In order to fix the eigenvalues of $A(u)$ and $D(u)$ to be 1, equation (6.11) implies that we have to require

$$1 = \alpha(u) \frac{Q(u-1)}{Q(u)}, \quad 1 = \delta(u) \frac{Q(u+1)}{Q(u)}. \quad (6.19)$$

This is the degenerate case of the Baxter equation (6.15) where each term on the r.h.s. is equal to 1. It leads to the required transfer matrix eigenvalue $\tau(u) = 2$, which is the rank of $\mathfrak{gl}(2)$. Assuming the regularity of $\alpha(u)$ and $\delta(u)$ at the Bethe roots $u = u_k$, one shows by taking the residue as in section 6.1 that (6.19) implies (6.18). Consequently, the problem of constructing common solutions of the eigenvalue equations in (6.16) has been reduced to solving (6.19).

To address (6.17) involving the off-diagonal monodromy elements, we use (6.16), which we already solved. We expand (6.17) using (3.26) to obtain

$$M_{11}^{(1)}|\Psi\rangle = 0, \quad M_{22}^{(1)}|\Psi\rangle = 0. \quad (6.20)$$

As discussed in the context of (3.28), the generators $-M_{ab}^{(1)}(u)$ form a $\mathfrak{gl}(2)$ algebra and thus (6.20) means that $|\Psi\rangle$ has $\mathfrak{gl}(2)$ weight $(0,0)$. The expansion of $C(u)|\Omega\rangle = 0$ from (6.5) implies $M_{21}^{(1)}|\Omega\rangle = 0$. Using the commutation relations (3.29) and (6.11) one shows

$$M_{21}^{(1)}|\Psi\rangle = - \sum_{k=1}^P (\alpha(u_k)Q(u_k - 1) + \delta(u_k)Q(u_k + 1)) \prod_{\substack{i=1 \\ i \neq k}}^P \frac{B(u_i)}{u_k - u_i} |\Omega\rangle = 0, \quad (6.21)$$

where we needed (6.18) for the last equality. As we are dealing with a finite-dimensional $\mathfrak{gl}(2)$ representation, (6.20) and (6.21) imply that $|\Psi\rangle$ is a $\mathfrak{gl}(2)$ singlet. Hence, also

$$M_{12}^{(1)}|\Psi\rangle = 0. \quad (6.22)$$

Finally, we obtain from (3.29) the relations

$$[M_{12}^{(1)}, A(u) - D(u)] = 2B(u), \quad [M_{21}^{(1)}, D(u) - A(u)] = 2C(u). \quad (6.23)$$

Acting with these on $|\Psi\rangle$ and using (6.16), (6.21) and (6.22), we see that also the off-diagonal part (6.17) of the Yangian invariance condition is satisfied.

In conclusion, we have reduced the problem of constructing invariants $|\Psi\rangle$ of the Yangian $\mathcal{Y}(\mathfrak{gl}(2))$ to the problem of solving the functional relations (6.19). Given a solution $(\alpha(u), \delta(u), Q(u))$ of (6.19), where the Q-function is of the form (6.12), and both $\alpha(u)$ and $\delta(u)$ are regular at the Bethe roots u_k , the Bethe vector $|\Psi\rangle$ given in (6.9) is Yangian invariant. It is convenient to represent the functional relations (6.19) in a slightly different form. Remarkably, the system of two equations in (6.19) can be decoupled into an equation that depends only on the eigenvalues (6.5) of the monodromy acting on the reference state and not on the Bethe roots,

$$1 = \alpha(u)\delta(u-1), \quad (6.24)$$

and a further equation also involving the Bethe roots contained in the Q-function,

$$\frac{Q(u)}{Q(u+1)} = \delta(u). \quad (6.25)$$

The main task is to understand the solutions of (6.24). As $\alpha(u)$ and $\delta(u)$ contain the representation labels and inhomogeneities, cf. (6.8), this equation determines those monodromies that correspond to a Yangian invariant, i.e. for which (3.30) admits a solution $|\Psi\rangle$. Once a suitable solution of (6.24) is found, the difference equation (6.25) can typically be solved with ease for the Bethe roots u_k . This is in stunning contradistinction to the usual situation in most spin chain spectral problems, where the Bethe equations are very hard to solve. Substituting the Bethe roots into (6.9) yields the Bethe state, and hence the invariant $|\Psi\rangle$. We term this construction a *Bethe ansatz for Yangian invariants*.

6.3 Sample solutions of $\mathfrak{gl}(2)$ functional relations

At present, we lack a complete understanding of the set of solutions to the functional relations (6.24) and (6.25). Gaining it should lead to a classification of invariants of the Yangian $\mathcal{Y}(\mathfrak{gl}(2))$, clearly an interesting problem for future research. In this paper we take first steps and analyze a few sample solutions. We show how the $\mathfrak{gl}(2)$ versions of our favorite invariants in oscillator form with representations of type $\mathfrak{s} = (s, 0)$ and $\bar{\mathfrak{s}} = (0, -s)$, cf. section 4, fit into the framework of the Bethe ansatz for Yangian invariants. In particular, we again discuss the invariant $|\Psi_{2,1}\rangle$, which was represented by a Baxter lattice with a single line, the three-vertices $|\Psi_{3,1}\rangle$ and $|\Psi_{3,2}\rangle$, as well as the four-vertex (R-matrix) $|\Psi_{4,2}(z)\rangle$. We also consider the invariant associated to a Baxter lattice of N lines. For all these examples the Bethe roots are given explicitly. They arrange themselves into strings in the complex plane.

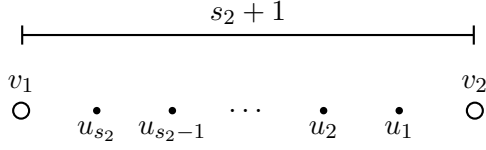


Figure 6.1: The Bethe roots u_k associated to the Yangian invariant $|\Psi_{2,1}\rangle$ of section 4.2.1 arrange into a string between the two inhomogeneities v_1 and v_2 , cf. (6.29) in the complex plane. This string consists of s_2 roots with a uniform real spacing of 1.

6.3.1 Line

Let us recall the representation labels and inhomogeneities for the $\mathfrak{gl}(2)$ case of the invariant $|\Psi_{2,1}\rangle$ discussed in section 4.2.1 and associated to the spin chain monodromy $M_{2,1}(u)$ with $L = 2$ sites, cf. (4.16) and (4.17):

$$\begin{aligned} \Xi_1 &= \bar{\mathbf{s}}_1, & \Xi_2 &= \mathbf{s}_2, \\ v_1 &= v_2 - 1 - s_2, & s_1 &= s_2. \end{aligned} \quad (6.26)$$

With these relations and the trivial normalization (4.18) of the monodromy, (6.8) simplifies to

$$\alpha(u) = \frac{u - v_2 + s_2}{u - v_2}, \quad \delta(u) = \frac{u - v_2 + 1}{u - v_2 + 1 + s_2}. \quad (6.27)$$

In this form one directly sees that the first functional relation (6.24) holds. The remaining relation (6.25) is solved by

$$Q(u) = \frac{\Gamma(u - v_2 + s_2 + 1)}{\Gamma(u - v_2 + 1)} = \prod_{k=1}^{s_2} (u - v_2 + k), \quad (6.28)$$

where the freedom of multiplying this solution by a function of period 1 in u has been fixed by imposing the polynomial form (6.12) of the Q-function. Because s_2 is a positive integer, the gamma functions in (6.28) indeed reduce to a polynomial and we can read off the Bethe roots as zeros of the Q-function,

$$u_k = v_2 - k \quad \text{for } k = 1, \dots, s_2. \quad (6.29)$$

They form a string in the complex plane, see figure 6.1. Note that, as is usual for a $\mathfrak{gl}(2)$ Bethe ansatz, the labels of the Bethe roots can be permuted because the operators $B(u)$ appearing in the Bethe vector (6.9) commute for different values of the spectral parameter u , cf. (6.10). Finally, we want to construct the Yangian invariant Bethe vector (6.9) corresponding to this solution of the functional relations. For this purpose we need the reference state (6.7) for the representations specified in (6.26). It is given by a tensor product of the highest weight states (4.2):

$$|\Omega\rangle = (\bar{\mathbf{b}}_2^1)^{s_2} (\bar{\mathbf{a}}_1^2)^{s_2} |0\rangle. \quad (6.30)$$

Then we can evaluate (6.9) using (6.26), (6.29) and (6.30), where we note that because of (4.18) also the normalization of the operators $B(u_k)$ is trivial. By direct case-by-case computation for small values of s_2 we obtain the explicit form of the Bethe vectors

$$|\Psi\rangle = B(u_1) \cdots B(u_{s_2}) |\Omega\rangle = (-1)^{s_2} (\bar{\mathbf{b}}^1 \cdot \bar{\mathbf{a}}^2)^{s_2} |0\rangle \propto |\Psi_{2,1}\rangle. \quad (6.31)$$

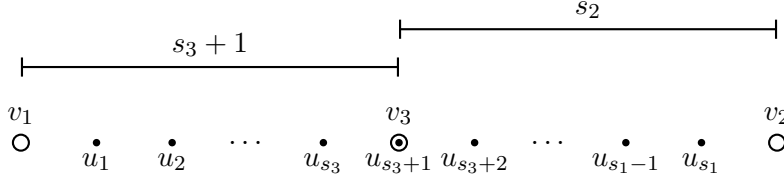


Figure 6.2: The invariant $|\Psi_{3,1}\rangle$ gives rise to a real string of s_1 uniformly spaced Bethe roots u_k in the complex plane, see (6.35). They lie in between the inhomogeneities v_1, v_2 and one root coincides with v_3 .

Thus, our Bethe ansatz for Yangian invariants nicely matches, up to a normalization, $|\Psi_{2,1}\rangle$ given in (4.19). It would be desirable to find a proof of (6.31) for general $s_2 \in \mathbb{N}$.

6.3.2 Three-vertices

In section 4.2.2 we discussed two different three-site invariants. For the $\mathfrak{gl}(2)$ case the monodromy $M_{3,1}(u)$ associated to the first invariant $|\Psi_{3,1}\rangle$ is defined by, cf. (4.22) and (4.23),

$$\begin{aligned} \bar{\Xi}_1 = \bar{\mathbf{s}}_1, \quad \bar{\Xi}_2 = \mathbf{s}_2, \quad \bar{\Xi}_3 = \mathbf{s}_3, \\ v_2 = v_1 + 1 + s_2 + s_3, \quad v_3 = v_1 + 1 + s_3, \quad s_1 = s_2 + s_3. \end{aligned} \quad (6.32)$$

With (6.32) and the trivial normalization of the monodromy (4.24), the eigenvalues of the monodromy on the reference state of the Bethe ansatz in (6.8) turn into

$$\alpha(u) = \frac{u - v_1 - 1}{u - v_1 - s_1 - 1}, \quad \delta(u) = \frac{u - v_1 - s_1}{u - v_1}. \quad (6.33)$$

Obviously, they obey (6.24). The other functional relation (6.25) is uniquely solved by

$$Q(u) = \frac{\Gamma(u - v_1)}{\Gamma(u - v_1 - s_1)} = \prod_{k=1}^{s_1} (u - v_1 - k), \quad (6.34)$$

because the Q-function is of the form (6.12). The zeros of (6.34) yield the Bethe roots

$$u_k = v_1 + k \quad \text{for } k = 1, \dots, s_1. \quad (6.35)$$

For this invariant the Bethe roots again form a string in the complex plane, see figure 6.2. We now turn to the construction of the associated Bethe vector. With (4.2) the reference state (6.7) for the Bethe ansatz with the representation labels found in (6.32) becomes

$$|\Omega\rangle = (\bar{\mathbf{b}}_2^1)^{s_2+s_3} (\bar{\mathbf{a}}_1^2)^{s_2} (\bar{\mathbf{a}}_1^3)^{s_3} |0\rangle. \quad (6.36)$$

Notice that one Bethe root is identical to an inhomogeneity, $u_{s_3+1} = v_3$. Consequently, the Lax operator $R_{\square_{s_3}}(u_{s_3+1} - v_3)$, cf. (4.4), contributing to $B(u_{s_3+1})$ in the Bethe vector (6.9) diverges. Nevertheless, we obtain a finite Bethe vector using an ad hoc prescription, which we verified for small values of s_2 and s_3 : First, all non-problematic Bethe roots are inserted into (6.9), while u_{s_3+1} is kept generic. In the resulting expression the divergence at $u_{s_3+1} = v_3$ disappears. Hence, in a second step, we can safely insert the last root, leading to

$$|\Psi\rangle = B(u_1) \cdots B(u_{s_1}) |\Omega\rangle = (-1)^{s_2+s_3} (\bar{\mathbf{b}}^1 \cdot \bar{\mathbf{a}}^2)^{s_2} (\bar{\mathbf{b}}^1 \cdot \bar{\mathbf{a}}^3)^{s_3} |0\rangle \propto |\Psi_{3,1}\rangle. \quad (6.37)$$

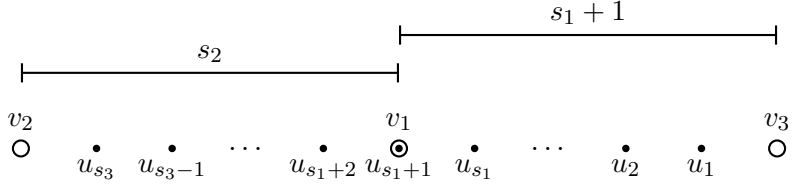


Figure 6.3: The string of Bethe roots u_k belonging to the invariant $|\Psi_{3,2}\rangle$. The roots lie between the inhomogeneities v_2 and v_3 . One of them coincides with v_1 .

Therefore, we have obtained also the three-site Yangian invariant $|\Psi_{3,1}\rangle$ presented in (4.25) from a Bethe ansatz. A derivation of (6.37) for general $s_2, s_3 \in \mathbb{N}$ and a better understanding of the divergence still have to be achieved.

So-called “singular solutions” of the Bethe equations leading naively to divergent Bethe vectors are well known for the homogeneous $\mathfrak{su}(2)$ spin $\frac{1}{2}$ chain, see e.g. the recent discussion [43], [44] and the references therein. Such solutions were already known to Bethe himself [14] and appeared also early on in the planar $\mathcal{N} = 4$ super Yang-Mills spectral problem [45]. There are several ways to treat them properly, cf. [43], which might also be applicable for the inhomogeneous spin chain with mixed representations needed for the three-site invariant $|\Psi_{3,1}\rangle$.

The $\mathfrak{gl}(2)$ version of the second three-site invariant discussed in section 4.2.2, $|\Psi_{3,2}\rangle$, is characterized by the monodromy $M_{3,2}(u)$ defined in (4.28) and (4.29),

$$\begin{aligned} \Xi_1 &= \bar{s}_1, & \Xi_2 &= \bar{s}_2, & \Xi_3 &= s_3, \\ v_1 &= v_3 - 1 - s_1, & v_2 &= v_3 - 1 - s_1 - s_2, & s_3 &= s_1 + s_2. \end{aligned} \quad (6.38)$$

The trivial normalization of this monodromy, cf. (4.30), together with (6.38) implies that (6.8) simplifies to

$$\alpha(u) = \frac{u - v_3 + s_3}{u - v_3}, \quad \delta(u) = \frac{u - v_3 + 1}{u - v_3 + 1 + s_3}, \quad (6.39)$$

which is a solution of the functional relation (6.24). The second relation (6.25) is then solved by

$$Q(u) = \frac{\Gamma(u - v_3 + s_3 + 1)}{\Gamma(u - v_3 + 1)} = \prod_{k=1}^{s_3} (u - v_3 + k). \quad (6.40)$$

Demanding this solution to be of the form (6.12) guarantees its uniqueness and allows us to read off the Bethe roots

$$u_k = v_3 - k \quad \text{for } k = 1, \dots, s_3. \quad (6.41)$$

Once again, they form a string, see figure 6.3. To obtain the corresponding Bethe vector, we first evaluate the reference state (6.7) with (4.2) and the representations labels given in (6.38). This leads to

$$|\Omega\rangle = (\bar{\mathbf{b}}_1^1)^{s_1} (\bar{\mathbf{b}}_2^2)^{s_2} (\bar{\mathbf{a}}_1^3)^{s_1 + s_2} |0\rangle. \quad (6.42)$$

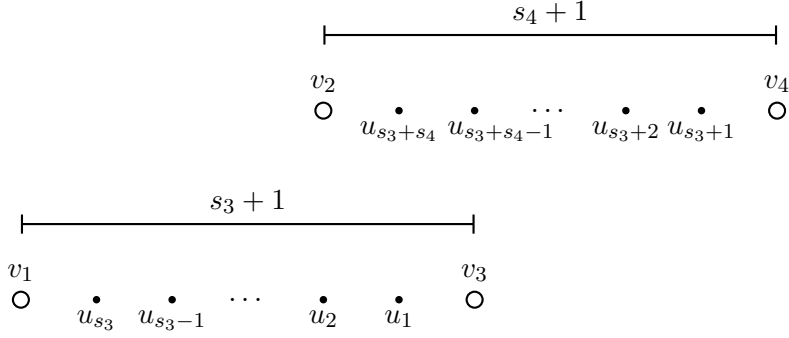


Figure 6.4: The Bethe roots u_k corresponding to the four site invariant $|\Psi_{4,2}(z)\rangle$, i.e. to the R-matrix $R_{s_3 s_4}(z)$, arrange into two real strings in the complex plane. The strings consist of s_3 and s_4 roots, respectively. The difference of their endpoints $z := v_3 - v_4$, cf. (4.39), is the spectral parameter of the R-matrix.

Just like the other three-site invariant, the operators $B(u_{s_1+1})$ diverges because $u_{s_1+1} = v_1$. With the same ad hoc prescription as above, we obtain again a finite Bethe vector that, for small values of s_1 and s_2 , has the explicit form

$$|\Psi\rangle = B(u_1) \cdots B(u_{s_1})|\Omega\rangle = (-1)^{s_1+s_2} (\bar{\mathbf{b}}^1 \cdot \bar{\mathbf{a}}^3)^{s_1} (\bar{\mathbf{b}}^2 \cdot \bar{\mathbf{a}}^3)^{s_2} |0\rangle \propto |\Psi_{3,2}\rangle. \quad (6.43)$$

This matches the form of the three-site invariant $|\Psi_{3,2}\rangle$ given in (4.31). Once again, at the moment we lack a derivation of (6.43) valid for all $s_1, s_2 \in \mathbb{N}$.

6.3.3 Four-vertex

The $\mathfrak{gl}(2)$ version of the four site invariant $|\Psi_{4,2}(v_3 - v_4)\rangle$ of section 4.2.3 is characterized by a monodromy matrix $M_{4,2}(u)$ that is specified by, cf. (4.34) and (4.35),

$$\begin{aligned} \Xi_1 &= \bar{\mathbf{s}}_1, & \Xi_2 &= \bar{\mathbf{s}}_2, & \Xi_3 &= \mathbf{s}_3, & \Xi_4 &= \mathbf{s}_4, \\ v_1 &= v_3 - 1 - s_3, & v_2 &= v_4 - 1 - s_4, & s_1 &= s_3, & s_2 &= s_4. \end{aligned} \quad (6.44)$$

For this monodromy the overall normalization (4.36) is once again trivial and with (6.44) the eigenvalues (6.8) become

$$\alpha(u) = \frac{u - v_3 + s_3}{u - v_3} \frac{u - v_4 + s_4}{u - v_4}, \quad \delta(u) = \frac{u - v_3 + 1}{u - v_3 + 1 + s_3} \frac{u - v_4 + 1}{u - v_4 + 1 + s_4}. \quad (6.45)$$

They obey the functional relation (6.24). A solution of (6.25) is given by

$$Q(u) = \frac{\Gamma(u - v_3 + s_3 + 1)}{\Gamma(u - v_3 + 1)} \frac{\Gamma(u - v_4 + s_4 + 1)}{\Gamma(u - v_4 + 1)} = \prod_{k=1}^{s_3} (u - v_3 + k) \prod_{k=1}^{s_4} (u - v_4 + k). \quad (6.46)$$

Because of (6.12) this solution is unique. The Bethe roots

$$\begin{aligned} u_k &= v_3 - k & \text{for } k &= 1, \dots, s_3, \\ u_{k+s_3} &= v_4 - k & \text{for } k &= 1, \dots, s_4, \end{aligned} \quad (6.47)$$

which we read off as the zeros of (6.46), form two strings, see figure 6.4. To construct the Bethe vector (6.9) we need the reference state (6.7) for the representation labels found in (6.44):

$$|\Omega\rangle = (\bar{\mathbf{b}}_2^1)^{s_3} (\bar{\mathbf{a}}_1^3)^{s_3} (\bar{\mathbf{b}}_2^2)^{s_4} (\bar{\mathbf{a}}_1^4)^{s_4} |0\rangle. \quad (6.48)$$

Then the explicit evaluation of (6.9) for small values of s_3 and s_4 yields

$$\begin{aligned} |\Psi\rangle &= B(u_1) \cdots B(u_{s_3}) B(u_{s_3+1}) \cdots B(u_{s_3+s_4}) |\Omega\rangle \\ &= (-1)^{s_3+s_4} s_3! s_4! \prod_{l=1}^{\min(s_3, s_4)} (v_3 - v_4 + s_4 - l + 1)^{-1} \sum_{k=0}^{\min(s_3, s_4)} \frac{1}{(s_3 - k)! (s_4 - k)! k!} \\ &\quad \cdot \prod_{l=k+1}^{\min(s_3, s_4)} (v_3 - v_4 - s_3 + l) (\bar{\mathbf{b}}^1 \cdot \bar{\mathbf{a}}^3)^{s_3-k} (\bar{\mathbf{b}}^2 \cdot \bar{\mathbf{a}}^4)^{s_4-k} (\bar{\mathbf{b}}^2 \cdot \bar{\mathbf{a}}^3)^k (\bar{\mathbf{b}}^1 \cdot \bar{\mathbf{a}}^4)^k |0\rangle \\ &\propto |\Psi_{4,2}(v_3 - v_4)\rangle, \end{aligned} \quad (6.49)$$

which matches the expression for $|\Psi_{4,2}(z)\rangle$ from (4.37) with (4.38), (4.39) and (4.41). Again, the derivation of this formula for general $s_3, s_4 \in \mathbb{N}$ remains to be done. As the invariant $|\Psi_{4,2}(z)\rangle$ can be understood as the R-matrix $R_{\mathbf{s}_3 \mathbf{s}_4}(z)$, we might say that this R-matrix is a special Bethe vector.

6.3.4 Baxter lattice with N lines

We know from section 4 that the invariants $|\Psi_{2,1}\rangle$ and $|\Psi_{4,2}(z)\rangle$ can be understood as a Baxter lattice with, respectively, one and two lines carrying conjugate symmetric representations. Here we work out the solution to the functional relations (6.24) and (6.25) for a Baxter lattice consisting of N lines of this type. In this case the monodromy has $L = 2N$ sites. According to the $\mathfrak{gl}(2)$ version of (4.15), the k -th line of the Baxter lattice with endpoints $i_k < j_k$, the representation $\Lambda_k = \bar{\mathbf{s}}_{i_k}$ and a spectral parameter θ_k gives rise to the two spin chain sites

$$\begin{aligned} \Xi_{i_k} &= \bar{\mathbf{s}}_{i_k}, \quad \Xi_{j_k} = \mathbf{s}_{j_k}, \\ v_{i_k} &= \theta_k, \quad v_{j_k} = \theta_k + s_{i_k} + 1, \quad s_{i_k} = s_{j_k}. \end{aligned} \quad (6.50)$$

This turns the monodromy eigenvalues (6.8) into

$$\begin{aligned} \alpha(u) &= \prod_{k=1}^N f_{\bar{\mathbf{s}}_{i_k}}(u - v_{i_k}) f_{\mathbf{s}_{j_k}}(u - v_{j_k}) \frac{u - v_{j_k} + s_{j_k}}{u - v_{j_k}} = \prod_{k=1}^N \frac{u - v_{j_k} + s_{j_k}}{u - v_{j_k}}, \\ \delta(u) &= \prod_{k=1}^N f_{\bar{\mathbf{s}}_{i_k}}(u - v_{i_k}) f_{\mathbf{s}_{j_k}}(u - v_{j_k}) \frac{u - v_{i_k} - s_{i_k}}{u - v_{i_k}} = \prod_{k=1}^N \frac{u - v_{j_k} + 1}{u - v_{j_k} + 1 + s_{j_k}}. \end{aligned} \quad (6.51)$$

For the last equality in both equations we used that each factor of the products corresponds to one line of the Baxter lattice. Using (6.50) the normalization factors belonging to each of these lines reduce to 1 analogously to the case of a single line explained before (4.18). Obviously, the eigenvalues in (6.51) satisfy (6.24). The relation (6.25) is solved by

$$Q(u) = \prod_{k=1}^N \frac{\Gamma(u - v_{j_k} + s_{j_k} + 1)}{\Gamma(u - v_{j_k} + 1)} = \prod_{k=1}^N \prod_{l=1}^{s_{j_k}} (u - v_{j_k} + l), \quad (6.52)$$

which is the unique solution because we also demand the Q-function to be of the form (6.12). We read off the Bethe roots as zeros of (6.52),

$$\begin{aligned} u_k &= v_{j_1} - k & \text{for } k = 1, \dots, s_{j_1}, \\ u_{k+s_{j_1}} &= v_{j_2} - k & \text{for } k = 1, \dots, s_{j_2}, \\ &\vdots \\ u_{k+s_{j_{N-1}}} &= v_{j_N} - k & \text{for } k = 1, \dots, s_{j_N}. \end{aligned} \tag{6.53}$$

They arrange into N strings. The k -th line of the Baxter lattice with representation $\Lambda_k = \bar{\mathbf{s}}_{i_k}$ leads to one string of $s_{i_k} = s_{j_k}$ Bethe roots with a uniform real spacing of 1 lying between the inhomogeneities v_{i_k} and v_{j_k} . The arrangement of these strings in the complex plane is determined by the spectral parameters $\theta_k = v_{i_k}$ of the lines. Next, we concentrate on the associated Bethe vector. With the form of the highest weight states (4.2) and (6.50) the reference state (6.7) turns into

$$|\Omega\rangle = \prod_{k=1}^N (\bar{\mathbf{b}}_2^{i_k})^{s_{j_k}} (\bar{\mathbf{a}}_1^{j_k})^{s_{j_k}} |0\rangle. \tag{6.54}$$

The Yangian invariant is then given by the Bethe vector (6.9). Note that as in the special cases of one- and two-line Baxter lattices discussed, respectively, in section 6.3.1 and section 6.3.3, for generic values of $\theta_k = v_{i_k}$ no Bethe root coincides with an inhomogeneity. Consequently, these Bethe vectors with an even number of spin chain sites are manifestly non-divergent.

We finish with a remark on the general structure of the set of solutions to the functional relations (6.24) and (6.25). Notice that the solution of these relations defined by (6.51) and (6.52) is actually the product of N line solutions of the type discussed in section 6.3.1. More generally, given two solutions $(\alpha_1(u), \delta_1(u), Q_1(u))$ and $(\alpha_2(u), \delta_2(u), Q_2(u))$ of the functional relations, a new one is obtained as the product

$$(\alpha_1(u)\alpha_2(u), \delta_1(u)\delta_2(u), Q_1(u)Q_2(u)). \tag{6.55}$$

Using this method one can construct new Yangian invariants by “superposing” known ones. For example, it should be possible to combine line solutions with the three-vertices discussed in section 6.3.2.

6.4 Relation to perimeter Bethe ansatz

In the previous section 6.3.4 we analyzed the solution to the functional relations (6.24) and (6.25) that corresponds to a Baxter lattice with N lines. Here we show that a special case of it reproduces the perimeter Bethe ansatz of section 2. Therefore, we first use special properties of the $\mathfrak{gl}(2)$ Lax operators. Then the Baxter lattice is specialized to the case where all lines carry the conjugate of the fundamental, i.e. the antifundamental, representation. This allows us to express the associated Yangian invariant $|\Psi\rangle$, which was discussed in section 6.3.4 in the algebraic formulation of the Bethe ansatz, in terms of a coordinate Bethe ansatz wave function. The resulting expression matches the perimeter Bethe ansatz formula (2.13) for the partition function $\mathcal{Z}(\mathbf{G}, \boldsymbol{\theta}, \boldsymbol{\alpha})$.

In order to obtain the special properties of the Lax operators, we employ a relation between representations \mathbf{s} and $\bar{\mathbf{s}}$, which is valid in the $\mathfrak{gl}(2)$ case but not for $\mathfrak{gl}(n)$ in general.

The generators (4.1) and the highest weight states (4.2) of both representations are linked by

$$UJ_{ab}U^{-1} = \bar{J}_{ab}|_{\mathbf{b}_a \mapsto \mathbf{a}_a} + s\delta_{ab}, \quad U|\sigma\rangle = (-1)^s|\bar{\sigma}\rangle|_{\mathbf{b}_a \mapsto \mathbf{a}_a}, \quad (6.56)$$

where the unitary operator

$$U = e^{\frac{\pi}{2}(\bar{\mathbf{a}}_1\mathbf{a}_2 - \bar{\mathbf{a}}_2\mathbf{a}_1)} \quad \text{obeys} \quad U|0\rangle = |0\rangle, \quad \bar{\mathbf{a}}_1U = U\bar{\mathbf{a}}_2, \quad \bar{\mathbf{a}}_2U = -U\bar{\mathbf{a}}_1. \quad (6.57)$$

To avoid spurious divergencies in the following, we introduce Lax operators with a different normalization than before,

$$\tilde{R}_{\square\mathbf{s}}(u-w) = (u-w)1 + \sum_{a,b=1}^2 e_{ab}\bar{\mathbf{a}}_b\mathbf{a}_a. \quad (6.58)$$

They build up a monodromy with inhomogeneities denoted by w_i ,

$$\tilde{M}(u) = \tilde{R}_{\square\mathbf{s}_1}(u-w_1) \cdots \tilde{R}_{\square\mathbf{s}_L}(u-w_L). \quad (6.59)$$

Using (6.56), the ordinary Lax operators (4.4) for the representation \mathbf{s} and (4.5) for $\bar{\mathbf{s}}$ can be expressed in terms of (6.58) as

$$R_{\square\mathbf{s}}(u) = \frac{f_{\mathbf{s}}(u)}{u}\tilde{R}_{\square\mathbf{s}}(u), \quad R_{\square\bar{\mathbf{s}}}(u)|_{\mathbf{b}_a \mapsto \mathbf{a}_a} = \frac{f_{\bar{\mathbf{s}}}(u)}{u}U\tilde{R}_{\square\mathbf{s}}(u-s)U^{-1}. \quad (6.60)$$

These properties at hand, any $\mathfrak{gl}(2)$ monodromy $M(u)$ consisting of $R_{\square\mathbf{s}}(u)$ and $R_{\square\bar{\mathbf{s}}}(u)$ can be reformulated as $\tilde{M}(u)$ that solely comprises Lax operators of the type $\tilde{R}_{\square\mathbf{s}}(u)$.

We will apply this observation to the monodromy specified in (6.50) which is associated to a Baxter lattice with N lines. To connect with the perimeter Bethe ansatz, we first need to specialize to lattices where each line carries the antifundamental representation,

$$\Lambda = (\overline{(1,0)}, \dots, \overline{(1,0)}), \quad (6.61)$$

cf. (3.1) for the notation. From (6.61) together with (6.50) we have $s_{i_k} = s_{j_k} = 1$. Hence, the strings of Bethe roots (6.53) degenerate into individual points in the complex plane,

$$u_k = \theta_k + 1 \quad \text{for} \quad k = 1, \dots, N. \quad (6.62)$$

This pattern of Bethe roots is identical to that of the perimeter Bethe ansatz in (2.12). Using (6.60), we express the monodromy defined by (6.50) and (6.61) as

$$M(u)|_{\mathbf{b}_a^{i_k} \mapsto \mathbf{a}_a^{i_k}} = \prod_{i=1}^{2N} \frac{1}{u-v_i} W\tilde{M}(u)W^{-1} \quad \text{with} \quad W = \prod_{k=1}^N U^{i_k}, \quad (6.63)$$

where the normalizations of the Lax operators cancel as explained after (6.51). The unitary U^{i_k} acts on site i_k . Thus W transforms all conjugate sites. The parameters of $\tilde{M}(u)$ are

$$\mathbf{s}_i = (1,0), \quad w_{i_k} = \theta_k + 1, \quad w_{j_k} = \theta_k + 2, \quad (6.64)$$

where the inhomogeneities w_{i_k} originating from the conjugate sites of $M(u)$ are shifted by 1 with respect to the v_{i_k} in (6.50). The inhomogeneities in (6.64) agree with those of

the perimeter Bethe ansatz in (2.12). To obtain the highest weight state $|\tilde{\Omega}\rangle$ in the total quantum space of $\tilde{M}(u)$, we apply (6.56) to $|\Omega\rangle$ in (6.54),

$$|\tilde{\Omega}\rangle = (-1)^N W^{-1} |\Omega\rangle \Big|_{\mathbf{b}_a^{i_k} \mapsto \mathbf{a}_a^{i_k}} = \bar{\mathbf{a}}_1^1 \cdots \bar{\mathbf{a}}_1^L |0\rangle. \quad (6.65)$$

Equations (6.63) and (6.65) allow us to express also the Bethe vector (6.9), i.e. the Yangian invariant $|\Psi\rangle$ of the Baxter lattice, as a Bethe vector that is constructed using the matrix elements $\tilde{M}_{12}(u) = \tilde{B}(u)$ of the new monodromy,

$$|\Psi\rangle \Big|_{\mathbf{b}_a^{i_k} \mapsto \mathbf{a}_a^{i_k}} = (-1)^N \prod_{k=1}^N \prod_{i=1}^{2N} \frac{1}{u_k - v_i} W |\tilde{\Psi}\rangle \quad \text{with} \quad |\tilde{\Psi}\rangle = \tilde{B}(u_1) \cdots \tilde{B}(u_N) |\tilde{\Omega}\rangle. \quad (6.66)$$

Next, the algebraic Bethe ansatz vector $|\tilde{\Psi}\rangle$ is represented by coordinate Bethe ansatz wave functions. For monodromies $\tilde{M}(u)$ of the type (6.59) with $\mathbf{s}_i = (1, 0)$ at all sites one has, see e.g. [46] and appendix 3.E of [47],⁶

$$|\tilde{\Psi}\rangle = \tilde{B}(u_1) \cdots \tilde{B}(u_P) |\tilde{\Omega}\rangle = \sum_{1 \leq x_1 < \cdots < x_P \leq L} \Phi(\mathbf{w}, \mathbf{z}, \mathbf{x}) J_{21}^{x_1} \cdots J_{21}^{x_P} |\tilde{\Omega}\rangle, \quad (6.67)$$

with generators $J_{ab}^i = \bar{\mathbf{a}}_a^i \mathbf{a}_b^i$ and the wave function $\Phi(\mathbf{w}, \mathbf{z}, \mathbf{x})$ in (2.8). The arguments \mathbf{w} , \mathbf{z} and \mathbf{x} denote respectively the inhomogeneities w_i , Bethe roots u_k and magnon positions x_k , cf. (2.7). We apply (6.67) in (6.66) with $L = 2N$ sites and $P = N$ Bethe roots.

To obtain a partition function from the Yangian invariant vector $|\Psi\rangle$, recall (3.19):

$$\mathcal{Z}(\mathbf{G}, \mathbf{\Lambda}, \boldsymbol{\theta}, \boldsymbol{\alpha}) \propto \langle \boldsymbol{\alpha} | \Psi \rangle. \quad (6.68)$$

For a Baxter lattice with the representations (6.61) the possible states are $|\boldsymbol{\alpha}\rangle = |\alpha_1\rangle \otimes \cdots \otimes |\alpha_{2N}\rangle$ with $\alpha_i = 1, 2$. After the replacement $|\boldsymbol{\alpha}\rangle \Big|_{\mathbf{b}_a^{i_k} \mapsto \mathbf{a}_a^{i_k}}$, the state at each site is either $|1\rangle = \bar{\mathbf{a}}_1^1 |0\rangle$ or $|2\rangle = \bar{\mathbf{a}}_2^1 |0\rangle$. The computation of the scalar product (6.68) reduces using (6.66) to that with each term of the sum in (6.67). This turns out to be only non-zero if the state labels $\boldsymbol{\alpha}$ obey the ice rule (2.6), and if in addition \mathbf{x} is determined in terms of \mathbf{G} and $\boldsymbol{\alpha}$ by (2.11). Then we have

$$\langle \boldsymbol{\alpha} | \Big|_{\mathbf{b}_a^{i_k} \mapsto \mathbf{a}_a^{i_k}} W J_{21}^{x_1} \cdots J_{21}^{x_N} |\tilde{\Omega}\rangle = (-1)^{\mathcal{K}(\mathbf{G}, \boldsymbol{\alpha})} \quad (6.69)$$

with $\mathcal{K}(\mathbf{G}, \boldsymbol{\alpha})$ defined in (2.14). The factors of -1 stem from sites transformed by W .

Finally, the combination of (6.66), (6.67) and (6.69) leads to an expression for the partition function (6.68). Again, it is only non-zero if the state labels $\boldsymbol{\alpha}$ satisfy (2.6). In this case

$$\mathcal{Z}(\mathbf{G}, \mathbf{\Lambda}, \boldsymbol{\theta}, \boldsymbol{\alpha}) \propto \langle \boldsymbol{\alpha} | \Psi \rangle = (-1)^N \prod_{k=1}^N \prod_{i=1}^{2N} \frac{1}{u_k - v_i} (-1)^{\mathcal{K}(\mathbf{G}, \boldsymbol{\alpha})} \Phi(\mathbf{w}, \mathbf{z}, \mathbf{x}). \quad (6.70)$$

Here $\mathbf{\Lambda}$ is fixed in (6.61), and the arguments \mathbf{w} , \mathbf{z} , \mathbf{x} of the wave function are determined by the variables \mathbf{G} , $\boldsymbol{\theta}$, $\boldsymbol{\alpha}$ of the partition function with (2.11) and (2.12). Up to an $\boldsymbol{\alpha}$ -independent normalization factor, the l.h.s. of (6.70) is the perimeter Bethe ansatz formula (2.13).

⁶See [48] for a proof of the corresponding relation in case of more general representations $\mathbf{s}_i = (s, 0)$ but no inhomogeneities, $w_i = 0$.

However, this factor cannot be directly determined by the Bethe ansatz. To show that its choice in (2.13) guarantees the agreement with the partition function (2.5), note the following. With the normalization of the Boltzmann weights in (2.3) it is easy to see that for the particular state labels $\alpha_0 = (1, \dots, 1)$ the partition function (2.5) equals $\mathcal{Z}(\mathbf{G}, \boldsymbol{\theta}, \alpha_0) = 1$. The α -independent normalization in (2.13) trivially guarantees that also this expression is equal to 1 for $\alpha = \alpha_0$. As we already know from (6.70) that the α -dependent part of (2.13) is proportional to the partition function (2.5), this concludes our derivation of (2.13). It shows that the perimeter Bethe ansatz as reviewed in section 2 is a special case of the Bethe ansatz for Yangian invariants.

6.5 Outline of $\mathfrak{gl}(n)$ functional relations

In section 6.2 we discussed in detail how the Bethe ansatz for $\mathfrak{gl}(2)$ spin chains can be specialized in such a way that the resulting Bethe vector $|\Psi\rangle$ is Yangian invariant. This leads to functional relations (6.19) which restrict the allowed representations and inhomogeneities of the monodromy and determine the Bethe roots. The derivation was based on the observation (6.2) that a Yangian invariant $|\Psi\rangle$ is a special eigenvector of a transfer matrix. Of course, this observation is also valid more generally for invariants of the Yangian of $\mathfrak{gl}(n)$. In this $\mathfrak{gl}(n)$ case the nested algebraic Bethe ansatz for monodromies with a finite-dimensional highest weight representation at each site can be found e.g. in [40]. In generalization of the discussion of the $\mathfrak{gl}(2)$ situation in section 6.2, it can be specialized to the case where the Bethe vectors are Yangian invariant. The details of this calculation will be presented in a separate publication [42].

Here we only state one of the main results, the set of functional relations determining the representation labels, inhomogeneities and Bethe roots of Yangian invariants in the $\mathfrak{gl}(n)$ case:

$$\begin{aligned}
1 &= \mu_1(u) \frac{Q_1(u-1)}{Q_1(u)}, \\
1 &= \mu_2(u) \frac{Q_1(u+1)}{Q_1(u)} \frac{Q_2(u-1)}{Q_2(u)}, \\
1 &= \mu_3(u) \frac{Q_2(u+1)}{Q_2(u)} \frac{Q_3(u-1)}{Q_3(u)}, \\
&\vdots \\
1 &= \mu_{n-1}(u) \frac{Q_{n-2}(u+1)}{Q_{n-2}(u)} \frac{Q_{n-1}(u-1)}{Q_{n-1}(u)}, \\
1 &= \mu_n(u) \frac{Q_{n-1}(u+1)}{Q_{n-1}(u)}.
\end{aligned} \tag{6.71}$$

Here $\mu_1(u), \dots, \mu_n(u)$ are the eigenvalues of the monodromy elements $M_{11}(u), \dots, M_{nn}(u)$ on the pseudo vacuum of the Bethe ansatz, cf. (6.5) for the $\mathfrak{gl}(2)$ case. For a monodromy (3.11), which is composed out of the Lax operators (3.21) with a finite-dimensional $\mathfrak{gl}(n)$ representation of highest weight $\Xi_i = (\xi_i^{(1)}, \dots, \xi_i^{(n)})$ at the local quantum space of the i -th site, these eigenvalues are given by

$$\mu_a(u) = \prod_{i=1}^L f_{\Xi_i}(u - v_i) \frac{u - v_i + \xi_i^{(a)}}{u - v_i}. \tag{6.72}$$

The Bethe roots are encoded into the Q-functions

$$Q_k(u) = \prod_{i=1}^{P_k} (u - u_i^{(k)}), \quad (6.73)$$

where $k = 1, \dots, n - 1$ is the nesting level with P_k Bethe roots $u_i^{(k)}$. Obviously, for $n = 2$ equation (6.71) reduces to the functional relations (6.19). As one can see from the Baxter equation for $\mathfrak{gl}(n)$, see e.g. [49], (6.71) is compatible with the fixed eigenvalue in (6.2). More precisely, each term in the Baxter equation is equal to one.

Interestingly, the functional relations (6.71) can also be written in the form

$$1 = \prod_{a=1}^n \mu_a(u - a + 1), \quad (6.74)$$

$$\frac{Q_k(u)}{Q_k(u+1)} = \prod_{a=k+1}^n \mu_a(u - a + k + 1) \quad (6.75)$$

for $k = 1, \dots, n - 1$. The first equation (6.74) does not involve the Bethe roots and only constrains the representation labels and inhomogeneities of the monodromy. Each of the remaining equations (6.75) only involves the Bethe roots of one nesting level k . The equations (6.74) and (6.75) generalize (6.24) and (6.25), respectively, to the $\mathfrak{gl}(n)$ case.

7 Conclusion and outlook

In this paper we have proposed a systematic approach to the construction of Yangian invariants by means of the quantum inverse scattering method (QISM). Our motivation is two-fold. The first is mathematical. It appears that the possibility to construct such invariants for a given algebra and representation in a methodical fashion has not yet been explored. This is clearly a rich field. The second is physical. Following [1], Yangian invariance appears as the hallmark of integrability in the form of a hidden symmetry of the tree-level scattering problem of planar $\mathcal{N} = 4$ super Yang-Mills theory. This opens the exciting possibility to directly construct such amplitudes by the techniques of integrability, such as the various versions of the Bethe ansatz.

The present work is complementary to [8, 9], where spectral parameter deformations of Yangian invariants in general, and of scattering amplitudes in particular were proposed. Here we can look at the spectral parameters z in [8, 9] from a slightly different perspective: In the above, these appear as (differences of) inhomogeneities of some auxiliary spin chain monodromies. The latter contain in turn a spectral parameter u , which is a very useful quantity in the QISM. However, the Yangian invariants and thus the amplitudes do not depend on this spectral parameter. We should also point the reader to the recent works [37, 38], which bear some similarities with our approach.

There is a large number of open problems. The first concerns completing the exploratory study of the $\mathfrak{gl}(n)$ invariants begun in this paper. Clearly it remains to construct the general L -site invariants, and to analyze the freedom in assigning the inhomogeneities (and thus the spectral parameters in the sense of [8, 9]). Furthermore, the attentive reader will have noticed that we essentially derived the 2, 3, 4-site invariants directly from (1.1), and subsequently proved that the Bethe ansatz equations are satisfied. We would really prefer to proceed in the opposite fashion: First solve the Bethe equations, which should

always be fairly trivial, as all roots are expected to assemble into exact strings. Then construct the invariants as the corresponding on-shell Bethe states. Bethe wave functions are in general very complicated. However, here it should help that the roots are so simple.

The second open problem concerns the replacement of compact representations of $\mathfrak{gl}(n)$ by the non-compact representations of $\mathfrak{gl}(4|4)$ appropriate for the study of the $\mathcal{N} = 4$ scattering amplitudes. The goal would clearly be to derive the Yangian invariant tree-level amplitudes from an appropriate “Bethe ansatz”. We suspect that functional methods will be important here, as the solution presumably involves considering infinite sets of Bethe roots. Q-operator methods [49, 50] might be helpful here.

The third and obviously most exciting open problem is the derivation of higher loop corrections to the tree-level amplitudes from a Bethe-like ansatz. Here there is a crucial open conceptual problem: What is the precise fate of Yangian invariance beyond one loop? See e.g. the discussion in [4]. The main trouble is that the infrared divergences of loop amplitudes naively break conformal symmetry and thus also Yangian symmetry. In [8, 9] it was proposed that parametric deformations of loop-level on-shell diagrams might regulate the divergences. Vexingly, however, exact Yangian invariance seems to clash with convergence. On the other hand, Yangian invariance appears to be a key feature of the on-shell diagrammatic approach of [30]. If it is true that the integrands of the higher-loop amplitudes may be constructed in a Yangian-invariant way, these integrands should definitely be constructible by an extension of the methods proposed in the present paper.

Acknowledgments

We thank Zoltan Bajnok, Ludvig Faddeev, Frank Göhmann, Vladimir Mitev, Nicolai Reshetikhin, and especially Livia Ferro, Tomek Łukowski, Carlo Meneghelli and Jan Plefka for very useful discussions. This research is supported in part by the SFB 647 “Raum-Zeit-Materie. Analytische und Geometrische Strukturen” and the Marie Curie network GATIS (gatis.desy.eu) of the European Union’s Seventh Framework Programme FP7/2007-2013/ under REA Grant Agreement No 317089. N.K. is supported by a *Promotionsstipendium* of the *Studienstiftung des Deutschen Volkes*, and receives partial support by the GK 1504 “Masse, Spektrum, Symmetrie”. Two of us (N.K. and M.S.) thank the Kavli IPMU for hospitality while working on parts of the manuscript, and acknowledge the support of the Marie Curie International Research Staff Exchange Network UNIFY.

A Some oscillator algebra representations

In this appendix we substantiate the representations of the oscillator algebra introduced formally in (5.16). It is easily seen that this algebra can be represented on holomorphic functions of one complex variable. The creation operator is realized as multiplication by this variable and the annihilation operator corresponds to differentiation. This was made precise by Bargmann [51] who provided an inner product guaranteeing that both operators are Hermitian conjugates of each other. We review his construction in section A.1.

In section 5 we reformulated the Yangian invariants of section 4 in a way that is reminiscent of planar $\mathcal{N} = 4$ super Yang-Mills scattering amplitudes. For this we also used a representation of the oscillator algebra which is “conjugate” to that of Bargmann in the sense that the role of the operators is exchanged: The creation operator acts by

differentiation and the annihilation operator as multiplication. Furthermore, the Fock vacuum is realized as a delta function of a complex argument.

Such a representation already appeared previously in rather different contexts, see e.g. [52–54], and it is even traced back in [55] to work by Dirac [56]. In contrast to these references, we explain this conjugate Bargmann representation in section A.2 completely within the Bargmann framework.

A.1 Bargmann representation

We start by reviewing the *Bargmann representation* [51], which is also called *holomorphic representation*, see e.g. [57, 58] for recent expositions. The oscillator algebra, the Hermiticity condition and the characterization of the Fock vacuum,

$$[\mathbf{a}, \bar{\mathbf{a}}] = 1, \quad \bar{\mathbf{a}}^\dagger = \mathbf{a}, \quad \mathbf{a}|0\rangle = 0, \quad (\text{A.1})$$

are realized in terms of a complex variable \mathcal{W} by

$$\bar{\mathbf{a}} \hat{=} \mathcal{W}, \quad \mathbf{a} \hat{=} \partial_{\mathcal{W}}, \quad |0\rangle \hat{=} 1. \quad (\text{A.2})$$

In this representation a state translates into a holomorphic function,

$$|\Sigma\rangle = \Sigma(\bar{\mathbf{a}})|0\rangle \hat{=} \Sigma(\mathcal{W}). \quad (\text{A.3})$$

The inner product of two states is defined as

$$\langle \Theta | \Sigma \rangle = \int_{\mathbb{C}} \frac{d\bar{\mathcal{W}} d\mathcal{W}}{2\pi i} e^{-\mathcal{W}\bar{\mathcal{W}}} \overline{\Theta(\bar{\mathcal{W}})} \Sigma(\mathcal{W}), \quad (\text{A.4})$$

where the integral is to be understood as a two-dimensional real integral with $d\bar{\mathcal{W}} d\mathcal{W} = 2i d\text{Re}\mathcal{W} d\text{Im}\mathcal{W}$. Because of the exponential function in the measure, the creation and annihilation operators are indeed related by Hermitian conjugation, i.e. $\mathcal{W}^\dagger = \partial_{\mathcal{W}}$. This is easily verified using partial integration. States with finite norm with respect to the inner product form a Hilbert space with an orthonormal basis

$$|k\rangle = \frac{\bar{\mathbf{a}}^k |0\rangle}{\sqrt{k!}} \hat{=} \frac{\mathcal{W}^k}{\sqrt{k!}}. \quad (\text{A.5})$$

Likewise, one defines an *antiholomorphic representation*, where a family of oscillators

$$[\mathbf{b}, \bar{\mathbf{b}}] = 1, \quad \bar{\mathbf{b}}^\dagger = \mathbf{b}, \quad \mathbf{b}|0\rangle = 0, \quad (\text{A.6})$$

is realized in terms of a complex conjugate variable $\bar{\mathcal{W}}$ as

$$\bar{\mathbf{b}} \hat{=} \bar{\mathcal{W}}, \quad \mathbf{b} \hat{=} \partial_{\bar{\mathcal{W}}}, \quad |0\rangle \hat{=} 1. \quad (\text{A.7})$$

Here the inner product is

$$\langle \Theta | \Sigma \rangle = \int_{\mathbb{C}} \frac{d\bar{\mathcal{W}} d\mathcal{W}}{2\pi i} e^{-\mathcal{W}\bar{\mathcal{W}}} \overline{\Theta(\bar{\mathcal{W}})} \Sigma(\bar{\mathcal{W}}). \quad (\text{A.8})$$

Let us employ both representations (A.2) and (A.7) in case of a simple example. Consider the operator

$$\mathcal{O}_\Psi = \sum_{k,l=0}^{\infty} \mathcal{O}_{kl} (\bar{\mathbf{a}}^2)^k |0\rangle \langle 0| (\mathbf{b}^1)^l \quad (\text{A.9})$$

mapping from a Fock space V_1 with oscillators $\bar{\mathbf{b}}^1, \mathbf{b}^1$ into V_2 with $\bar{\mathbf{a}}^2, \mathbf{a}^2$. It should be thought of as a simple analogue of the Yangian invariants discussed in section 4, see e.g. (4.21). Of course, for generic coefficients \mathcal{O}_{kl} and with only one family of oscillators per space, it is not an actual invariant of the Yangian $\mathcal{Y}(\mathfrak{gl}(n))$. We use the representation (A.2) for the oscillators in V_2 and (A.7) for those in V_1 . Then the action of the operator on a “test state” $|f\rangle \in V_1$ becomes

$$\mathcal{O}_\Psi |f\rangle = \int_{\mathbb{C}} \frac{d\bar{\mathcal{W}}^1 d\mathcal{W}^1}{2\pi i} e^{-\mathcal{W}^1 \bar{\mathcal{W}}^1} \mathcal{O}_\Psi(\mathcal{W}^2, \mathcal{W}^1) f(\bar{\mathcal{W}}^1) \quad (\text{A.10})$$

with the kernel

$$\mathcal{O}_\Psi(\mathcal{W}^2, \mathcal{W}^1) = \sum_{k,l=0}^{\infty} \mathcal{O}_{kl} (\mathcal{W}^2)^k (\mathcal{W}^1)^l. \quad (\text{A.11})$$

In this article we mostly work with the vector version $|\Psi\rangle = \mathcal{O}_\Psi^{\dagger 1}$ of operators like (A.9), see e.g. (4.19). Written in terms of this vector, (A.10) turns into

$$\mathcal{O}_\Psi |f\rangle = \overline{\langle f | \Psi \rangle}^1. \quad (\text{A.12})$$

Note that the inner product is only in the space V_1 and not in V_2 . The complex conjugation affects also only V_1 .

A.2 Conjugate Bargmann representation

Motivated by (A.12) of this example we employ the representation (A.7) to study the inner product of two states $|\Sigma\rangle$ and $|f\rangle$, where the latter will play the role of a test state. Choosing $|\Sigma\rangle = |0\rangle$ to be the Fock vacuum we write

$$\langle f | 0 \rangle = \overline{f(0)} = \int_{\mathbb{C}} \frac{d\bar{\mathcal{W}} d\mathcal{W}}{2\pi i} \bar{f}(\mathcal{W}) \delta(\mathcal{W}) \quad \text{with} \quad \delta(\mathcal{W}) := e^{-\mathcal{W} \bar{\mathcal{W}}}. \quad (\text{A.13})$$

Here we interpreted the exponential function of the measure in (A.8) as a “delta function of a complex argument”, cf. [58]. This delta function does *not* coincide with the reproducing kernel, which usually plays the role of a delta function in the Bargmann representation. However, this interpretation of the exponential function is essential for our purpose, see below. For a general state $|\Sigma\rangle$ we obtain

$$\langle f | \Sigma \rangle = \int_{\mathbb{C}} \frac{d\bar{\mathcal{W}} d\mathcal{Y}}{2\pi i} \bar{f}(\mathcal{W}) \hat{\Sigma}(\mathcal{W}), \quad \text{with} \quad \hat{\Sigma}(\mathcal{W}) := \Sigma(-\partial_{\mathcal{W}}) \delta(\mathcal{W}). \quad (\text{A.14})$$

The action of the oscillators (A.7) translates into

$$\begin{aligned} \langle f | \bar{\mathbf{b}} | \Sigma \rangle &= \int_{\mathbb{C}} \frac{d\bar{\mathcal{W}} d\mathcal{W}}{2\pi i} \bar{f}(\mathcal{W}) (-\partial_{\mathcal{W}}) \hat{\Sigma}(\mathcal{W}), \\ \langle f | \mathbf{b} | \Sigma \rangle &= \int_{\mathbb{C}} \frac{d\bar{\mathcal{W}} d\mathcal{W}}{2\pi i} \bar{f}(\mathcal{W}) \mathcal{W} \hat{\Sigma}(\mathcal{W}). \end{aligned} \quad (\text{A.15})$$

Also the inner product (A.8) can be expressed in terms of $\hat{\Sigma}(\mathcal{W})$ and $\hat{\Theta}(\mathcal{W})$,⁷

$$\langle \Theta | \Sigma \rangle = \sum_{n=0}^{\infty} \overline{\langle n | \Theta \rangle} \langle n | \Sigma \rangle = \int_{\mathbb{C}} \frac{d\bar{\mathcal{Y}} d\mathcal{Y}}{2\pi i} \int_{\mathbb{C}} \frac{d\bar{\mathcal{W}} d\mathcal{W}}{2\pi i} e^{+\bar{\mathcal{Y}} \mathcal{W}} \overline{\hat{\Theta}(\mathcal{Y})} \hat{\Sigma}(\mathcal{W}). \quad (\text{A.16})$$

⁷As similar inner product was introduced in [53].

With this one easily verifies $(-\partial_{\mathcal{W}})^\dagger = \mathcal{W}$ after identifying $\mathcal{W} \leftrightarrow \mathcal{Y}$. Notice the positive sign in the exponential function in (A.16), whereas it is negative in the measure of (A.8). In particular, this leads to a finite norm of $\hat{\Sigma}(\mathcal{W}) = \delta(\mathcal{W})$, while that of $\hat{\Sigma}(\mathcal{W}) = 1$ diverges.

In conclusion, (A.13) and (A.15) together with (A.16) constitute a realization of the oscillators (A.6) which we call *conjugate Bargmann representation*:

$$\bar{\mathbf{b}} \doteq -\partial_{\mathcal{W}}, \quad \mathbf{b} \doteq \mathcal{W}, \quad |0\rangle \doteq \delta(\mathcal{W}). \quad (\text{A.17})$$

The fact that we can realize the creation operator as differentiation and the annihilation operator as multiplication (and not the other way around) depends crucially on the reinterpretation of the exponential factor in the measure as a delta function, cf. (A.13). In this sense the representation (A.17) can also be thought of as (A.7) “in disguise”. With (A.17) a general state, cf. (A.14), and the orthonormal states from above respectively take the form

$$|\Sigma\rangle \doteq \hat{\Sigma}(\mathcal{W}) = \Sigma(-\partial_{\mathcal{W}})\delta(\mathcal{W}), \quad |k\rangle \doteq \frac{(-\partial_{\mathcal{W}})^k \delta(\mathcal{W})}{\sqrt{k!}}. \quad (\text{A.18})$$

Given a state $|\Sigma\rangle$, the representative $\Sigma(\mathcal{W})$ in the Bargmann representation (A.2) and $\hat{\Sigma}(\mathcal{W})$ in its conjugate (A.17) are formally related by a complex generalization of the Fourier transform.⁸

We return to the example from the end of section A.1. Realizing the oscillators in space V_1 by (A.17) and those in V_2 by (A.2), the vector version of the operator (A.9) becomes

$$|\Psi\rangle = \mathcal{O}_\Psi^\dagger = \sum_{k,l=0}^{\infty} \mathcal{O}_{kl}(\bar{\mathbf{a}}^2)^k(\bar{\mathbf{b}}^1)^l|0\rangle \doteq \mathcal{O}_\Psi(\mathcal{W}^2, -\partial_{\mathcal{W}^1})\delta(\mathcal{W}^1). \quad (\text{A.19})$$

This example illustrates the use of these oscillator algebra representations for the Yangian invariants in section 5. There the Bargmann representation (A.2) is employed for oscillators at sites carrying a totally symmetric representation \mathbf{s} of $\mathfrak{gl}(n)$ and the conjugate Bargmann representation (A.17) appears at sites with a conjugate $\bar{\mathbf{s}}$ of a totally symmetric $\mathfrak{gl}(n)$ representation. Equation (A.19) is also an example of how our expressions for Yangian invariants in terms of delta functions are related to the kernels, cf. (A.11), of the corresponding intertwiners.

References

- [1] J. Drummond, J. Henn, and J. Plefka, “Yangian Symmetry of Scattering Amplitudes in N=4 Super Yang-Mills Theory,” *JHEP* **0905** (2009) 046, [arXiv:0902.2987](#).
- [2] J. M. Drummond, J. Henn, G. P. Korchemsky, and E. Sokatchev, “Dual Superconformal Symmetry of Scattering Amplitudes in N=4 Super-Yang-Mills Theory,” *Nucl. Phys. B* **828** (2010) 317, [arXiv:0807.1095](#).
- [3] N. Beisert, C. Ahn, L. F. Alday, Z. Bajnok, J. M. Drummond, L. Freyhult, N. Gromov, R. A. Janik, V. Kazakov, T. Kloze, G. P. Korchemsky, C. Kristjansen, M. Magro, T. McLoughlin, J. A. Minahan, R. I. Nepomechie, A. Rej, R. Roiban, S. Schäfer-Nameki, C. Sieg, M. Staudacher, A. Torrielli, A. A. Tseytlin, P. Vieira,

⁸A definition of a complex Fourier transform can be found e.g. in [59].

- D. Volin, and K. Zoubos, “Review of AdS/CFT Integrability: An Overview,” *Lett. Math. Phys.* **99** (2012) 3, [arXiv:1012.3982](#).
- [4] N. Beisert, “On Yangian Symmetry in Planar N=4 SYM,” in *Gribov-80 Memorial Volume: Quantum Chromodynamics and Beyond*, Y. L. Dokshitzer, P. Lévai, and J. Nyíri, eds., p. 413. World Scientific Publishing, 2011. [arXiv:1004.5423](#).
- [5] B. Basso, A. Sever, and P. Vieira, “Space-Time S-Matrix and Flux-Tube S-Matrix at Finite Coupling,” *Phys. Rev. Lett.* **111** (2013) 091602, [arXiv:1303.1396](#).
B. Basso, A. Sever, and P. Vieira, “Space-Time S-Matrix and Flux Tube S-Matrix II. Extracting and Matching Data,” [arXiv:1306.2058](#).
- [6] R. J. Baxter, “Perimeter Bethe Ansatz,” *J. Phys. A* **20** (1987) 2557.
- [7] J. M. Drummond and L. Ferro, “The Yangian Origin of the Grassmannian Integral,” *JHEP* **1012** (2012) 010, [arXiv:1002.4622](#).
- [8] L. Ferro, T. Łukowski, C. Meneghelli, J. Plefka, and M. Staudacher, “Harmonic R Matrices for Scattering Amplitudes and Spectral Regularization,” *Phys. Rev. Lett.* **110** (2013) 121602, [arXiv:1212.0850](#).
- [9] L. Ferro, T. Łukowski, C. Meneghelli, J. Plefka, and M. Staudacher, “Spectral Parameters for Scattering Amplitudes in N=4 Super Yang-Mills Theory,” [arXiv:1308.3494](#).
- [10] N. Arkani-Hamed, F. Cachazo, C. Cheung, and J. Kaplan, “A Duality for the S Matrix,” *JHEP* **1003** (2010) 020, [arXiv:0907.5418](#).
- [11] R. J. Baxter, *Exactly Solved Models in Statistical Mechanics*. Dover Publications, 2007.
- [12] E. H. Lieb, “Residual Entropy of Square Ice,” *Phys. Rev.* **162** (1967) 162.
E. H. Lieb, “Exact Solution of the F Model of an Antiferroelectric,” *Phys. Rev. Lett.* **18** (1967) 1046.
B. Sutherland, “Exact Solution of a Two-Dimensional Model for Hydrogen-Bonded Crystals,” *Phys. Rev. Lett.* **19** (1967) 103.
- [13] R. J. Baxter, “Solvable Eight Vertex Model on an Arbitrary Planar Lattice,” *Phil. Trans. Roy. Soc. Lond. A* **289** (1978) 315.
- [14] H. Bethe, “Zur Theorie der Metalle. I. Eigenwerte und Eigenfunktionen der Linearen Atomkette,” *Z. Phys.* **71** (1931) 205.
- [15] M. Karbach and G. Müller, “Introduction to the Bethe Ansatz I,” *Phys. Comp.* **11** (1997) 36, [arXiv:cond-mat/9809162](#).
B. Sutherland, *Beautiful Models: 70 Years of Exactly Solved Quantum Many-Body Problems*. World Scientific Publishing, 2004.
- [16] C. N. Yang, “Some Exact Results for the Many Body Problems in One Dimension with Repulsive Delta Function Interaction,” *Phys. Rev. Lett.* **19** (1967) 1312.
M. Gaudin, “Un Systeme a Une Dimension de Fermions en Interaction,” *Phys. Lett. A* **24** (1967) 55.

- [17] L. D. Faddeev, “Algebraic Aspects of the Bethe Ansatz,” *Int. J. Mod. Phys. A* **10** (1995) 1845, [arXiv:hep-th/9404013](#).
- [18] A. Molev, *Yangians and Classical Lie Algebras*. American Mathematical Society, 2007.
- [19] V. Drinfel’d, “Hopf Algebras and the Quantum Yang-Baxter Equation,” *Sov. Math. Dokl.* **32** (1985) 254.
V. G. Drinfel’d, “Quantum Groups,” *J. Sov. Math.* **41** (1988) 898.
- [20] D. Bernard, “An Introduction to Yangian Symmetries,” *Int. J. Mod. Phys. B* **7** (1993) 3517, [arXiv:hep-th/9211133](#).
N. J. MacKay, “Introduction to Yangian Symmetry in Integrable Field Theory,” *Int. J. Mod. Phys. A* **20** (2005) 7189, [arXiv:hep-th/0409183](#).
- [21] A. B. Zamolodchikov, “Integrable Field Theory from Conformal Field Theory,” *Adv. Stud. Pure Math* **19** (1989) 641.
- [22] P. Dorey, “Exact S-Matrices,” in *Conformal Field Theories and Integrable Models*, Z. Horváth and L. Palla, eds., p. 85. Springer, 1997.
- [23] L. Samaj and Z. Bajnok, *Introduction to the Statistical Physics of Integrable Many-Body Systems*. Cambridge University Press, 2013.
- [24] L. C. Biedenharn and J. D. Louck, *Angular Momentum in Quantum Physics*. Addison-Wesley Publishing, 1981.
- [25] B. Berg, M. Karowski, P. Weisz, and V. Kurak, “Factorized U(n) Symmetric S-Matrices in Two Dimensions,” *Nucl. Phys. B* **134** (1978) 125.
- [26] P. P. Kulish, N. Y. Reshetikhin, and E. K. Sklyanin, “Yang-Baxter Equation and Representation Theory: I,” *Lett. Math. Phys.* **5** (1981) 393.
- [27] J. M. Drummond, “Tree-Level Amplitudes and Dual Superconformal Symmetry,” *J. Phys. A* **44** (2011) 454010, [arXiv:1107.4544](#).
- [28] T. Bargheer, N. Beisert, W. Galleas, F. Loebbert, and T. McLoughlin, “Exacting N=4 Superconformal Symmetry,” *JHEP* **0911** (2009) 056, [arXiv:0905.3738](#).
- [29] T. Bargheer, N. Beisert, and F. Loebbert, “Exact Superconformal and Yangian Symmetry of Scattering Amplitudes,” *J. Phys. A* **44** (2011) 454012, [arXiv:1104.0700](#).
- [30] N. Arkani-Hamed, J. L. Bourjaily, F. Cachazo, A. B. Goncharov, A. Postnikov, and J. Trnka, “Scattering Amplitudes and the Positive Grassmannian,” [arXiv:1212.5605](#).
- [31] E. Witten, “Perturbative Gauge Theory as a String Theory in Twistor Space,” *Commun. Math. Phys.* **252** (2004) 189, [arXiv:hep-th/0312171](#).
- [32] J. M. Drummond and L. Ferro, “Yangians, Grassmannians and T-duality,” *JHEP* **1007** (2010) 027, [arXiv:1001.3348](#).

- [33] L. Ferro, “Yangian Symmetry in N=4 Super Yang-Mills,” [arXiv:1107.1776](#).
- [34] L. Mason and D. Skinner, “Dual Superconformal Invariance, Momentum Twistors and Grassmannians,” *JHEP* **0911** (2009) 045, [arXiv:0909.0250](#).
- [35] M. Abramowitz and I. A. Stegun, *Handbook of Mathematical Functions*. Dover Publications, 1964.
- [36] N. Arkani-Hamed, F. Cachazo, C. Cheung, and J. Kaplan, “The S-Matrix in Twistor Space,” *JHEP* **1003** (2010) 110, [arXiv:0903.2110](#).
- [37] D. Chicherin and R. Kirschner, “Yangian Symmetric Correlators,” *Nucl. Phys. B* **877** (2013) 484, [arXiv:1306.0711](#).
- [38] D. Chicherin, S. Derkachov, and R. Kirschner, “Yang-Baxter Operators and Scattering Amplitudes in N=4 Super-Yang-Mills Theory,” [arXiv:1309.5748](#).
- [39] L. D. Faddeev, “How Algebraic Bethe Ansatz Works for Integrable Model,” in *Symmetries Quantiques/Quantum Symmetries: Les Houches, Session LXIV*, A. Connes, K. Gawedzki, and J. Zinn-Justin, eds., p. 149. North-Holland Publishing, 1998. [arXiv:hep-th/9605187](#).
- [40] P. P. Kulish and N. Y. Reshetikhin, “Diagonalisation of GL(N) Invariant Transfer Matrices and Quantum N-Wave System (Lee Model),” *J. Phys. A* **16** (1983) L591.
- [41] R. J. Baxter, “Partition Function of the Eight-Vertex Lattice Model,” *Ann. Phys.* **70** (1972) 193.
- [42] R. Frassek, N. Kanning, Y. Ko, and M. Staudacher. To appear.
- [43] R. I. Nepomechie and C. Wang, “Algebraic Bethe Ansatz for Singular Solutions,” *J. Phys. A* **46** (2013) 325002, [arXiv:1304.7978](#).
- [44] R. J. Baxter, “Completeness of the Bethe Ansatz for the Six and Eight Vertex Models,” *J. Stat. Phys.* **108** (2002) 1, [arXiv:cond-mat/0111188](#).
- [45] N. Beisert, J. A. Minahan, M. Staudacher, and K. Zarembo, “Stringing Spins and Spinning Strings,” *JHEP* **0309** (2003) 010, [arXiv:hep-th/0306139](#).
- [46] A. A. Ovchinnikov, “Coordinate Space Wave Function from the Algebraic Bethe Ansatz for the Inhomogeneous Six-Vertex Model,” *Phys. Lett. A* **374** (2010) 1311, [arXiv:1001.2672](#).
- [47] F. H. L. Essler, H. Frahm, F. Göhmann, A. Klümper, and V. E. Korepin, *The One-Dimensional Hubbard Model*. Cambridge University Press, 2010.
- [48] L. V. Avdeev and A. A. Vladimirov, “On Exceptional Solutions of the Bethe Ansatz Equations,” *Theor. Math. Phys.* **69** (1987) 1071.
- [49] V. V. Bazhanov, R. Frassek, T. Łukowski, C. Meneghelli, and M. Staudacher, “Baxter Q-Operators and Representations of Yangians,” *Nucl. Phys. B* **850** (2011) 148, [arXiv:1010.3699](#).

- [50] R. Frassek, T. Łukowski, C. Meneghelli, and M. Staudacher, “Oscillator Construction of $\mathfrak{su}(n|m)$ Q-Operators,” *Nucl. Phys. B* **850** (2011) 175, [arXiv:1012.6021](#).
- R. Frassek, T. Łukowski, C. Meneghelli, and M. Staudacher, “Baxter Operators and Hamiltonians for ‘Nearly All’ Integrable Closed $\mathfrak{gl}(n)$ Spin Chains,” *Nucl. Phys. B* **874** (2013) 620, [arXiv:1112.3600](#).
- R. Frassek and C. Meneghelli, “From Baxter Q-Operators to Local Charges,” *J. Stat. Mech.* **1302** (2013) P02019, [arXiv:1207.4513](#).
- [51] V. Bargmann, “On a Hilbert Space of Analytic Functions and an Associated Integral Transform Part I,” *Commun. Pure Appl. Math.* **14** (1961) 187.
- [52] H. Fan, Z. Liu, and T. Ruan, “Does the Creation Operator a_+ Possess Eigenvectors?,” *Commun. Theor. Phys.* **3** (1984) 175.
- [53] A. Ashtekar, C. Rovelli, and L. Smolin, “Self Duality and Quantization,” *J. Geom. Phys.* **8** (1992) 7, [arXiv:hep-th/9202079](#).
- [54] A. D. Ribeiro, F. Parisio, and M. A. M. de Aguiar, “A Conjugate for the Bargmann Representation,” *J. Phys. A* **42** (2009) 105301, [arXiv:0809.1759](#).
- [55] F. Hong-Yi and J. R. Klauder, “On the Common Eigenvectors of Two-Mode Creation Operators and the Charge Operator,” *Mod. Phys. Lett. A* **9** (1994) 1291.
- [56] P. A. M. Dirac, “Quantum Electrodynamics,” *Commun. Dublin Inst. Adv. Stud. A* **1** (1943) 1.
- [57] L. A. Takhtajan, *Quantum Mechanics for Mathematicians*. American Mathematical Society, 2008.
- [58] J. Zinn-Justin, *Path Integrals in Quantum Mechanics*. Oxford University Press, 2005.
- [59] J. A. Dubinskii, *Analytic Pseudo-Differential Operators and their Applications*. Kluwer, 1991.